Universiteit Utrecht

Master's Thesis

Radiative Symmetry Breaking in Classically Conformal Extensions of the Standard Model

---

Leonardo Chataignier Moreira da Rocha

Supervisor:
Dr. Tomislav Prokopec

Institute for Theoretical Physics
Department of Physics and Astronomy
Faculty of Science
Utrecht University

Abstract

We examine the dynamical breakdown of the electroweak symmetry in classically conformal extensions of the Standard Model of Particle Physics known as Higgs Portal Models. Since quantum corrections are responsible for symmetry breaking in these extensions, we study the effective potential up to one-loop order and discuss the application of the renormalisation group to ensure the validity of perturbation theory for arbitrary field values. We emphasise how a judicious choice of the renormalisation scale can minimise the effect of large logarithmic contributions from quantum corrections. In particular, we present a method to re-sum the largest logarithms in models with several scalar fields without resorting to multi-scale techniques. In this way, the improved potential admits a perturbative expansion if the renormalised coupling parameters are small. Non-trivial minima of the effective potential correspond to vacua of the underlying quantum field theory and signal the dynamical breakdown of symmetry. By identifying such points, we conclude that certain Higgs Portal Models can accommodate the radiative generation of the electroweak scale, as well as physics beyond the Standard Model. We also comment on the available literature on the subject and discuss the advantages and shortcomings of the different approaches to radiative symmetry breaking.

To my parents

Ackowledgements

I would like to thank my supervisor, Dr. Tomislav Prokopec, and our collaborators Prof. Dr. Michael G. Schmidt and Dr. Bogumiła Świeżewska for the invaluable discussions, orientation and time they dedicated to clarify fundamental aspects and concepts of this Master's Thesis. Our meetings were indispensable to the development of this project.

I would also like to thank my Master's programme colleagues Adriana Correia, António Rebelo, Lǐ Chōngchuò, Đại-Thành L. Châu, Domingo Gallegos, Emma Minarelli, Enea Mauri, Folkert Kuipers, Guilherme Brando, Jette van den Broeke, Kevin Kavanagh, Pedro Cal, Peter Cats, Rafael Aoude and Ward Vleeshouwers for their friendship and companionship, and my parents for their unconditional support.

Contents

Notations and Conventions 5
Introduction 6

1 Effective Actions **8**
1.1 The Effective Action 8
1.2 The One-Loop Effective Potential 12

2 Dynamical Symmetry Breaking **18**
2.1 Massless ϕ^4-theory 18
2.1.1 Perturbative Structure, Renormalisation and Stability 18
2.1.2 Radiative Extrema 21
2.2 Scalar Quantum Electrodynamics 22
2.3 Flat Directions 24
2.4 A Panoramic View of the Dynamical Breakdown of Symmetry 26

3 Renormalisation Group Improvement of Effective Potentials **28**
Fixing the Notation 28
3.1 Re-summation of Logarithmic Terms 29
3.2 RG Improvement 31
3.2.1 Pivot Logarithm 32
3.2.2 Improvement Along a Characteristic Curve 34

4 The Conformal Standard Model **39**
4.1 The Tree-Level Mass Spectrum 39
4.2 The One-Loop Effective Potential 40
4.2.1 Radiative Extrema 44
4.2.2 RG Improvement 46

5 Conformal Standard Model with a Real Scalar Singlet **50**
5.1 An Overview of Classically Conformal Extensions of the Standard Model 50
5.2 The One-Loop Effective Potential 51
5.3 Flat Directions 53
5.4 Radiative Extrema 55

6 Conformal Standard Model with a hidden $SU(2)$ Gauge Group **58**
6.1 The One-Loop Effective Potential 58
6.2 Hierarchy of Couplings 61
6.3 RG Improvement 66
6.4 A Gildener-Weinberg Example 68

Conclusions 71

A The Method of Characteristics **74**
Fixing the Notation 74
A.1 The Cauchy Boundary Value Problem 74
A.1.1 The Characteristic Form 75
A.1.2 (Non)Characteristic Hypersurfaces 76
A.1.3 First-Order PDEs 77

B The Hypersurface of Vanishing Loop Corrections: A General Approach **80**
Fixing the Notation 80
B.1 The Perturbative Structure of the Effective Potential 81
B.2 (Sub)Leading Contributions in the Pivot Logarithm Expansion 83
B.3 Vanishing Loop Corrections: General Formulas 84

C An Application of RG-Improvement **89**
C.1 Massless $O(N)$-symmetric ϕ^4-theory 89

References **94**

Notations and Conventions

- Unless we specify otherwise, we work in units in which $\hbar = c = 1$.
- We will use the Euclidean metric to evaluate functional integrals and Feynman diagrams. Results in the Euclidean theory can be converted to results with Minkowski metric by a Wick rotation.
- Divergent integrals will be regularised with dimensional regularisation and we will use the $\overline{MS}$ renormalisation scheme, in which the counter-terms are proportional to the combination
$$\frac{1}{\epsilon} + \frac{1}{2}\gamma_E - \frac{1}{2}\log(4\pi) \ ,$$
where $\gamma_E = 0.577\cdots$ is Euler's constant, $\log$ is the natural logarithm and the number of dimensions is $d = 4 + \epsilon$. Divergent terms are expressed as poles in ϵ and the renormalised Lagrangian density is finite in the limit $\epsilon \to 0$.
- We will adopt the Landau gauge throughout the text, unless we state otherwise. This gauge is fixed by adding to the lagrangian density of a gauge field A_μ the term [54]
$$-\frac{1}{2}\lambda^2 \left(\sum_\mu \partial_\mu A^\mu\right)^2$$
and by taking the limit $\lambda \to \infty$ after computing the gauge field propagator. In momentum space and four spacetime dimensions, the gauge field propagator in the Landau gauge reads
$$\Delta_{\mu\nu}(k) = \frac{1}{i(2\pi)^4}\frac{1}{k^2}\left(\eta_{\mu\nu} - \frac{k_\mu k_\nu}{k^2}\right) \ ,$$
where $\eta_{\mu\nu} = \mathrm{diag}(-,+,+,+)$ is the Minkowski metric.
- The reduced Planck mass is
$$M_P = 2.435 \times 10^{18}\ \mathrm{GeV} \ .$$

Introduction

The origin of the electroweak scale is not yet known. While the discovery of a Higgs boson completes the experimental corroboration of the Standard Model of Particle Physics, several questions remain unanswered and an extension of the model is warranted. On the other hand, the current lack of evidence for physics beyond the Standard Model favours the simple proposal that it remains a valid effective theory for energies up to the Planck mass, at which gravitational effects are expected to become important. If this is the case, then there will be no intermediate scale between the electroweak and Planck scales [9, 16]. Although extensions of the model are needed to incorporate dark energy, dark matter and gravity, for example, one can envisage ways to minimally modify the theory without introducing new physical scales.

In the Standard Model, the masses of fermions, excluding neutrinos, and vector bosons are generated by the Brout-Englert-Higgs mechanism. The underlying electroweak symmetry is spontaneously broken by a non-vanishing vacuum expectation value of the physical Higgs field. The condensation of this field is achieved by including a negative mass-squared parameter in the lagrangian. The current experimental data indicate that this mass term nearly vanishes at large energies, which means the Standard Model is nearly-conformal in the ultraviolet (UV). In this scenario, classically conformal extensions of the current theory are promising candidates to address open problems such as how the Higgs boson mass is generated. Moreover, the measured value of the Higgs mass of approximately 125 GeV signals that the electroweak vacuum is metastable [9], which motivates the search for models in which the vacuum is stabilised.

Since classical scale invariance forbids the notion of an intrinsic energy scale, the lagrangian of classically conformal models cannot contain any mass terms. By removing the Higgs mass parameter, the Standard Model lagrangian becomes scale invariant and the breakdown of the electroweak symmetry no longer occurs at tree level [14]. Nature clearly displays different physical scales, which implies some mechanism must be responsible for the breakdown of classical conformal symmetry.

Sidney Coleman and Erick Weinberg studied such a mechanism [3]. Their key insight was that quantum corrections break scale invariance and consequently can lead to non-trivial vacuum expectation values of the fields. Indeed, this is a manifestation of the dimensional transmutation phenomenon, in which dimensionful quantities arise from quantum loops as a consequence of renormalisation. Loop corrections thus modify the classical potential into an effective counterpart and if the effective potential exhibits a non-trivial minimum, then symmetry breaking occurs dynamically. In this case, all mass parameters are generated by the quantum corrections. In other words, mass originates from the quantum theory.

Although current data rule out the Coleman-Weinberg mechanism for the Standard Model, this interesting idea has propelled research into classically conformal extensions of the model, first considered by Hempfling in [15]. These extensions are, in principle, sufficiently robust to accommodate phenomena such as baryogenesis and particle dark matter [17, 24, 32], yet they are simple enough to be predictive. In particular, they are alternatives to supersymmetric models, for which no evidence has been gathered so far.

Classically conformal models can also pave the way to a technical resolution of the hierarchy problem [29, 15, 19], which is also addressed by supersymmetry. One way to understand this problem is to realise that, in the absence of a symmetry that guarantees the vanishing of the Higgs mass term, one needs fine-tuning to explain the small ratio between the electroweak scale and the Planck scale. However, since the electroweak scale arises as a radiative effect in classically conformal models, it can be radiatively stable, thus resolving the hierarchy problem. In other words, classical conformal symmetry serves as a custodial symmetry which protects the Higgs mass from radiative corrections, as was suggested by Bardeen [14]. However, it is

important to notice that such conclusions are still rather speculative, since little is known about the relevant effects of a UV-complete Planckian theory. Nevertheless, there is sufficient motivation to seriously consider classically conformal extensions of the Standard Model as gateways to new physics.

In this work, we will systematically analyse how such models dynamically generate the electroweak scale, placing special emphasis on what are the conditions for the occurrence of the radiative breakdown of symmetry and how one can use the renormalisation group to extended the validity of perturbation theory to all scales below the Planck scale. We will see that perturbativity is guaranteed if the running couplings continue to be small parameters at high energies and no Landau poles occur below the Planck mass. We will show that there is no need to employ several subtraction masses when multiple scalar fields are present, contrary to what has been done in the literature [42, 35, 43, 44], as long as the theory is weakly coupled across a large range of scales.

The thesis is structured as follows. We begin with a review of the theory of effective actions and the one-loop effective potential in Chapter 1. In Chapter 2, we present a systematic way of understanding different cases in which the breakdown of symmetry is realised via radiative corrections. In Chapter 3, we will present a practical alternative to multi-scale techniques. By using the renormalisation-group (RG) equation with a single subtraction mass, we will develop a method to improve potentials with an arbitrary number of scalar fields. With the technique of RG-improvement presented, the one-loop effective potential will be sufficient for our purposes. In Chapter 4, the Conformal Standard Model will be studied in preparation for the classically conformal extensions in Chapters 5 and 6. Finally, we will conclude that a particular class of classically conformal models, known as Higgs Portal Models, is capable of radiatively generating the electroweak vacuum and of ensuring vacuum stability.

Chapter 1

Effective Actions

The phenomenon of spontaneous symmetry breaking and the presence of unsymmetrical solutions is intimately related to the vacuum degrees of freedom of a quantum field theory. Since the vacuum expectation values (VEVs) of field-operators are classical fields, one can envisage an effective theory that describes the dynamics of the field-VEVs and of macroscopic excitations in the vacuum. Such a theory can be achieved with the Method of the Effective Action, introduced by Goldstone, Salam and Weinberg [1] and Jona-Lasinio [2]. In the following section, we will follow references [2, 4, 7].

1.1 The Effective Action

For simplicity*, let us consider the dynamics of a single scalar field ϕ in d dimensions, given by an action functional S. The n-point correlation functions are generated by a functional Z defined as

$$Z[j] := \int \mathcal{D}\phi \, e^{-S[\phi]+(j,\phi)} \ , \tag{1}$$

where j is a source for the field ϕ, viz.

$$(j,\phi) := \int \mathrm{d}^d x \; j(x)\phi(x) \ , \tag{2}$$

such that one can compute the n-point functions by functional differentiation

$$G^{(n)}(x_1,...,x_n) := \frac{1}{Z[0]} \left. \frac{\delta^n Z[j]}{\delta j(x_1)\cdots\delta j(x_n)} \right|_{j=0} \ . \tag{3}$$

The functional Z thus admits the series expansion

$$\frac{Z[j]}{Z[0]} = 1 + \sum_{n=1}^{\infty} \frac{1}{n!} \int \mathrm{d}^d x_1 \cdots \mathrm{d}^d x_n \; G^{(n)}(x_1,...,x_n) j(x_1)\cdots j(x_n) \ . \tag{4}$$

The connected n-point functions are generated by the related functional

$$\log \frac{Z[j]}{Z[0]} = \sum_{n=1}^{\infty} \frac{1}{n!} \int \mathrm{d}^d x_1 \cdots \mathrm{d}^d x_n \; G_c^{(n)}(x_1,...,x_n) j(x_1)\cdots j(x_n) \ . \tag{5}$$

*The generalisation of the definitions and computations of this section to an arbitrary number N_ϕ of scalar fields is straightforward. One promotes the single scalar field ϕ to a collection of scalar fields $\phi_i \ , \ (i = 1, ..., N_\phi)$ and the single source j to a corresponding collection of sources $j_i \ , \ (i = 1, ..., N_\phi)$.

For example, the connected two-point function is given by

$$G_c^{(2)}(x_1,x_2) = \left.\frac{\delta^2 \log Z[j]}{\delta j(x_1)\delta j(x_2)}\right|_{j=0} = G^{(2)}(x_1,x_2) - G^{(1)}(x_1)G^{(1)}(x_2)\,.$$

In an interacting theory, the connected two-point function is related to the free propagator by Dyson's equation,

$$\left[G_c^{(2)}\right]^{-1}(x_1,x_2) = \left[G_{\text{free}}^{(2)}\right]^{-1}(x_1,x_2) - \Sigma(x_1,x_2)\,, \tag{6}$$

where $\Sigma(x_1,x_2)$ is called the self-energy and encodes the corrections to the inverse free propagator. In perturbation theory, such corrections are comprised of amputated one-particle irreducible Feynman diagrams. Amputated diagrams are those obtained by removing the external lines from a connected diagram that contributes to a connected correlation function. In this way, we can define an amputated correlation function as follows.

$$G_{\text{amp}}^{(n)}(x_1,...,x_n) := \prod_{k=1}^{n}\int \mathrm{d}^d y_k \left[G^{(2)}\right]^{-1}(x_k,y_k)G^{(n)}(y_1,...,y_n) \tag{7}$$

One-particle irreducible diagrams cannot be split into disconnected terms when an arbitrary internal line is removed. We define the proper vertices $\Gamma^{(n)}(x_1,...,x_n)$ of the theory as the amputated one-particle irreducible correlation functions. In particular, we have $\Gamma^{(2)}(x_1,x_2) = \left[G_c^{(2)}\right]^{-1}(x_1,x_2)$. In the same way that the inverse connected two-point function includes corrections from the self-energy diagrams, the n-point proper vertex will include corrections from the interactions terms of the theory. Therefore, if we are interested in the effective counterpart of the theory, it will be convenient to find a generating functional for the proper vertices.

Let us now define

$$\phi_c(x;j) := \frac{\delta \log Z}{\delta j(x)}[j]\,, \tag{8}$$

and assume this relation can be inverted to yield the current $j_c(x;\phi_c)$. We can interpret eq. (8) as the VEV of the field operator in the presence of a source. We also note that

$$\phi_c(x;0) = \left.\frac{\delta \log Z[j]}{\delta j(x)}\right|_{j=0} = G^{(1)}(x)\,. \tag{9}$$

To build the effective theory, we will trade the functional dependence on j by a dependence on the classical field variable ϕ_c, sometimes also referred to as average or mean field variable. We can then write the Legendre transform of $-\log Z[j]$ as

$$\Gamma[\phi_c] := \left\{-\log Z[j] + \int \mathrm{d}^d x\; j(x)\phi_c(x)\right\}_{j(x)=j_c(x,\phi_c)}\,, \tag{10}$$

which is a functional of the classical field[†]. This transform is referred to as the effective action, because it is, in fact, the generating functional of the proper vertices of the theory. Indeed, its first functional derivative reads

$$\frac{\delta\Gamma}{\delta\phi_c(x)}[\phi_c] = j_c(x;\phi_c)\,, \tag{11}$$

[†]In what follows, we will write only one argument for the classical field, viz. $\phi_c(x)$, since the current is to be evaluated as $j_c(x,\phi_c)$.

as can be easily checked from eqs. (8) and (10). If in the absence of sources the field-VEV is

$$\phi_c(x;0) = v \,, \tag{12}$$

then eq. (11) implies

$$\left.\frac{\delta\Gamma}{\delta\phi_c(x)}\right|_{\phi_c=v} = 0 \,, \tag{13}$$

i.e., the field-VEV is a stationary point of the effective action if no external sources are present. The second functional derivative of the effective action can be computed from eq. (8) as follows.

$$\begin{aligned}
\delta(x_1 - x_2) &= \int \mathrm{d}^d x_3 \, \frac{\delta j(x_3)}{\delta\phi_c(x_2)} \left.\frac{\delta^2 \log Z}{\delta j(x_3)\delta j(x_1)}\right|_{j=j_c(v)=0} = \\
&= \int \mathrm{d}^d x_3 \, \left.\frac{\delta^2\Gamma}{\delta\phi_c(x_2)\delta\phi_c(x_3)}\right|_{\phi_c=v} G_c^{(2)}(x_3, x_1) \\
\left.\frac{\delta^2\Gamma}{\delta\phi_c(x_1)\delta\phi_c(x_2)}\right|_{\phi_c=v} &= \left[G_c^{(2)}\right]^{-1}(x_1, x_2) = \Gamma^{(2)}(x_1, x_2) \,,
\end{aligned}$$

which is the two-point proper vertex. In a similar fashion, taking further functional derivatives of eq. (8) will yield the n-point proper vertices.

$$\left.\frac{\delta^n\Gamma}{\delta\phi_c(x_1)\cdots\delta\phi_c(x_n)}\right|_{\phi_c=v} = \prod_{k=1}^{n} \int \mathrm{d}^d y_k \left[G_c^{(2)}\right]^{-1}(x_k, y_k) G_c^{(n)}(y_1, ..., y_n) = \Gamma^{(n)}(x_1, ..., x_n)$$

We can therefore expand the effective action as follows.

$$\Gamma[\phi_c] = \Gamma[v] + \sum_{n=2}^{\infty} \frac{1}{n!} \int \mathrm{d}^d x_1 \cdots \mathrm{d}^d x_n \, \Gamma^{(n)}(x_1, ..., x_n) \, (\phi_c(x_1) - v) \, ... \, (\phi_c(x_n) - v) \tag{14}$$

It is, however, more convenient to expand the effective action about the zero-field configuration,

$$\Gamma[\phi_c] = \Gamma[0] + \sum_{n=1}^{\infty} \frac{1}{n!} \int \mathrm{d}^d x_1 \cdots \mathrm{d}^d x_n \, \Gamma_0^{(n)}(x_1, ..., x_n) \phi_c(x_1) ... \phi_c(x_n) \,, \tag{15}$$

where $\Gamma_0^{(n)}(x_1, ..., x_n)$ are amputated one-particle irreducible correlation functions computed in the presence of the source $j_c(x;0)$, which does not necessarily vanish.

We are interested in field-VEVs which are translationally invariant. For this reason, it is convenient to consider the Fourier transform of the correlation functions

$$\Gamma_0^{(n)}(x_1, ..., x_n) = \prod_{i=1}^{n} \left[\int \frac{\mathrm{d}^d p_i}{(2\pi)^d}\right] (2\pi)^d \delta\left(\sum_i p_i\right) \tilde{\Gamma}_0^{(n)}(p_1, ..., p_n) \exp\left(i \sum_i x_i \cdot p_i\right) \,, \tag{16}$$

such that the the effective action can be written as

$$\Gamma[\phi_c] = \Gamma[0] + \sum_{n=1}^{\infty} \frac{1}{n!} \int \mathrm{d}^d x \, \prod_{i=1}^{n} \left[\frac{\mathrm{d}^d x_i \mathrm{d}^d p_i}{(2\pi)^d} \phi_c(x_i)\right] \, \tilde{\Gamma}_0^{(n)}(p_1, ..., p_n) \exp\left(i \sum_i (x_i - x) \cdot p_i\right) \,.$$

By expanding the correlation functions in powers of momenta,

$$\begin{aligned}
\Gamma_0^{(n)}(p_1, ..., p_n) = \Gamma_0^{(n)}(0, ..., 0) &+ \sum_{i,\mu} \left.\frac{\partial}{\partial p_i^\mu} \Gamma_0^{(n)}(p_1, ..., p_n)\right|_{p=0} p_{i,\mu} + \\
&+ \frac{1}{2} \sum_{i,j,\mu,\nu} \left.\frac{\partial^2}{\partial p_i^\mu \partial p_j^\nu} \Gamma_0^{(n)}(p_1, ..., p_n)\right|_{p=0} p_{i,\mu} p_{j,\nu} + \cdots \,,
\end{aligned}$$

we obtain a derivative expansion for the effective action,

$$\Gamma[\phi_c] = \Gamma[0] + \int \mathrm{d}^d x \sum_{n=1}^{\infty} \frac{\phi_c^n(x)}{n!} \tilde{\Gamma}_0^{(n)}(0,...,0) + \frac{1}{2} \sum_{\mu} \int \mathrm{d}^d x \, Z(\phi_c) \frac{\partial \phi_c}{\partial x^\mu} \frac{\partial \phi_c}{\partial x_\mu} + \cdots \,, \tag{17}$$

which resembles a classical action functional. The normalisation $Z(\phi_c)$ of the kinetic term will be determined by the amputated one-particle irreducible correlation functions $\Gamma_0^{(n)}$ evaluated at zero momenta. The non-derivative terms are interpreted as an effective potential, i.e., we define the effective potential of the theory as

$$\int \mathrm{d}^d x \, V_{\text{eff}}(\phi_c) := \Gamma[0] + \int \mathrm{d}^d x \sum_{n=1}^{\infty} \frac{\phi_c^n(x)}{n!} \tilde{\Gamma}_0^{(n)}(0,...,0) \,. \tag{18}$$

For field-VEVs that are translationally invariant, $\phi_c(x) = \phi_c(0) \equiv \phi_c$, we have

$$\left[V_{\text{eff}}(\phi_c) - \sum_{n=1}^{\infty} \frac{\phi_c^n}{n!} \tilde{\Gamma}_0^{(n)}(0,...,0) \right] (2\pi)^d \delta(0) - \Gamma[0] = 0 \,.$$

By defining $\Gamma[0] = -(2\pi)^d \delta(0) V(0)$, we obtain a formula for the effective potential of translationally invariant VEVs

$$V_{\text{eff}}(\phi_c) = V(0) + \sum_{n=1}^{\infty} \frac{\phi_c^n}{n!} \tilde{\Gamma}_0^{(n)}(0,...,0) \,. \tag{19}$$

From eq. (13), we then obtain

$$\begin{aligned} 0 = \frac{\delta \Gamma}{\delta \phi_c(x)}\bigg|_{\phi_c = v} &= \frac{\partial V_{\text{eff}}}{\partial \phi_c}\bigg|_{\phi_c = v} (2\pi)^d \delta(0) \,, \\ \Rightarrow \frac{\partial V_{\text{eff}}}{\partial \phi_c}\bigg|_{\phi_c = v} &= 0 \,, \end{aligned} \tag{20}$$

i.e., translationally invariant field-VEVs are stationary points of the effective potential in the absence of external sources. In this thesis, we will exploit this fact to probe for non-trivial vacua in classically conformal extensions of the Standard Model. If such non-trivial minima are present in these models, then the breakdown of symmetry is entirely due to the quantum corrections of the theory.

With eq. (19), one may compute the effective potential of the theory up to any loop order. It is useful to recall that the loop expansion is equivalent to an expansion in powers of $\hbar$. To see this, one reinstates $\hbar$ in eq. (1),

$$Z[j] := \int \mathcal{D}\phi \, e^{-\frac{1}{\hbar} S[\phi] + \frac{1}{\hbar}(j,\phi)} \,, \tag{21}$$

and notices that eq. (21) implies that vertices contribute with $\hbar^{-1}$ and propagators contribute with $\hbar$ in each diagram. In amputated one-particle irreducible diagrams, the power P of $\hbar$ is then given by $P = I - V$, where I is the number of internal lines and V is the number of vertices. Moreover, in momentum space, each internal line is accompanied with a momentum integral, while each vertex is associated with a δ-function. Conservation of the external momenta of the diagram prevents one δ-function from being integrated, in such a way that we can reduce the I integration variables by $V - 1$ only. The number of loops in a diagram is equal to the number of remaining integration variables, i.e., $L = I - V + 1 = P + 1$.

For our purposes, the one-loop effective potential will be sufficient. Indeed, as we will see in section (3.2), one can use the renormalisation group to re-sum certain terms of higher powers of $\hbar$ with limited knowledge of lower loop-orders. In this thesis, our strategy to study the radiative breakdown of symmetry in classically conformal extensions of the Standard Model will rely only on one-loop quantities. We will then use the renormalisation group to incorporate certain higher loop-order terms, in a procedure known as renormalisation-group improvement of the effective potential, which will be discussed in Chapter 3.

In the following section, we will follow references [4, 7, 8].

1.2 The One-Loop Effective Potential

The one-loop effective potential is given by eq. (19) with the amputated one-particle irreducible correlation functions truncated at one-loop order. It is, however, more practical to obtain a concrete expression for the potential in terms of a momentum integral that can be computed in a given regularisation scheme. To obtain such an expression, we can expand the effective action up to first order in $\hbar$.

Let us then expand the action functional around an arbitrary field configuration φ

$$\begin{aligned} S[\phi+\varphi] = S[\varphi] + \int \mathrm{d}^d x \ \left.\frac{\delta S}{\delta\phi(x)}\right|_{\phi=\varphi} \phi(x) + \\ + \frac{1}{2}\int \mathrm{d}^d x_1 \mathrm{d}^d x_2 \ \phi(x_1) \left.\frac{\delta^2 S}{\delta\phi(x_1)\delta\phi(x_2)}\right|_{\phi=\varphi} \phi(x_2) + I(\varphi;\phi) \ , \end{aligned}$$

where $I(\varphi;\phi)$ represents higher order terms in the expansion. Let us also define

$$\Delta^{-1}(\varphi; x_1, x_2) := \left.\frac{\delta^2 S}{\delta\phi(x_1)\delta\phi(x_2)}\right|_{\phi=\varphi} \ . \tag{22}$$

We can now rewrite eq. (21) as

$$Z[j] = \exp\left\{-\frac{1}{\hbar}S[\varphi] + \frac{1}{\hbar}(j,\varphi)\right\} Z'[j] \ , \tag{23}$$

where

$$\begin{aligned} Z'[j] &:= N\int \mathcal{D}\phi \ \exp\left\{-\frac{1}{\hbar}\left[\left(\frac{\delta S}{\delta\phi} - j, \phi\right) + \frac{1}{2}(\phi, \Delta^{-1}\phi) + I(\varphi;\phi)\right]\right\} \ , \\ (\phi, \Delta^{-1}\phi) &:= \int \mathrm{d}^d x_1 \mathrm{d}^d x_2 \ \phi(x_1)\Delta^{-1}(\varphi; x_1, x_2)\phi(x_2) \ . \end{aligned} \tag{24}$$

The factor of N is the overall normalisation of the functional integral, which was not included in eq. (21). In particular,

$$N\int \mathcal{D}\phi \ \exp\left\{-\frac{1}{2\hbar}(\phi, \Delta^{-1}\phi)\right\} = \left(\det \Delta^{-1}\right)^{-1/2} \ . \tag{25}$$

It is now convenient to choose φ to obey the classical equation of motion

$$\frac{\delta S}{\delta\phi(x)}[\varphi] = j(x) \ , \tag{26}$$

which defines φ as a functional of j. We are going to assume this relation can be inverted to yield $j(x;\varphi)$. With this choice, eq. (24) reduces to

$$Z'[j] = N \int \mathcal{D}\phi \, \exp\left\{-\frac{1}{\hbar}\left[\frac{1}{2}(\phi, \Delta^{-1}\phi) + I(\varphi;\phi)\right]\right\} . \tag{27}$$

Moreover,

$$\begin{aligned}\left(\det \Delta^{-1}\right)^{1/2} Z'[j] &= \frac{\int \mathcal{D}\phi \, \exp\left\{-\frac{1}{\hbar}\left[\frac{1}{2}(\phi, \Delta\phi) + I(\varphi;\phi)\right]\right\}}{\int \mathcal{D}\phi \, \exp\left\{-\frac{1}{2\hbar}(\phi, \Delta\phi)\right\}} = \\ &= \exp\left\{-\frac{1}{\hbar} I\left(\varphi; \frac{\delta}{\delta K}\right)\right\} \exp\left\{\frac{1}{2}(K, \hbar\Delta K)\right\}\Big|_{K=0} = \\ &= 1 + \mathcal{O}(\hbar) .\end{aligned}$$

In this way, we can write

$$\begin{aligned} Z'[j] &= \left(\det \Delta^{-1}\right)^{-1/2} + \mathcal{O}(\hbar) , \\ -\hbar \log Z[j] &= S[\varphi] - (j,\varphi) + \frac{\hbar}{2}\mathrm{Tr}\log\Delta^{-1} + \mathcal{O}(\hbar^2) . \end{aligned} \tag{28}$$

From eqs. (8) and (26), we obtain

$$-\hbar\frac{\delta \log Z[j]}{\delta j(x;\varphi)} = -\varphi(x) + \mathcal{O}(\hbar) \equiv -\phi_c(x) . \tag{29}$$

The effective action can then be written as (cf.eq. (10))

$$\begin{aligned}\Gamma[\phi_c] &= S[\varphi] + (j_c, \phi_c - \varphi) + \frac{\hbar}{2}\mathrm{Tr}\log\Delta^{-1} + \mathcal{O}(\hbar^2) = \\ &= S[\phi_c] + \left(\frac{\delta S}{\delta\phi_c}, \varphi - \phi_c\right) + (j_c, \phi_c - \varphi) + \frac{\hbar}{2}\mathrm{Tr}\log\Delta^{-1} + \mathcal{O}(\hbar^2) .\end{aligned}$$

Since $\phi_c - \varphi = \mathcal{O}(\hbar)$, we have $(\frac{\delta S}{\delta\phi_c} - j_c, \varphi - \phi_c) = \mathcal{O}(\hbar^2)$. The effective action then reads

$$\Gamma[\phi_c] = S[\phi_c] + \frac{\hbar}{2}\mathrm{Tr}\log\Delta^{-1} + \mathcal{O}(\hbar^2) , \tag{30}$$

where the inverse propagator Δ^{-1} is to be evaluated at ϕ_c. We thus see that the effective action for the translationally invariant field-VEV is comprised of the tree-level action evaluated at ϕ_c and the quantum corrections, which are contained in the logarithmic term (see also [4, 7]). Terms with higher powers in $\hbar$ correspond to contributions from higher loop orders to the effective action. Indeed, from the diagrammatic relation $L = P + 1$ and the Legendre transform $-\hbar\log Z[j_c] + (j_c, \phi_c)$, we see that the l-th loop order contributions to the effective action are accompanied by a factor of $\hbar^{l-1+1} = \hbar^l$.

Since ϕ_c is translationally invariant, the propagator $\Delta(\phi_c; x_1, x_2)$ depends only on $x_1 - x_2$ and is, therefore, diagonal in momentum space.

$$\begin{aligned}\tilde{\Delta}^{-1}(\phi_c; k_1, k_2) &= \frac{1}{(2\pi)^d}\int \mathrm{d}^d x_1 \mathrm{d}^d x_2 \exp\left(-ik_1\cdot x_1 + ik_2\cdot x_2\right)\Delta^{-1}(\phi_c; x_1 - x_2) = \\ &= \delta(k_1 - k_2)\tilde{\Delta}^{-1}(\phi_c; k_1)\end{aligned}$$

This implies the functional trace in eq. (30) reads

$$\begin{aligned}\mathrm{Tr}\log\Delta^{-1} &= \int \mathrm{d}^d k_1 \mathrm{d}^d k_2\ \delta(k_1-k_2)\ \mathrm{tr}\log\tilde{\Delta}^{-1}(\phi_c;k_1,k_2) = \\ &= \delta(0)\int \mathrm{d}^d k\ \mathrm{tr}\log\tilde{\Delta}^{-1}(\phi_c;k)\ ,\end{aligned}$$

where the remaining trace sums over spin or internal degrees of freedom in models with multiple fields (see below). We can now write the non-derivative terms in eq. (30) as

$$\int \mathrm{d}^d x\ V_{\text{eff}}(\phi_c) = \int \mathrm{d}^d x\ V^{(0)}(\phi_c) + \frac{\hbar}{2}\int \mathrm{d}^d x \int \frac{\mathrm{d}^d k}{(2\pi)^d}\mathrm{tr}\log\tilde{\Delta}^{-1}(\phi_c;k) + \mathcal{O}(\hbar^2)\ ,$$

where $V^{(0)}$ is the tree-level potential. The one-loop term is

$$V^{(1)}(\phi_c) = \frac{1}{2}\int \frac{\mathrm{d}^d k}{(2\pi)^d}\mathrm{tr}\log\tilde{\Delta}^{-1}(\phi_c;k) \tag{31}$$

and the effective potential can be written as

$$\begin{aligned}V_{\text{eff}}(\phi_c) &= V^{(0)}(\phi_c) + \hbar V^{(1)}(\phi_c) + \mathcal{O}(\hbar^2) = \\ &= V^{(0)}(\phi_c) + \frac{\hbar}{2}\mathrm{tr}\int \frac{\mathrm{d}^d k}{(2\pi)^d}\log\tilde{\Delta}^{-1}(\phi_c;k) + \mathcal{O}(\hbar^2)\ .\end{aligned} \tag{32}$$

The One-Loop Effective Potential for Scalar Bosons

To obtain the expression for the one-loop effective potential in the scalar sector of the theory, let us begin by considering the simple example of massive ϕ^4-theory, with the (euclidean) lagrangian density given by

$$\begin{aligned}\mathcal{L} = &\frac{1}{2}\sum_\mu \frac{\partial\phi}{\partial x^\mu}\frac{\partial\phi}{\partial x_\mu} + \frac{1}{2}m^2\phi^2 + \frac{1}{4}\lambda\phi^4 + \\ &+ \frac{A}{2}\sum_\mu \frac{\partial\phi}{\partial x^\mu}\frac{\partial\phi}{\partial x_\mu} + \frac{1}{2}B\phi^2 + \frac{1}{4}C\phi^4 + \Omega + D\ ,\end{aligned} \tag{33}$$

where Ω is a constant and A, B, C, D are counterterms that render the loop expansion finite in four spacetime dimensions. Moreover, ϕ is the quantum field to be integrated in the generating functional $Z[j]$. The tree-level effective potential is then given by

$$V^{(0)}(\phi_c) = \frac{1}{2}m^2\phi_c^2 + \frac{1}{4}\lambda\phi_c^4 + \Omega\ . \tag{34}$$

The inverse propagator in momentum space reads

$$\tilde{\Delta}^{-1}(\phi_c;k) = k^2 + m^2 + 3\lambda\phi_c^2\ , \tag{35}$$

such that the one-loop term in the effective potential is[‡]

$$V^{(1)}(\phi_c) = \frac{1}{2}\int \frac{\mathrm{d}^d k}{(2\pi)^d}\log\left(k^2 + m^2 + 3\lambda\phi_c^2\right) + \frac{1}{2}B^{(1)}\phi_c^2 + \frac{1}{4}C^{(1)}\phi_c^4 + D^{(1)}\ . \tag{36}$$

[‡]Note that counterterms were not explicitly written in eq. (32) and that $B^{(1)}$, $C^{(1)}$ and $D^{(1)}$ are the counterterms in the one-loop approximation.

In four spacetime dimensions, the momentum integral diverges. To regularise the theory, we take $d = 4 + \epsilon\ ,\ 0 < \epsilon < 1$, and use dimensional regularisation. The result is

$$\begin{aligned} B^{(1)} &= -\frac{6m^2\lambda}{16\pi^2}\left(\frac{1}{\epsilon} + \frac{1}{2}\gamma_E - \frac{1}{2}\log 4\pi\right)\ , \\ C^{(1)} &= -\frac{9\lambda^2}{8\pi^2}\left(\frac{1}{\epsilon} + \frac{1}{2}\gamma_E - \frac{1}{2}\log 4\pi\right)\ , \\ D^{(1)} &= -\frac{m^4}{32\pi^2}\left(\frac{1}{\epsilon} + \frac{1}{2}\gamma_E - \frac{1}{2}\log 4\pi\right)\ , \\ V^{(1)} &= \frac{(m^2 + 3\lambda\phi_c^2)^2}{64\pi^2}\left[\log\frac{m^2 + 3\lambda\phi_c^2}{\mu^2} - \frac{3}{2}\right]\ . \end{aligned} \tag{37}$$

In four spacetime dimensions, the renormalised effective potential of massive ϕ^4-theory then reads

$$V_{\text{eff}}(\phi_c) = \Omega + \frac{1}{2}m^2\phi_c^2 + \frac{1}{4}\lambda\phi_c^4 + \hbar\frac{(m^2 + 3\lambda\phi_c^2)^2}{64\pi^2}\left[\log\frac{m^2 + 3\lambda\phi_c^2}{\mu^2} - \frac{3}{2}\right] + \mathcal{O}(\hbar^2)\ . \tag{38}$$

It is straightforward to generalise this result to a model where $N_\phi > 1$ scalar fields are present. The inverse propagator now reads

$$\begin{aligned} \tilde{\Delta}^{-1}_{ab}(\phi_c; k) &= k^2 + M^2_{ab}(\phi_c)\ , \\ M^2_{ab}(\phi_c) &= \frac{\partial^2 V^{(0)}}{\partial\phi_{c,a}\partial\phi_{c,b}}\ , \end{aligned} \tag{39}$$

and the renormalised effective potential in four spacetime dimensions is

$$V_{\text{eff}}(\phi_c) = V^{(0)}(\phi_c) + \frac{\hbar}{64\pi^2}\text{tr}\left\{M^4(\phi_c)\left[\log\frac{M^2(\phi_c)}{\mu^2} - \frac{3}{2}\right]\right\} + \mathcal{O}(\hbar^2)\ . \tag{40}$$

The One-Loop Effective Potential for Vector Bosons

To compute the one-loop effective potential for gauge fields, it is practical to choose the Landau gauge, in which the Faddeev-Popov ghosts decouple from the scalars. We will thus fix the Landau gauge and ignore the ghost-field contributions to the effective potential. The inverse propagator for gauge fields then reads

$$\tilde{\Delta}^{-1}_{\mu\alpha,\nu\beta}(\phi_c; k) = \sum_s \epsilon^{(s)}_\alpha \epsilon^{(s)}_\beta \left(k^2 + \mathbb{M}^2(\phi_c)\right)\left(\delta_{\mu\nu} - \frac{k_\mu k_\nu}{k^2}\right)\ , \tag{41}$$

where $\mathbb{M}$ is the tree-level mass matrix for vector fields and $\epsilon^{(s)}$ is an eigenvector of $\mathbb{M}$ [7]. The computation of the renormalised effective potential in the vector-boson sector proceeds in an entirely analogous way to the one in the previous section. The one-loop contribution is

$$\begin{aligned} V^{(1)}_{\text{vectors}} &= \frac{1}{2}\text{tr}\int\frac{\mathrm{d}^d k}{(2\pi)^d}\log\tilde{\Delta}^{-1}(\phi_c; k) + \text{counterterms} = \\ &= \frac{d-1}{2}\text{tr}\int\frac{\mathrm{d}^d k}{(2\pi)^d}\log\left(k^2 + \mathbb{M}^2(\phi_c)\right) + \text{counterterms}\ , \end{aligned}$$

where the factor of $d-1$ is comes from summing over the polarisations of massive vector fields. In four spacetime dimensions, we find

$$V^{(1)}_{\text{vectors}}(\phi_c) = \frac{3}{64\pi^2}\text{tr}\left\{\mathbb{M}^4(\phi_c)\left[\log\frac{\mathbb{M}^2(\phi_c)}{\mu^2} - \frac{5}{6}\right]\right\}\ . \tag{42}$$

The One-Loop Effective Potential for Dirac Fermions

The derivation of the one-loop renormalised expression for the effective potential in the fermionic sector is analogous to the scalar and vector-boson counterparts. The important difference that arises in the fermionic case is the inclusion of an overall factor of -2 coming from the logarithm of the Gaussian integral in the analogue of eq. (25) for Grassmann variables. We thus obtain

$$V^{(1)}_{\text{fermions}} = -\text{tr}\int \frac{\mathrm{d}^d k}{(2\pi)^d} \log \tilde{\Delta}^{-1}(\phi_c; k) + \text{counterterms} \,, \tag{43}$$

where the inverse propagator reads

$$\tilde{\Delta}^{-1}(\phi_c; k) = \sum_\mu \gamma_\mu k^\mu + \mathbf{M}(\phi_c) \,, \tag{44}$$

where $\mathbf{M}(\phi_c)$ is the tree-level mass matrix for fermions, which is a linear function of ϕ_c. We find the one-loop renormalised contribution

$$V^{(1)}_{\text{fermions}}(\phi_c) = -\frac{4}{64\pi^2}\text{tr}\left\{\left(\mathbf{M}(\phi_c)\mathbf{M}^\dagger(\phi_c)\right)^2\left(\frac{\mathbf{M}(\phi_c)\mathbf{M}^\dagger(\phi_c)}{\mu^2}\right) - \frac{3}{2}\right\} \,, \tag{45}$$

where the factor of 4 comes from summing over the Dirac indices, i.e., it is the number of degrees of freedom of a Dirac fermion. The remaining trace in the above expression sums over the internal degrees of freedom and colour charges of the fermions.

The General One-Loop Term

In a model with scalars, vectors and fermions in four spacetime dimensions, by working in the Landau gauge and adopting the $\overline{MS}$ scheme, we can write the renormalised one-loop term in the effective potential as

$$V^{(1)}(\phi_c) = \frac{1}{64\pi^2}\sum_a \xi_a m_a^4(\phi_c)\left(\log\frac{m_a^2(\phi_c)}{\mu^2} - \chi_a\right) \,, \tag{46}$$

where the index a runs over all mass eigenvalues, the tree-level field-dependent mass eigenvalues have been generically denoted by $m_a(\phi_c)$ and the constants ξ_a and χ_a read

$$\xi_a = \begin{cases} 1 & \text{for scalars} \\ -4 & \text{for Dirac fermions} \\ 3 & \text{for vector bosons} \end{cases} \,,$$

$$\chi_a = \begin{cases} \frac{3}{2} & \text{for scalars and Dirac fermions} \\ \\ \frac{5}{6} & \text{for vector bosons} \end{cases} \,.$$

A convenient way of writing the one-loop term is obtained by rewriting each mass logarithm as

$$\log\frac{m_a^2(\phi_c)}{\mu^2} = \log\frac{m_a^2(\phi_c)}{\mathcal{M}^2} + \log\frac{\mathcal{M}^2}{\mu^2} \,, \tag{47}$$

where $\mathcal{M}$ is any function with mass dimension equal to one and will be referred to as the pivot mass. For example, if there are N_ϕ scalar fields, we can choose $\mathcal{M}$ to be the radial variable in the scalar-field configuration space

$$\mathcal{M}^2 := \rho^2 = \sum_{a=1}^{N_\phi} \phi_{a,c}^2 \,.$$

We can then rewrite eq. (46) as

$$V^{(1)}(\phi_c) = \mathcal{M}^4 \left(\mathbb{A} + \mathbb{B} \log \frac{\mathcal{M}^2}{\mu^2} \right) , \tag{48}$$

where we defined the functions

$$\begin{aligned} \mathbb{A} &= \frac{1}{64\pi^2 \mathcal{M}^4} \sum_a \xi_a \left(m_a^4(\phi_c) \log \frac{m_a^2(\phi_c)}{\mathcal{M}^2} - \chi_a m_a^4(\phi_c) \right) , \\ \mathbb{B} &= \frac{1}{64\pi^2 \mathcal{M}^4} \sum_a \xi_a m_a^4(\phi_c) . \end{aligned} \tag{49}$$

Since $\mathcal{M}$ is arbitrary, we note that different choices $\mathcal{M}$ and $\mathcal{M}'$ are related by the transformations

$$\begin{aligned} \mathbb{A}\mathcal{M}^4 &= \frac{1}{64\pi^2} \sum_a \xi_a \left(m_a^4(\phi_c) \log \frac{m_a^2(\phi_c)}{\mathcal{M}'^2} - \chi_a m_a^4(\phi_c) \right) + \frac{1}{64\pi^2} \sum_a \xi_a m_a^4(\phi_c) \log \frac{\mathcal{M}'^2}{\mathcal{M}^2} \equiv \\ &\equiv \mathbb{A}'\mathcal{M}'^4 + \mathbb{B}'\mathcal{M}'^4 \log \frac{\mathcal{M}'^2}{\mathcal{M}^2} , \\ \mathbb{B}\mathcal{M}^4 &\equiv \mathbb{B}'\mathcal{M}'^4 . \end{aligned} \tag{50}$$

The one-loop term (48) is evidently invariant under the above transformations. Using expression (48) is advantageous since the explicit dependence on the subtraction mass is contained only in the logarithm $\log \frac{\mathcal{M}^2}{\mu^2}$ if $\mathcal{M}$ is independent of μ. We will refer to this logarithm as the pivot logarithm. In the following chapters, we will use the form of the one-loop contribution of eq. (48).

Chapter 2

Dynamical Symmetry Breaking

The radiative corrections encoded in the effective action studied in Chapter 1 can be sufficiently large so as to generate non-trivial vacua for a quantum field theory. Indeed, from eq. (20), we see that the stationary points of the effective potential correspond to translationally invariant vacuum expectation values of the scalar fields if no external sources are present. It is, therefore, of crucial importance to determine whether or not the quantum corrections can considerably alter the vacuum structure of a given model. In this chapter, we will review the archetypical examples of radiative symmetry breaking, which were originally studied in [3, 5], and discuss the limit of applicability of the one-loop approximation to the effective potential.

2.1 Massless ϕ^4-theory

We begin by considering ϕ^4-theory. The one-loop effective potential was given in eq. (38). With a view to classically conformal models, we set the tree-level mass parameter and vacuum energy to zero, $m^2 = 0$, $\Omega = 0$, which is consistent with eq. (37). This is the simplest classically conformal model and is referred to as massless ϕ^4-theory. For convenience, we drop the "eff" and "c" subscripts from the effective potential and classical field, respectively, and we include the subtraction mass μ and coupling λ as explicit arguments of the effective potential,

$$V(\mu;\lambda,\phi) = \frac{1}{4}\lambda\phi^4 + \frac{9\hbar\lambda^2\phi^4}{64\pi^2}\left[\log\frac{3\lambda\phi^2}{\mu^2} - \frac{3}{2}\right] + \mathcal{O}(\hbar^2)\,. \tag{51}$$

2.1.1 Perturbative Structure, Renormalisation and Stability

In general, the one-loop approximation (48) will be reliable if the $\mathcal{O}(\hbar^2)$ terms in the effective potential are not large. Otherwise, perturbation theory ceases to be valid. Perturbativity is guaranteed if the couplings are small parameters and there are no large logarithmic contributions in the loop corrections.

To better understand the perturbative structure of the effective potential, let us analyse the potential in massless ϕ^4-theory. The mass logarithm in eq. (51) originated from the momentum integral in eq. (32). In general, a momentum integral will exhibit a logarithmic divergence which, upon regularisation, is converted into a mass logarithm $\log\frac{3\lambda\phi^2}{\mu^2}$. In this way, there can be at most n such logarithmic factors in an n-loop Feynman diagram. The n-th loop-order effective potential will thus contain products of the coupling and logarithm with powers given by, at

most, $\lambda^{n+1}\left[\hbar\log\frac{3\lambda\phi^2}{\mu^2}\right]^n$. Such terms are referred to as the leading logarithms of massless ϕ^4-theory. The loop expansion of the effective potential is thus a power series in λ and in $\hbar\lambda\log\frac{3\lambda\phi^2}{\mu^2}$ and truncations at a given loop-order will be useful approximations if both parameters are small.

If there are large logarithms, i.e., $\hbar\left|\lambda\log\frac{3\lambda\phi^2}{\mu^2}\right| > 4\pi$, then one may use the freedom of choosing the subtraction mass μ to regain perturbativity. Indeed, the subtraction mass is an arbitrary parameter and the value of the effective potential, for fixed values of the couplings and fields, cannot depend on it. The renormalised parameters of the theory will, however, vary for different choices of μ, due to the addition of counterterms. In general, for each coupling parameter and field*, one defines the renormalisation group (RG) functions

$$\begin{aligned}\beta \equiv \beta(\lambda,\epsilon) &:= \mu\left.\frac{\partial\lambda}{\partial\mu}\right|_{\lambda_0,\epsilon\text{ fixed}}\,,\\ \gamma \equiv \gamma(\lambda,\epsilon) &:= \mu\left.\frac{\partial\log Z}{\partial\mu}\right|_{\lambda_0,\epsilon\text{ fixed}}\,,\end{aligned} \tag{52}$$

which are referred to as β-functions and anomalous dimensions, respectively. For massless ϕ^4-theory, the relation between the renormalised coupling λ and the bare coupling λ_0 is (cf. eqs. (37))

$$\lambda_0 = \mu^\epsilon\left(\lambda + \hbar C^{(1)} + \mathcal{O}(\hbar^2)\right)\,.$$

Upon differentiating with respect to μ, one finds

$$0 = \epsilon\left(\lambda + \hbar C^{(1)}\right) + \left(1 + \hbar\frac{\mathrm{d}C^{(1)}}{\mathrm{d}\lambda}\right)\beta + \mathcal{O}(\hbar^2)\,,$$

which leads to

$$\begin{aligned}\beta &= \epsilon\left(\lambda - \hbar\lambda\frac{\mathrm{d}C^{(1)}}{\mathrm{d}\lambda} + \hbar C^{(1)}\right) + \mathcal{O}(\hbar^2) =\\ &= \epsilon\left\{\lambda + \frac{9\hbar\lambda^2}{8\pi^2}\left(\frac{1}{\epsilon} + \frac{1}{2}\gamma_E - \frac{1}{2}\log 4\pi\right)\right\} + \mathcal{O}(\hbar^2) \overset{\epsilon\to 0}{=}\\ &\overset{\epsilon\to 0}{=} \frac{9\hbar\lambda^2}{8\pi^2} + \mathcal{O}(\hbar^2) \equiv \hbar\beta^{(1)} + \mathcal{O}(\hbar^2)\,.\end{aligned} \tag{53}$$

Analogously, we see from eqs. (37) that the one-loop anomalous dimension of the scalar field vanishes, which implies that, at one-loop order, the field variable ϕ is independent of the choice of subtraction mass.

By integrating the first of eqs. (52) and using the result of eq. (53), we obtain the one-loop running coupling

$$\lambda(\mu) = \frac{\lambda_0}{1 - \frac{9\hbar\lambda_0}{8\pi^2}\log\frac{\mu}{\mu_0}}\,, \tag{54}$$

where $\lambda_0 = \lambda(\mu_0)$ and μ_0 is an arbitrary reference mass. We interpret $\lambda(\mu)$ as the value of the coupling parameter when the subtraction mass is chosen to be μ, which is related to the corresponding value at μ_0 by terms of all orders in λ_0 and $\hbar\lambda_0\log\frac{\mu}{\mu_0}$ (cf. eq. (54)). This observation

*Recall that the relation between the bare field and the renormalised field is given by $\phi_0 = \sqrt{Z}\phi$.

is the key to regaining perturbativity in the case of large logarithms. Indeed, the closed form in eq. (54) guarantees that, as long as $|\lambda(\mu)| \leq 4\pi$, the logarithm in the denominator can grow large. Therefore, if the potential evaluated at the mass μ_0 exhibits large logarithmic terms, then we should evaluate the potential at the mass μ, where these logarithms have been re-summed into $\lambda(\mu)$. More precisely, we see that

$$\lambda(\mu^2 = 3\lambda_0\phi^2) = \sum_{n=0}^{\infty} \lambda_0^{n+1} \left[\frac{9\hbar}{16\pi^2} \log \frac{3\lambda_0\phi^2}{\mu_0^2}\right]^n \ , \tag{55}$$

i.e., the renormalised coupling at the mass-squared $\mu^2 = 3\lambda_0\phi^2$ corresponds to the sum of all leading logarithms at a reference mass μ_0. We thus see that the one-loop RG running of the coupling parameter is sufficient to re-sum into a closed form the highest powers of the mass logarithm that appear at each loop-level. Perturbativity is then guaranteed if $\lambda(\mu^2 = 3\lambda_0\phi^2)$ is small.

Since the effective potential itself is independent of the choice of μ, it must satisfy the equation

$$0 = \mu \frac{\mathrm{d}V}{\mathrm{d}\mu} = \mu\hbar \frac{\partial V^{(1)}}{\partial \mu} + \hbar\beta^{(1)} \frac{\partial V^{(0)}}{\partial \lambda} + \mathcal{O}(\hbar^2) \ , \tag{56}$$

which is referred to as the renormalisation group (RG) equation for the effective potential. From eqs. (51) and (53), it is straightforward to verify that eq. (56) indeed holds. This implies that eq. (51) may be regarded as a perturbative solution of the RG equation (56) and, thus, λ in eq. (51) should be interpreted as $\lambda(\mu)$. Moreover, from eqs. (54) and (55), we see that

$$V^{(0)}(\lambda(\mu^2 = 3\lambda_0\phi^2), \phi) = \frac{\lambda(\mu^2 = 3\lambda_0\phi^2)}{4}\phi^4 = \frac{1}{4}\frac{\lambda_0\phi^4}{1 - \frac{9\hbar\lambda_0}{16\pi^2}\log\frac{3\lambda_0\phi^2}{\mu_0^2}} \ , \tag{57}$$

i.e., the tree-level form evaluated at the mass-squared $\mu^2 = 3\lambda_0\phi^2$ corresponds to a re-summation of all leading logarithms at the mass μ_0. This statement can be recast into a double interpretation of eq. (57). On the left hand side, it is the lowest order effective potential at the mass-squared $\mu^2 = 3\lambda_0\phi^2$. On the right hand side, it is the potential at the mass μ_0 for which terms of all orders in $\hbar$ have been included. For this reason, eq. (57) is frequently referred to as the one-loop RG-improved potential. The one-loop form $V^{(1)}$ evaluated at $\mu^2 = 3\lambda_0\phi^2$ will contain the re-summation of subleading logarithms. In general, one may define terms of the kind

$$\lambda^{n+k+1}\hbar^{n+k}\left[\log\frac{3\lambda\phi^2}{\mu^2}\right]^k \ , \ k = 0, 1, 2, \dots \ , \tag{58}$$

to be of n-th-to-leading logarithmic order. From the re-summation of leading logarithms in eq. (55), we expect that the stability of the tree-level form implies the stability of the full effective potential. In what follows, we will argue that this is indeed the case. In the next chapter, we will analyse the RG-improvement of effective potentials in more detail and prove this result.

It is also possible to define a choice for the subtraction mass implicitly. For example, the logarithm in eq. (38) may be removed by evaluating the effective potential at the mass $\mu^2 = 3\lambda(\mu)\phi^2$, which yields

$$V = \frac{1}{4}\lambda(\mu)\phi^4 - \hbar\frac{27\lambda^2(\mu)\phi^4}{128\pi^2} + \mathcal{O}(\hbar^2) \ . \tag{59}$$

When evaluated at this mass, the effective potential contains no logarithmic terms. From eq (55), it is clear that this choice is related to the previous one,

$$\mu = 3\lambda(\mu)\phi^2 = 3\lambda_0\phi^2 + \mathcal{O}(\hbar) \ , \tag{60}$$

and re-sums the leading logarithms evaluated at the mass μ_0.

We will be interested in the stability of the effective potential. It is generally more convenient to analyse the stability of the tree-level term than that of a given loop-order approximation. Loop corrections introduce new terms, most importantly logarithms, which will affect the stability of the potential. It is therefore of practical interest to evaluate the effective potential at a subtraction mass for which loop corrections vanish and the effective potential has the tree-level form. In massless ϕ^4-theory at one-loop level, such a choice corresponds to

$$\mu_*^2 = 3\lambda(\mu_*)\phi^2 \exp\left(-\frac{3}{2}\right) , \tag{61}$$

at which the one-loop approximation reads

$$V = \frac{1}{4}\lambda(\mu_*)\phi^4 + \mathcal{O}(\hbar^2) . \tag{62}$$

This potential will be bounded from below if $\lambda(\mu_*) > 0$ for large values of the field. Since the effective potential cannot depend on the choice of μ, we then conclude that a sufficient condition for the potential to be bounded from below in massless ϕ^4-theory is

$$\lim_{\phi\to\infty} \lambda(\mu_*) > 0 . \tag{63}$$

In the literature, the stability of the tree-level form is sometimes taken be to a sufficient indicator of the stability of the effective potential without justification. As we commented, it is an expected result from the leading-logarithm re-summation and, indeed, for the simple one-loop approximation (51), the stability of the effective potential can be directly verified. However, we will prove in the next chapter that there always exists a choice of μ for which the one-loop effective potential can be written as the tree-level form.

In this way, we see that, for a general model with an arbitrary number of scalar fields, one can verify whether or not the one-loop approximation of the effective potential will be bounded from below by analysing the stability of the tree-level potential at the mass μ_*, with one-loop running parameters. In appendix B, we will go further and prove that it is always possible to choose μ such that the full effective potential (to all loop orders) can be written as the tree-level form.

Furthermore, it is clear that choice (61) will also re-sum leading logarithms at the mass μ_0, for it differs from eq. (60) by a multiplicative constant. At the mass given by eq. (61), the logarithmic term reads

$$\log\frac{3\lambda(\mu_*)\phi^2}{\mu_*^2} = \frac{3}{2} .$$

In this way, if $\frac{3}{2}\lambda(\mu_*) \leq 4\pi$, the $\mathcal{O}(\hbar^2)$ terms in eq. (62) contain no large logarithms.

2.1.2 Radiative Extrema

The stationary points of eq. (51), up to $\mathcal{O}(\hbar^2)$ terms, are solutions of the equation

$$0 = \phi^3\left\{\lambda + \frac{9\hbar\lambda^2}{16\pi^2}\left(\log\frac{3\lambda\phi^2}{\mu^2} - 1\right)\right\} .$$

In this way, non-trivial extrema are given by

$$\hbar\lambda\log\frac{3\lambda\phi^2}{\mu^2} = -\frac{16\pi^2}{9} + \hbar\lambda . \tag{64}$$

We note that eq. (64) can only be satisfied if either the coupling is large or the logarithm is large. This implies that non-trivial extrema are located outside the range of validity of the one-loop approximation, as S. Coleman and E. Weinberg first noticed in [3]. To overcome this limitation, we may RG-improve the effective potential.

The leading logarithms are re-summed into the tree-level form (57). This result was obtained in [3, 36, 42, 46]. As we noted above, a related RG improvement may be obtained by choosing $\mu = \mu_*$ as in eq. (61), which can be approximated by

$$\mu_* = 3\lambda(\mu_*)\phi^2 \exp\left(-\frac{3}{2}\right) = 3\lambda_0\phi^2 \exp\left(-\frac{3}{2}\right) + \mathcal{O}(\hbar) \, .$$

The improved potential in eq. (62) is then approximated by

$$V^{(0)}(\lambda(\mu_*), \phi) = \frac{1}{4} \frac{\lambda_0}{1 - \frac{9\hbar\lambda_0}{16\pi^2}\left(\log\frac{3\lambda_0\phi^2}{\mu_0^2} - \frac{3}{2}\right)} \phi^4 \, . \tag{65}$$

Both eqs. (57) and (65) represent improvements of the one-loop effective potential in the sense that higher orders in λ_0 (formally higher orders in $\hbar$) are included as a result of integrating the one-loop β-function. Evidently, one can obtain better approximations of the full effective potential if knowledge of the RG functions up to higher loop-orders is available.

Moreover, as we noted above, the running coupling $\lambda(\mu)$ is small for a large range of values of the logarithm $\log\frac{\mu}{\mu_0}$, which alleviates the constraint on the size of the logarithmic contribution. The stationary points of the improved potential (57) or (65) are given by

$$0 = \phi^3 \left\{ \lambda(\mu) + \frac{9\lambda^2(\mu)}{32\pi^2} \right\} \, . \tag{66}$$

Therefore, we note that non-trivial extrema are determined by the running of the coupling. This is a general feature which will also be present in more complicated models. The extrema of the RG-improved potential are determined by the running of the parameters of the model.

We see that eq. (66) implies that non-trivial extrema correspond to a large running coupling

$$\lambda(\mu) = -\frac{32\pi^2}{9} \, , \tag{67}$$

which renders the RG improved potential non-perturbative as well. We thus conclude, as S. Coleman and E. Weinberg observed [3], that quantum corrections to massless ϕ^4-theory are not capable of generating non-trivial minima in the perturbative regime[†]. In appendix B, we examine the more general case of $O(N)$-symmetric ϕ^4-theory.

2.2 Scalar Quantum Electrodynamics

One of the key ideas that S. Coleman and E. Weinberg presented in [3] was that the hierarchy between different couplings plays an important role in realising the dynamical breakdown of symmetry in a perturbative regime. This is not evident in pure ϕ^4-theory, which displays a single coupling parameter. However, scalar quantum electrodynamics (scalar QED) is a simple classically conformal model in which the magnitudes of the scalar coupling and the gauge coupling can be exploited to obtain perturbative non-trivial minima.

[†]This conclusion holds up to subleading logarithmic orders.

The one-loop effective potential for scalar QED reads[‡]

$$V(\phi) = \frac{\lambda}{4}\phi^4 + \\ + \frac{\hbar\phi^4}{64\pi^2}\left(9\lambda^2 \log\frac{3\lambda\phi^2}{\mu^2} + \lambda^2\log\frac{\lambda\phi^2}{\mu^2} + \frac{3e'^4}{16}\log\frac{e'^2\phi^2}{4\mu^2} - 15\lambda^2 - \frac{5e'^4}{32}\right) , \tag{68}$$

where $\phi^2 = \phi_1^2 + \phi_2^2$, λ is the scalar-sector coupling and e' is the gauge coupling. Non-trivial and real stationary points given by[§] $\phi = \phi_1 = v \neq 0$ and $\phi_2 = 0$ impose the following constraint on the couplings.

$$-\lambda = \frac{\hbar}{16\pi^2}\left(9\lambda^2 \log\frac{3\lambda v^2}{\mu^2} + \lambda^2\log\frac{\lambda v^2}{\mu^2} + \frac{3e'^4}{16}\log\frac{e'^2 v^2}{4\mu^2} - 10\lambda^2 - \frac{e'^4}{16}\right) .$$

We can solve this equation for λ iteratively. This is equivalent to assuming $\lambda = \mathcal{O}(\hbar e'^4)$. Indeed, to lowest order in the gauge coupling, we find

$$\lambda = -\frac{\hbar e'^4}{16\pi^2}\left(\frac{3}{16}\log\frac{e'^2 v^2}{4\mu^2} - \frac{1}{16}\right) + \mathcal{O}(\hbar^2 e'^8) , \tag{69}$$

where the $\mathcal{O}(\hbar^2 e^8)$ terms are obtained by including the contributions proportional to λ^2. We can further simplify eq. (69) by choosing the subtraction mass to be the field VEV, i.e., $\mu = v$. This choice eliminates explicit factors of v in eq. (69). We obtain

$$\lambda = -\frac{\hbar e'^4}{16\pi^2}\left(\frac{3}{16}\log\frac{e'^2}{4} - \frac{1}{16}\right) + \mathcal{O}(\hbar^2 e'^8) . \tag{70}$$

We then have the effective potential

$$V(\phi) = \frac{3\hbar e'^4\phi^4}{1024\pi^2}\left(\log\frac{\phi^2}{v^2} - \frac{1}{2}\right) + \mathcal{O}(\hbar^2 e'^8) . \tag{71}$$

Some important comments about eqs. (69), (70) and (71) are in order. First and foremost, eq. (70) guarantees that the stationary-point equations are satisfied in a perturbative regime. Indeed, if the gauge coupling is sufficiently small, then λ is also a small parameter and no large logarithms are present, since the logarithmic term in eq. (71) vanishes at $\phi = v$. Secondly, having $\lambda = \mathcal{O}(\hbar e'^4)$ renders the tree-level potential of the same order as the one-loop contribution, since both are now of order $\hbar e'^4$. This does not invalidate perturbation theory, it merely reorganises it. The potential (71) should be viewed as the leading order term, while contributions of higher loops or, more generally, of order $\hbar^2 e'^8$ contain the subleading terms. In particular, the other logarithms present in eq. (68) are now subleading and small. Indeed, if e' is such that $e' \ll 1$, then $e'^4 \log e'^2 \ll 1$ and the subleading logarithms are at most of order

$$e'^8\left(\log e'^2\right)^2 \ll e'^4 \log e'^2 \ll 1 ,$$

so the remaining logarithms in eq. (68) are small.

[‡]The one-loop potential (68) can be obtained straightforwardly with the method presented in section (1.2). We omit the details for the case of scalar QED, since we will give a detailed derivation of the one-loop effective potential of the Conformal Standard Model in Chapter 4.

[§]This is, in fact, a gauge choice.

We then find the second derivative

$$m_\phi^2 \equiv \left.\frac{\mathrm{d}^2 V}{\mathrm{d}\phi^2}\right|_{\phi=v} = \frac{3\hbar e'^4}{128\pi^2} v^2 > 0 \tag{72}$$

which signals that radiative symmetry breaking occurs and there is a non-trivial minimum at $\phi = v$. This result is correct up to order $\hbar^2 e'^8$. The vector boson acquires a mass given by

$$m_V^2 = \frac{e'^2}{4} v^2 \,,$$

such that we find the ratio

$$\frac{m_\phi^2}{m_V^2} = \frac{3\hbar e'^2}{32\pi^2} \,, \tag{73}$$

as was computed in [3]. We expect that this perturbative calculation reproduces a local minimum of the effective potential reliably, even though it will cease to be valid near the origin of the scalar-field configuration space or for very large fields, where logarithmic terms are large. To probe the potential at all scales with a limited knowledge of the loop expansion, one needs RG improvement. The improvement of scalar QED was studied by S. Coleman and E. Weinberg in [3], where they concluded that indeed the minimum found above is reliable. We will analyse a similar, yet more complicated, case in the Chapter 4.

2.3 Flat Directions

Some years after S. Coleman and E. Weinberg published their seminal paper [3], E. Gildener and S. Weinberg published a complementary work contemplating the case in which several scalar fields are present, as opposed to the single scalar in ϕ^4-theory and scalar QED. Here we will briefly review and comment on their results.

In the previous section, we concluded that radiative symmetry breaking occurs in scalar QED as long as the one-loop contribution in the effective potential was of the same order of the tree-level term, i.e., both are of order $\hbar e'^4$ at the scale of the minimum $\phi = v$. However, we can easily imagine scenarios where this is not realised, as we will analyse below.

Let us consider a classically conformal model with N_ϕ scalar fields, N_λ coupling parameters and N_m mass logarithms, where the tree-level term is of lower order than the one-loop term. In this case, any correction to the tree-level stationary point will be formally of order $\hbar$. We write the tree-level as

$$V^{(0)} = \frac{1}{4} \sum_{ijkl} \lambda_{ijkl} \phi_i \phi_j \phi_k \phi_l \,, \tag{74}$$

where the coupling parameters have been collected in the symmetric symbol λ_{ijkl}. The one-loop contribution is given by eq. (48). Let us denote the tree-level minimum by $v^{(0)}$ and the one-loop VEV correction by $v^{(1)}$. We can then formally expand the stationary point equation in powers of $\hbar$ to obtain

$$\begin{aligned} 0 = \left.\frac{\partial}{\partial\phi_i}\left(V^{(0)} + \hbar V^{(1)}\right)\right|_{\phi=v^{(0)}+\hbar v^{(1)}} = \\ = \left.\frac{\partial V^{(0)}}{\partial\phi_i}\right|_{\phi=v^{(0)}} + \sum_j \left.\frac{\partial^2 V^{(0)}}{\partial\phi_i\partial\phi_j}\right|_{\phi=v^{(0)}} \hbar v_j^{(1)} + \hbar \left.\frac{\partial V^{(1)}}{\partial\phi_i}\right|_{\phi=v^{(0)}} + \mathcal{O}(\hbar^2) = \end{aligned}$$

$$= \sum_j \frac{\partial^2 V^{(0)}}{\partial\phi_i \partial\phi_j}\bigg|_{\phi=v^{(0)}} \hbar v_j^{(1)} + \hbar \left.\frac{\partial V^{(1)}}{\partial\phi_i}\right|_{\phi=v^{(0)}} + \mathcal{O}(\hbar^2) \,. \tag{75}$$

If $v^{(0)} = 0$, this equation is trivially satisfied, since the first and second derivatives of $V^{(0)}$ and the first derivative of $V^{(1)}$ vanish at the origin of the scalar-field configuration space. Let us then assume the tree-level potential exhibits a non-trivial minimum, i.e.,

$$\begin{aligned} \left.\frac{\partial V^{(0)}}{\partial\phi_i}\right|_{\phi=v^{(0)}} &= \sum_{jkl} \lambda_{ijkl} v_j^{(0)} v_k^{(0)} v_l^{(0)} = 0 \,, \\ V^{(0)}(\mu;\lambda,v^{(0)}) &= \frac{1}{4}\sum_i v_i^{(0)} \sum_{jkl} \lambda_{ijkl} v_j^{(0)} v_k^{(0)} v_l^{(0)} = 0 \,. \end{aligned} \tag{76}$$

Evidently, the condition (76) will not be satisfied for arbitrary values of the couplings, i.e., it is a constraint on the coupling parameters of the model, which must be satisfied for the choice of subtraction mass at which the effective potential is computed. Thus, we assume that there exists a choice $\mu = \mu_{\text{GW}}$ for which eq. (76) is satisfied and we compute the effective potential at this mass. Moreover, eq. (76) is satisfied for any value of the radial variable in the scalar-field configuration space,

$$\begin{aligned} &\varphi^2 := \sum_i \left(v_i^{(0)}\right)^2 \,,\; N_i := \frac{v_i^{(0)}}{\varphi} \\ &\Rightarrow \sum_{jkl} \lambda_{ijkl} N_j N_k N_l = 0 \,, \end{aligned}$$

i.e., a non-trivial tree-level minimum corresponds to a flat direction of the tree-level potential in classically conformal models. Only the angles N can be determined, while the radius φ remains undetermined at lowest order. We see that eq. (75) leads to

$$\begin{aligned} 0 &= 3\sum_{jkl} \lambda_{ijkl} v_k^{(0)} v_l^{(0)} v_j^{(1)} + \left.\frac{\partial V^{(1)}}{\partial\phi_i}\right|_{\phi=v^{(0)}} \,, \\ 0 &= 3\sum_{ijkl} \lambda_{ijkl} N_i v_k^{(0)} v_l^{(0)} v_j^{(1)} + \sum_i N_i \left.\frac{\partial V^{(1)}}{\partial\phi_i}\right|_{\phi=N\varphi} = \\ &= 0 + \frac{\partial V^{(1)}}{\partial\varphi} \,, \end{aligned}$$

i.e., we can determine the lowest order radial coordinate of the VEV by the stationary point condition on the one-loop term

$$\frac{\partial V^{(1)}}{\partial\varphi} = 0 \,. \tag{77}$$

Once φ is determined, one can use eq. (75) again to determine $v^{(1)}$. We will, however, be mostly interested in the lowest order VEV. Using eq. (48), we write $V^{(1)}$ along the flat direction as

$$V^{(1)}(\mu_{\text{GW}};\lambda,\varphi) = \mathbb{A}(N,\lambda)\varphi^4 + \mathbb{B}(N,\lambda)\varphi^4 \log\frac{\varphi^2}{\mu_{\text{GW}}^2} \,. \tag{78}$$

From eq. (77), we find

$$\log\frac{\varphi^2}{\mu_{\text{GW}}^2} = -\frac{1}{2} - \frac{\mathbb{A}}{\mathbb{B}} \,. \tag{79}$$

From this result, we conclude that the one-loop approximation of the effective potential will exhibit no large logarithms along the flat direction if $\mathbb{A}$ and $\mathbb{B}$ are of the same order. In a theory with gauge couplings, this can be achieved by assuming the scalar-sector couplings are all of order $\mathbf{g}^2$, where $\mathbf{g}$ is a typical gauge coupling, for in this case we have $\mathbb{A} \sim \mathbb{B} \sim \mathcal{O}(\mathbf{g}^4)$. In the case of large logarithms, RG improvement has to be employed.

Using eq. (79), we find that the potential up to one-loop order evaluated at the stationary point reads

$$V(\mu_{\text{GW}}; \lambda, N\varphi) = -\frac{\hbar\mathbb{B}}{2}\varphi^4 \,.$$

Therefore, we must have $\mathbb{B} > 0$ along the flat direction in order to obtain a radiative minimum. Indeed, in a similar fashion to eq. (75), we obtain

$$\begin{aligned} \left.\frac{\partial^2 V}{\partial\phi_i\partial\phi_j}\right|_{v^{(0)}+\hbar v^{(1)}} &= 3\varphi^2 \sum_{kl} \lambda_{ijkl} N_k N_l + 6\hbar\varphi \sum_{kl} \lambda_{ijkl} N_k v_l^{(1)} + \hbar \left.\frac{\partial^2 V^{(1)}}{\partial\phi_i\partial\phi_j}\right|_{v^{(0)}} \\ \Rightarrow \sum_{ij} N_i N_j \left.\frac{\partial^2 V}{\partial\phi_i\partial\phi_j}\right|_{v^{(0)}+\hbar v^{(1)}} &= \hbar\frac{\partial^2 V^{(1)}}{\partial\varphi^2} = 8\hbar\mathbb{B}\varphi^2 \,, \end{aligned} \tag{80}$$

i.e., we obtain a minimum along the flat direction if $\mathbb{B} > 0$.

2.4 A Panoramic View of the Dynamical Breakdown of Symmetry

From the above analysis of radiative symmetry breaking in classically conformal models, we identify the following important cases in which radiative extrema can be found.

- **Case I**: $V^{(0)} > V^{(1)}$, the Gildener-Weinberg case.
  The first case corresponds to the scenario in which the tree-level term is of lower order than the one-loop correction. Since quantum corrections are small compared to the classical level, a radiative minimum can only be generated if the tree-level term exhibits a flat direction, which can be slightly deformed by the one-loop contribution. This was studied by E. Gildener and S.Weinberg in [5] and holds for an arbitrary number of scalar fields.

  The caveat is in the flat-direction constraint (76), for it is necessarily an assumption (albeit not a strong one) that the Gildener-Weinberg mass μ_{GW} exists for a given model. This constraint is related to the stability of the tree-level potential. Indeed, for classically conformal models at tree level, boundedness from below is typically expressed as a constraint on the couplings [28]. If we assume that the tree-level potential in eq. (74) exhibits Z_2 symmetry besides conformal symmetry, we can write it as

  $$V^{(0)} = \frac{1}{4}\sum_{ijkl} \lambda_{ijkl}\phi_i\phi_j\phi_k\phi_l \equiv \frac{1}{4}\sum_{a,b=1}^{N_\phi} \tilde{\lambda}_{ab}\phi_a^2\phi_b^2 \,.$$

  This form makes the invariance of the potential under $\phi_a \to -\phi_a$ explicit. The tree-level potential will be bounded from below if the coupling matrix $\tilde{\lambda}$ satisfies

  $$\eta^T\tilde{\lambda}\eta = \sum_{a,b} \tilde{\lambda}_{ab}\eta_a\eta_b > 0 \,, \tag{81}$$

where η is a vector with non-negative components in the basis $(\phi_1^2, ..., \phi_{N_\phi}^2)$. A matrix $\tilde{\lambda}$ which satisfies eq. (81) is called copositive [50]. Schematically, we can write the stability conditions of the tree-level potential as follows,

$$\eta^T \tilde{\lambda} \eta < 0 \Rightarrow \text{unbounded from below} ,$$
$$\eta^T \tilde{\lambda} \eta = 0 \Rightarrow \text{flat direction} ,$$
$$\eta^T \tilde{\lambda} \eta > 0 \Rightarrow \text{bounded from below} .$$

Concerning a hierarchy of the coupling parameters, as E. Gildener and S. Weinberg considered, Case I will be free of large logarithms at the mass μ_{GW} if, for example, the scalar-sector couplings are all of order $\mathbf{g}^2$, where $\mathbf{g}$ is a typical gauge coupling. The one-loop term will then be of order $\mathbf{g}^4$. Let us define $\lambda_{\max} := \mathbf{g}^2$. We can then say, more generally, that Case I can be identified with the case in which the tree-level is effectively of order $\lambda_{\max}$, while the one-loop term is of order $\hbar\lambda_{\max}^2$, when the potential is evaluated at a stationary point.

- **Case II**: $V^{(0)} \lesssim V^{(1)}$, the Coleman-Weinberg case.
  Although the loop expansion of the effective potential must converge, it is conceivable that the one-loop term is of the order of the tree-level potential. This was the case studied by S. Coleman and E. Weinberg in [3]. Intuitively, it corresponds to the expectation that quantum corrections need to be as large as the classical potential to produce a (global) minimum. As the example of scalar QED made clear, this corresponds to a hierarchy of the coupling parameters, in which the scalar-sector couplings are of order $\mathbf{g}^4$, where $\mathbf{g}$ is a typical gauge coupling. More generally, Case II can be identified with the case in which both the tree-level and the one-loop terms are effectively of order $\hbar\lambda_{\max}^2$, when the potential is evaluated at an extremum[¶].

- **RG Improvement**: Re-summation, stability.
  We will analyse different methods of RG-improving the effective potential in the next chapter. In particular, we will see that it is always possible to choose the subtraction mass such that the full effective potential has the tree-level form, as we also commented in section (2.1.1). In this way, the (RG-improved) potential will be bounded from below if the running coupling matrix is copositive in the large-field limit.

  As we will see in concrete examples in the following chapters, it is not necessary to resum all leading logarithms, for one can always consider a model in Case I or II, in which large logarithms are avoided near the radiative minimum and only appear near the origin and near infinity. RG-improvement can be performed in the hypersurface of vanishing quantum corrections (see Chapter 3), up to subleading logarithmic errors, as long as the running couplings of the model remain small over a large range of scales. In this way, we can study the effective potential for a large range of field values, incorporating contributions that are formally of all loop-orders.

In Chapters 4, 5 and 6, we will apply Cases I or II and RG-improvement to study classically conformal extensions of the Standard Model.

[¶]In this way, the expansion is powers of $\lambda_{\max}$ does not need to coincide with the loop expansion in powers of $\hbar$, since both the tree-level and the one-loop terms could be of the same order in $\lambda_{\max}$.

Chapter 3

Renormalisation Group Improvement of Effective Potentials

In this chapter, we will use the renormalisation group (RG) to improve the one-loop approximation of the effective potential, i.e., to re-sum contributions from higher loop-orders. This was first done by S. Coleman and E. Weinberg in the case of a single massless scalar field [3]. B. Kastening extended the method to the massive case [36]. In both cases, knowledge of the RG functions to one-loop order is sufficient to re-sum the highest powers of logarithmic terms (referred to as leading logarithms) to a closed-form expression.

When more scalar fields are present or, more precisely, different mass eigenvalues are featured in the effective potential, it is necessary to employ multi-scale techniques to re-sum all of the leading logarithms [42, 35, 43, 44, 48]. These techniques introduce several subtraction masses instead of a single μ, and are also related to the use of the decoupling theorem in mass-independent renormalisation schemes [41, 45].

We will be interested in practical alternatives to multi-scale methods to analyse the effective potential across a large range of scales when an arbitrary number of scalar fields are present. For convenience, we focus on the one-loop improvement of a general theory. We will prove that the one-loop effective potential can be written as the tree-level form for a specific choice of the subtraction mass. As we will see, this corresponds to a re-summation of the leading contributions from higher-loop orders and does not require multi-scale techniques. The method presented in this chapter will be generalised to an arbitrary number of loops in appendix B, where we show that the full effective potential (to all loop-orders) can be written as the tree-level form.

Fixing the Notation

We consider a theory with N_ϕ scalar fields and N_λ couplings in addition to vector and fermionic fields. We denote the couplings (possibly including mass terms) by $\lambda = (\lambda_1, ..., \lambda_{N_\lambda})$ and the classical scalar fields by $\phi = (\phi_1, ..., \phi_{N_\phi})$. There will be N_m field-dependent mass eigenvalues, denoted by $m = (m_1, ..., m_{N_m})$. Note that each eigenvalue is a function of the couplings as well as the fields.

We will also denote the effective potential by $V(\mu; \lambda, \phi)$, making its dependence on the couplings explicit. As we will see, the full effective potential cannot depend on the arbitrary subtraction mass μ. Nevertheless, its truncations to a given loop order will depend on μ. For this

reason, we choose to include μ as a separate argument of V. We will consider the effective potential $V(\mu;\lambda,\phi)$ as a function defined on a domain of the parameter space spanned by $(\mu;\lambda,\phi)$, i.e., by the subtraction mass, the couplings and scalar fields of the theory and we will keep factors of $\hbar$ explicit in this chapter.

3.1 Re-summation of Logarithmic Terms

The effective potential can be computed in perturbation theory as the loop expansion (cf.eq. (30))

$$V(\mu;\lambda,\phi)=\sum_{l=0}^{\infty}\hbar^{l}V^{(l)}(\mu,\lambda,\phi)\ , \tag{82}$$

where $V^{(l)}(\mu,\lambda,\phi)$ is the l-th loop-order contribution and, in particular, $V^{(0)}(\lambda,\phi)$ is the tree-level term. In general, the highest powers of the mass logarithms that appear in the renormalised l-th loop order term will be of the form [37, 41, 42]

$$\hbar^{l}\prod_{a=1}^{N_m}\left(\log\frac{m_a^2(\lambda,\phi)}{\mu^2}\right)^{n_a}\ ,\ \sum_{a=1}^{N_m}n_a=l\ ,\ n_a=0,1,...\ , \tag{83}$$

and are referred to as the leading logarithms of the theory. The appearance of explicit logarithmic terms can jeopardise the validity of perturbation theory if the mass logarithms are large. In particular, this implies that for large field values, which will generally yield large logarithms, the loop expansion is not reliable. If one is interested in the large field behaviour of the effective potential, e.g., to study the vacuum stability of a given model, then one needs to enlarge the region of parameter space for which perturbation theory holds.

In the one-field case ($N_\phi=N_m=1$), this is accomplished by re-summing the (sub)leading logarithms by choosing μ to be the only mass eigenvalue, as was done in eq. (59). When $N_\phi>1$, it is not possible to suppress all logarithms individually, since there is only one subtraction mass. For this reason, one needs to employ multi-scale techniques in order to re-sum the leading logarithms, as they are defined in eq. (83), with correct coefficients. These techniques employ several arbitrary subtraction masses. Work in this direction was initiated in [35] and later pursued in [42, 43, 44, 48].

In this chapter, we will develop an alternative way of re-summing logarithms in the effective potential. To achieve this, we begin by noting that we can express the potential as an expansion in powers of a pivot logarithm, as was done in [37, 42]. Such an expansion is very instructive because it allows us to collect all the explicit dependence on the subtraction mass in only one term. To achieve this, we use eq. (47) and we define $\log\frac{\mathcal{M}^2}{\mu^2}$ to be the pivot logarithm. Inserting eq. (47) into eq. (82) leads to the series

$$V(\mu,\lambda,\phi)=\sum_{l=0}^{\infty}\hbar^{l}\sum_{n=0}^{l}w_n^{(l)}(\lambda,\phi)\left[\log\frac{\mathcal{M}^2}{\mu^2}\right]^{n}\ , \tag{84}$$

where $w_n^{(l)}(\lambda,\phi)$ may include logarithms of the ratios $\frac{\phi}{\mathcal{M}}$, which correspond to the angular variables if $\mathcal{M}$ is chosen to be the radius. Furthermore, we have $\mathbb{A}\mathcal{M}^4=w_0^{(1)}$ and $\mathbb{B}\mathcal{M}^4=w_1^{(1)}$ in eq. (48).

The expansion in powers of a pivot logarithm was used in [37]. It is best suited when the pivot logarithm is the dominant one, i.e., when logarithms of the ratios $\frac{\phi}{\mathcal{M}}$ are subleading and

we have the relation

$$\left|\log\frac{\mathcal{M}^2}{\mu^2}\right| \gg \max_a\left\{\left|\log\frac{m_a^2}{\mathcal{M}^2}\right|\right\} . \tag{85}$$

For example, this can be achieved in a region of parameter space where the subtraction mass is at most the smallest mass parameter, $\mu \leq \min_a\{m_a(\lambda,\phi)\}$, and the pivot mass is at least the largest mass parameter, $\mathcal{M} \geq \max_a\{m_a(\lambda,\phi)\}$ or in the converse case. In particular, when $\left|\log\frac{\mathcal{M}^2}{\mu^2}\right| \gg \max_a\left\{\left|\log\frac{m_a^2}{\mathcal{M}^2}\right|\right\}$, we see from eq. (47) that all logarithms are approximately equal and we recover the one-field case. A concrete example of this situation is obtained by defining the pivot mass to be the radius in the scalar-field configuration space and taking the large-field limit, i.e., $\mathcal{M} = \rho \to \infty$ at fixed values of the ratios (angles) $\frac{\phi}{\rho}$. In in this limit, all logarithms are equal to the radial logarithm. For very large values of the fields along a particular direction in parameter space, we thus conclude that the angular logarithms are subleading, as expected. Both re-summations in leading logarithms and in the leading powers of the pivot logarithm will yield the same result if all the mass eigenvalues are degenerate ($N_m = 1$). If they are not, the re-summation in leading powers of the pivot logarithm will only be reliable when condition (85) is satisfied. In the next sections, we will see how to overcome this limitation.

We may change the summation variables in eq. (84) to obtain

$$\begin{aligned} V(\mu,\lambda,\phi) &= \sum_{l=0}^{\infty}\hbar^l\sum_{n=0}^{l} w_n^{(l)}(\lambda,\phi)\left[\log\frac{\mathcal{M}^2}{\mu^2}\right]^n = \\ &= \sum_{l=0}^{\infty}\sum_{n=0}^{\infty}\hbar^{l+n} w_n^{(l+n)}(\lambda,\phi)\left[\log\frac{\mathcal{M}^2}{\mu^2}\right]^n = \\ &=: \sum_{l=0}^{\infty}\hbar^l f_l(\hbar;\mu,\lambda,\phi) , \end{aligned}$$

where we defined the functions

$$f_l(\hbar;\mu,\lambda,\phi) = \sum_{n=0}^{\infty}\hbar^n w_n^{(n+l)}(\lambda,\phi)\left[\log\frac{\mathcal{M}^2}{\mu^2}\right]^n , \tag{86}$$

which will be referred to as the l-th-to-leading functions. It is also convenient to define

$$w_n(\lambda,\phi) = \sum_{k=n}^{\infty}\hbar^k w_n^{(k)}(\lambda,\phi) = \mathcal{O}(\hbar^n) , \tag{87}$$

such that the potential can be written as

$$V(\mu,\lambda,\phi) = \sum_{n=0}^{\infty} w_n(\lambda,\phi)\left[\log\frac{\mathcal{M}^2}{\mu^2}\right]^n . \tag{88}$$

From the above considerations, we see that a practical alternative to the re-summation of the l-th-to-leading logarithms is to work with the pivot logarithm, if it is the dominant one, and to re-sum the l-th-to-leading functions of eq. (86). This amounts to changing the set of relevant logarithms,

$$\mathbb{S}_1 = \left\{\log\frac{m_a^2}{\mu^2},\ a=1,...,N_m\right\} \leftrightarrow \mathbb{S}_2 = \left\{\log\frac{\mathcal{M}^2}{\mu^2}\ ,\ \log\frac{m_a^2}{\mathcal{M}^2},\ a=1,...,N_m\right\} . \tag{89}$$

If one chooses to work with the set $\mathbb{S}_1$, multi-scale techniques are needed to re-sum all the logarithms with correct coefficients. On the other hand, if the pivot logarithm is the dominant one, we can work with the set $\mathbb{S}_2$ and use a single subtraction mass to re-sum the logarithms to a closed-form expression, which, when expanded in powers of the pivot logarithm, reproduces the correct coefficients of the elements of the set $\mathbb{S}_2$ in the effective potential. We will prove this is true to leading order in the next section, whereas the general case is left for appendix B.

Evidently, the field-dependent mass eigenvalues will vary for different regions of parameter space. Thus, one would have, in principle, to make different choices of the pivot mass $\mathcal{M}$ for different domains, such that eq. (85) is satisfied. In section (3.2.1), we will not address this issue. This difficulty will then be overcome in section (3.2.2), in which we will also prove that it is possible to write the effective potential as the tree-level form, i.e., there exists a scale at which quantum corrections vanish. In appendix B, we prove that this scale can be determined in perturbation theory, without resorting to multi-scale techniques.

3.2 RG Improvement

When one computes the renormalised effective action, inevitably a spurious mass is introduced, since the loop corrections will in general depend explicitly on the subtraction mass μ, which is also referred to as the renormalisation mass scale. Changes in this renormalisation scale are accompanied by changes in the parameters of the theory, which are encoded by the standard renormalisation group equations

$$\begin{aligned}\beta_i \equiv \beta_i(\lambda) &= \mu\frac{\mathrm{d}}{\mathrm{d}\mu}\lambda_i(\mu) = \sum_{l=1}^{\infty}\hbar^l\beta_i^{(l)}\,,\\ \gamma_a \equiv \gamma_a(\lambda) &= \mu\frac{\mathrm{d}}{\mathrm{d}\mu}\log Z_a(\mu) = \sum_{l=1}^{\infty}\hbar^l\gamma_a^{(l)}\,,\end{aligned} \tag{90}$$

where $i = 1, ..., N_\lambda,\ a = 1, ..., N_\phi$ and Z_a is the normalisation of the field ϕ_a. The above derivatives are referred to as β-functions and anomalous dimensions, respectively. Given the anomalous dimensions, one can compute the β-functions in perturbation theory from the loop expansion of the effective potential. Examples will be given in the following chapters.

Since the physical content of the theory must be independent of the choice of μ, it follows that the effective action cannot depend on the subtraction mass. This statement is translated into a RG equation for the effective action

$$\mu\frac{\mathrm{d}}{\mathrm{d}\mu}\Gamma[\phi] = \left(\mu\frac{\partial}{\partial\mu} + \sum_{i=1}^{N_\lambda}\beta_i\frac{\partial}{\partial\lambda_i} - \frac{1}{2}\sum_{a=1}^{N_\phi}\gamma_a\int \mathrm{d}^4x\ \phi_a(x)\frac{\delta}{\delta\phi_a(x)}\right)\Gamma[\phi] = 0\,. \tag{91}$$

The effective potential inherits its own RG equation from eq. (91), given by

$$\mu\frac{\mathrm{d}V}{\mathrm{d}\mu} \equiv \left(\mu\frac{\partial}{\partial\mu} + \sum_{i=1}^{N_\lambda}\beta_i\frac{\partial}{\partial\lambda_i} - \frac{1}{2}\sum_{a=1}^{N_\phi}\gamma_a\phi_a\frac{\partial}{\partial\phi_a}\right)V(\mu;\lambda,\phi) = \left(\mu\frac{\partial}{\partial\mu} + \sum_{i=1}^{N_\lambda}\beta_i\frac{\partial}{\partial\lambda_i}\right)V(\mu;\lambda,0)\,.$$

Note that the left hand side of the above equation is only zero if the vacuum energy $V(\mu;\lambda,0)$ is scale invariant*. It is always possible to make a field-independent shift to the potential such

*This was not taken into account in eq. (56) because the vacuum energy was set to zero in massless ϕ^4-theory.

that the scale dependence of the vacuum energy is cancelled [39, 42]. We define

$$\begin{aligned}\tilde{V}(\mu;\lambda,\phi) &:= V(\mu;\lambda,\phi) + \delta\Lambda(\mu,\lambda)\,,\\ \Lambda(\mu,\lambda) &:= V(\mu;\lambda,0) + \delta\Lambda(\mu,\lambda)\,,\end{aligned} \tag{92}$$

and demand

$$\left(\mu\frac{\partial}{\partial\mu} + \sum_{i=1}^{N_\lambda}\beta_i\frac{\partial}{\partial\lambda_i}\right)\Lambda(\mu,\lambda) = 0\,.$$

In this way, the potential $\tilde{V}(\mu;\lambda,\phi)$ satisfies the equation

$$\mu\frac{\mathrm{d}\tilde{V}}{\mathrm{d}\mu}(\mu;\lambda,\phi) = \left(\mu\frac{\partial}{\partial\mu} + \sum_{i=1}^{N_\lambda}\beta_i\frac{\partial}{\partial\lambda_i} - \frac{1}{2}\sum_{a=1}^{N_\phi}\gamma_a\phi_a\frac{\partial}{\partial\phi_a}\right)\tilde{V}(\mu;\lambda,\phi) = 0\,, \tag{93}$$

which can be interpret as a partial differential equation on a domain of the parameter space spanned by $(\mu;\lambda,\phi)$. In what follows, it will be useful to define the l-th loop-order derivative as

$$\mathrm{d}^{(l)} := \sum_{i=1}^{N_\lambda}\beta_i^{(l)}\frac{\partial}{\partial\lambda_i} - \frac{1}{2}\sum_{a=1}^{N_\phi}\gamma_a^{(l)}\phi_a\frac{\partial}{\partial\phi_a}\,. \tag{94}$$

3.2.1 Pivot Logarithm

Following eqs. (86) and (88), we may write the potential $\tilde{V}(\mu;\lambda,\phi)$ as

$$\begin{aligned}\tilde{V}(\mu;\lambda,\phi) &= \sum_{n=0}^{\infty}\tilde{w}_n(\lambda,\phi)\left[\log\frac{\mathcal{M}^2}{\mu^2}\right]^n = \sum_{n=0}^{\infty}\sum_{k=0}^{\infty}\hbar^{k+n}\tilde{w}_n^{(k+n)}(\lambda,\phi)\left[\log\frac{\mathcal{M}^2}{\mu^2}\right]^n = \\ &= \sum_{k=0}^{\infty}\hbar^k f_k(\hbar;\mu,\lambda,\phi)\,, \\ f_k(\hbar;\mu,\lambda,\phi) &= \sum_{n=0}^{\infty}\hbar^n\tilde{w}_n^{(n+k)}(\lambda,\phi)\left[\log\frac{\mathcal{M}^2}{\mu^2}\right]^n\,.\end{aligned} \tag{95}$$

The derivatives of the coefficients $\tilde{w}_n$ can also be treated in perturbation theory (cf.eq. (94)).

$$\begin{aligned}\mu\frac{\mathrm{d}}{\mathrm{d}\mu}\tilde{w}_n(\lambda,\phi) &\equiv \sum_{l=1}^{\infty}\hbar^l\left(\sum_{i=1}^{N_\lambda}\beta_i^{(l)}\frac{\partial}{\partial\lambda_i} - \frac{1}{2}\sum_{a=1}^{N_\phi}\gamma_a^{(l)}\phi_a\frac{\partial}{\partial\phi_a}\right)\tilde{w}_n(\lambda,\phi) \equiv \\ &\equiv \sum_{l=1}^{\infty}\hbar^l\mathrm{d}^{(l)}\tilde{w}_n(\lambda,\phi)\,.\end{aligned} \tag{96}$$

Inserting eqs. (90), (95) and (96) into eq. (93) yields

$$\sum_{s=n+1}^{\infty}\hbar^s\sum_{l=1}^{s-n}\mathrm{d}^{(l)}\tilde{w}_n^{(s-l)} = 2(n+1)\sum_{s=n+1}^{\infty}\hbar^s\tilde{w}_{n+1}^{(s)} - 2\frac{n+1}{\mathcal{M}}\sum_{s=n+2}^{\infty}\hbar^s\sum_{l=1}^{s-n-1}\tilde{w}_{n+1}^{(s-l)}\mathrm{d}^{(l)}\mathcal{M}\,,$$

which leads to the two recursive relations

$$\mathrm{d}^{(1)}\tilde{w}_n^{(n)} = 2(n+1)\tilde{w}_{n+1}^{(n+1)}\,, \tag{97}$$

$$\sum_{l=1}^{s-n} \mathrm{d}^{(l)} \tilde{w}_n^{(s-l)} = 2(n+1)\tilde{w}_{n+1}^{(s)} - 2\frac{n+1}{\mathcal{M}} \sum_{l=1}^{s-n-1} \tilde{w}_{n+1}^{(s-l)} \mathrm{d}^{(l)} \mathcal{M} \ , \ s > n+1 \ . \tag{98}$$

By solving eq. (97), we obtain the relation

$$\left[\mathrm{d}^{(1)}\right]^n \tilde{V}^{(0)} \equiv \left[\mathrm{d}^{(1)}\right]^n \tilde{w}_0^{(0)} = 2^n n! \tilde{w}_n^{(n)} \ . \tag{99}$$

The leading function in the effective potential reads

$$f_0(\hbar; \mu, \lambda, \phi) = \sum_{n=0}^{\infty} \hbar^n \tilde{w}_n^{(n)} (\lambda, \phi) \left[\log \frac{\mathcal{M}^2}{\mu^2}\right]^n \ . \tag{100}$$

We can now use eq. (99) to write eq. (100) in closed form.

$$\begin{aligned} f_0(\hbar; \mu, \lambda, \phi) &= \sum_{n=0}^{\infty} \hbar^n \frac{1}{2^n n!} \left\{ \left[\mathrm{d}^{(1)}\right]^n \tilde{V}^{(0)}(\lambda, \phi) \right\} \left[\log \frac{\mathcal{M}^2}{\mu^2}\right]^n = \\ &= \sum_{n=0}^{\infty} \left\{ \frac{1}{n!} \left[\hbar \mathrm{d}^{(1)}\right]^n \tilde{V}^{(0)}(\lambda, \phi) \right\} \left[\frac{1}{2} \log \frac{\mathcal{M}^2}{\mu^2}\right]^n = \\ &= \tilde{V}^{(0)} \left(\bar{\lambda}(t_{\mathcal{M}}), \bar{\phi}(t_{\mathcal{M}})\right) \ , \end{aligned} \tag{101}$$

where we defined the one-loop running parameters

$$\begin{aligned} &\bar{\lambda}(t) : \frac{\mathrm{d}\bar{\lambda}}{\mathrm{d}t} = \hbar \beta^{(1)}(\bar{\lambda}) \ , \ \bar{\lambda}(0) = \lambda \ , \\ &\bar{\phi}(t) : \frac{\mathrm{d}\bar{\phi}}{\mathrm{d}t} = -\frac{\hbar}{2} \gamma^{(1)}(\bar{\lambda}) \bar{\phi} \ , \ \bar{\phi}(0) = \phi \ , \\ &t_{\mathcal{M}} := \frac{1}{2} \log \frac{\mathcal{M}^2}{\mu^2} \ . \end{aligned} \tag{102}$$

Thus, we can RG-improve the effective potential by re-summing the leading powers of the pivot logarithm into a closed-form expression which is the tree-level term evaluated at the point $\left(\bar{\lambda}(t_{\mathcal{M}}), \bar{\phi}(t_{\mathcal{M}})\right)$. Re-summation of subleading terms can be done with the aid of eq. (98). However, to find closed-form expressions for subleading terms, it is more convenient to use recursive relations for the f_k functions instead of eqs. (97) and (98), as was done in [37]. This will be reviewed in appendix B.

To see that it is not possible to re-sum all the leading logarithms with the above method, it is sufficient to note that f_0 only re-sums the highest powers of the pivot logarithm, which have the coefficients $\tilde{w}_n^{(n)}$. These coefficients do not, in general, coincide with the coefficients of the leading logarithms of eq. (83). For example, we have

$$\tilde{w}_1^{(1)} = \mathbb{B}\mathcal{M}^4 \ ,$$

which is a sum of coefficients of leading logarithms (cf. eq (49)). This remains true to higher loop-orders. A concrete example is given in appendix B. Moreover, the above results imply that, starting from the tree-level form

$$\tilde{V}^{(0)} \left(\bar{\lambda}(t), \bar{\phi}(t)\right) \ , \tag{103}$$

where $\bar{\lambda}$ and $\bar{\phi}$ are the one-loop running parameters given in eq. (102), there is no choice of t (choice of pivot mass) for which a Taylor expansion of eq. (103) would generate the leading

logarithms of eq. (83). Thus, multi-scale techniques, for which the running parameters have several arguments $t_1, t_2, ...$, are needed, as was argued in [35, 42, 43, 44, 48].

Nevertheless, if the pivot logarithm is the dominant one, the above method correctly re-sums the (sub)leading terms in the effective potential. In particular, a Taylor expansion of f_0 reproduces the correct coefficients of the leading powers of the pivot logarithm in the effective potential. For this result to hold it is paramount that the pivot logarithm is dominant.

Indeed, consider the case in which $N_m = 1$. The pivot mass can be chosen to be the only mass eigenvalue of the theory, $\mathcal{M} = m$, such that eq. (101) re-sums leading logarithms (cf. section (2.1.1)). This is not true if the theory contains different mass eigenvalues because in this case the coefficients $\tilde{w}_n^{(k)}$ with $k > n+1$ include logarithms of the ratios $\frac{\phi}{\mathcal{M}}$. If the theory contains many large logarithms, subleading terms in the expansion (95) might become comparable to or greater than the leading function, invalidating the perturbative expansion.

Therefore, eq. (101) will only be a valid truncation of eq. (95) in regions of parameter space in which the logarithms of the ratios $\frac{\phi}{\mathcal{M}}$ are smaller than or negligible in comparison to the pivot logarithm. As we commented in the end of section (3.1), the choice in eq. (85) varies for different domains in parameter space and it can thus be difficult to choose the pivot mass. In the next section, we will solve this issue.

3.2.2 Improvement Along a Characteristic Curve

Given boundary data, the Cauchy problem for eq. (93) can be solved by the method of characteristics (cf. appendix A). The characteristic equations for eq. (93) along a particular characteristic curve can be written as

$$\begin{aligned} \frac{\mathrm{d}\mu}{\mathrm{d}t} &= \mu \,, \\ \frac{\mathrm{d}\lambda_i}{\mathrm{d}t} &= \beta_i \,, \\ \frac{\mathrm{d}\phi_a}{\mathrm{d}t} &= -\frac{1}{2}\gamma_a \phi_a \,, \\ \frac{\mathrm{d}\tilde{V}}{\mathrm{d}t} &= 0 \,, \end{aligned} \tag{104}$$

where the last equation is the condition for the scale independence of $\tilde{V}$. Quantities run along characteristic curves in parameter space and the characteristic parameter t sets the scale of the subtraction mass and physical quantities. The bare quantities are the boundary values determined by Cauchy data on a regular noncharacteristic hypersurface in parameter space.

A hypersurface defined by $\Sigma(\mu, \lambda, \phi) = 0$ is said to be regular if $\nabla\Sigma = (\partial_\mu\Sigma, \partial_\lambda\Sigma, \partial_\phi\Sigma) \neq 0$. It is said to be noncharacteristic if

$$\Xi(\nabla\Sigma) = \mu\frac{\partial\Sigma}{\partial\mu} + \sum_{i=1}^{N_\lambda}\beta_i\frac{\partial\Sigma}{\partial\lambda_i} - \frac{1}{2}\sum_{a=1}^{N_\phi}\gamma_a\phi_a\frac{\partial\Sigma}{\partial\phi_a} \neq 0 \,.$$

A typical example of boundary is the hyperplane $\mu = \mu_0 \neq 0$, which is clearly regular. It is noncharacteristic, since $\Xi(e_\mu) = \mu_0 \neq 0$. This hyperplane is parametrised by the bare quantities

$$\xi = (\lambda_0, \phi_0) \,.$$

A particular choice of boundary conditions, i.e., a choice of ξ, corresponds to a characteristic

curve in parameter space. The solution of eq. (104) along a particular curve is then

$$\begin{aligned}
\mu(t) &= \mu_0 e^t \,, \\
\lambda_i &\equiv \lambda_i(t) \,, \\
\phi_a(t) &= \phi_{a,0} Z_a(t)^{-\frac{1}{2}} \,, \\
Z_a(t) &= Z_a(0) e^{\int_0^t \gamma_a(\lambda(\eta))\mathrm{d}\eta} \,, \\
\tilde{V}(\mu(t);\lambda(t),\phi(t)) &= \tilde{V}(\mu_0;\lambda_0,\phi_0) \,.
\end{aligned} \tag{105}$$

We do not include an explicit solution for the couplings, since it depends on the functional form of the β-functions. Usually the bare field-normalisation is set to[†] $Z_a(0) = 1$.

Solution (105) implies that running along a characteristic curve does not alter the value of the effective potential and, hence, it is scale invariant. Any choice of characteristic parameter (any choice of μ) is equally valid, as long as the Cauchy problem is well defined. Running can thus improve the validity of the perturbative expansion of the effective potential at a given loop order. If we know how the couplings, masses and fields run along characteristic curves, the scale independence of the effective potential provides a way to RG-improve it by incorporating the effect of the running of its parameters, such that the contributions from radiative corrections are minimised by a suitable choice of scale.

For example, it is not possible to choose the hypersurface $\tilde{V}(\mu;\lambda,\phi) = 0$ as a boundary. It is evidently characteristic because the effective potential satisfies the RG equation (93). In this case, the Cauchy problem is ill-posed. This also implies that it is not possible to choose t (choose μ) in eq. (105) such that the full effective potential (92) vanishes.

It is, however, possible to choose t such that loop contributions to the effective potential vanish. In what follows, we will examine this choice for the one-loop approximation of the effective potential. In appendix B, we will generalise the method to any loop order.

The Hypersurface of Vanishing Loop-Corrections: A First Approach

From eq. (48), we see that we may choose a field-dependent value for the subtraction mass such that the one-loop contribution vanishes. This choice defines a hypersurface in the parameter space spanned by $(\mu;\lambda,\phi)$, which is given by the equation

$$\mu_* = \mathcal{M} \exp\left\{ \frac{1}{2} \frac{\mathbb{A}\left(\lambda, \frac{\phi}{\mathcal{M}}\right)}{\mathbb{B}\left(\lambda, \frac{\phi}{\mathcal{M}}\right)} \right\} \,. \tag{106}$$

We note that this choice can be motivated by the consideration that, while it is not possible to suppress all logarithms individually with a single subtraction mass, one can suppress the quantum corrections altogether, when evaluating the potential on the hypersurface given in eq. (106). Along a particular characteristic curve given in eq. (105), the characteristic displacement to the hypersurface of eq. (106) is a solution to the implicit equation

$$t_* = \frac{1}{2}\log\frac{\mu^2(t_*)}{\mu_0^2} = \frac{1}{2}\log\frac{\mathcal{M}^2}{\mu_0^2} + \frac{1}{2}\frac{\mathbb{A}\left(\lambda(t_*), \frac{\phi(t_*)}{\mathcal{M}}\right)}{\mathbb{B}\left(\lambda(t_*), \frac{\phi(t_*)}{\mathcal{M}}\right)} \,, \tag{107}$$

[†]This can be always done by a suitable global rescaling of fields.

which can also be written as

$$t_* = \frac{V^{(1)}\left(\mu_0, \lambda(t_*), \phi(t_*)\right)}{2\mathbb{B}\left(\lambda(t_*), \frac{\phi(t_*)}{\mathcal{M}}\right)\mathcal{M}^4} \,. \tag{108}$$

At this scale, the effective potential reads

$$\begin{aligned} V(\mu_*; \lambda_*, \phi_*) &= V^{(0)}(\lambda_*, \phi_*) + \mathcal{O}(\hbar^2) \,, \\ \mu_* &\equiv \mu(t_*) \,, \\ \lambda_* &\equiv \lambda(t_*) \,, \\ \phi_* &\equiv \phi(t_*) \,. \end{aligned} \tag{109}$$

It is straightforward to verify that eqs. (106) and (108) remain unchanged under a redefinition of the pivot mass[‡], given in eqs. (50). To understand that the formula (109) represents an RG improvement with respect to a reference mass μ_0, we note that λ_* and ϕ_* contain terms in all orders in $\hbar$, due to the integration of the β-functions and anomalous dimensions (cf. eq. (105)).

In section (2.1.1), in the case of massless ϕ^4-theory, we concluded that the $\mathcal{O}(\hbar^2)$ terms in eq. (109) contained no large logarithms and that the displacement (108) re-summed the leading logarithms of the theory. When more scalar fields are present and different mass eigenvalues are featured in the effective potential, the choice (106) will unfortunately not re-sum the all the leading logarithms at an arbitrary reference mass μ_0, due to the results of section (3.2.1).

Nevertheless, the results of that section also imply that logarithmic terms contained in $\mathcal{O}(\hbar^2)$ will be of subleading order with respect to a dominant pivot logarithm at an arbitrary reference mass μ_0. This can be seen as follows. We first approximate eq. (107) by

$$t_* = \frac{1}{2}\log\frac{\mathcal{M}^2}{\mu_0^2} + \frac{1}{2}\frac{\mathbb{A}\left(\lambda_0, \frac{\phi_0}{\mathcal{M}}\right)}{\mathbb{B}\left(\lambda_0, \frac{\phi_0}{\mathcal{M}}\right)} + \mathcal{O}(\hbar) \,, \tag{110}$$

which is invariant under redefinitions of $\mathcal{M}$ due to eqs. (50). We exploit this invariance of the above equation to redefine $\mathcal{M}$ (starting from any arbitrary initial definition) as

$$\left|\log\frac{\mathcal{M}^2}{\mu_0^2}\right| \gg \max_a\left\{\log\frac{m_a^2(\lambda_0, \phi_0)}{\mathcal{M}^2}\right\} \,. \tag{111}$$

We then note that eq. (109) can be expanded in a Taylor series

$$\begin{aligned} V^{(0)}(\lambda_*, \phi_*) &= \sum_{n=0}^{\infty} \hbar^n \tilde{w}_n^{(n)}(\lambda_0, \phi_0)(2t_*)^n = \\ &= \sum_{n=0}^{\infty} \hbar^n \tilde{w}_n^{(n)}(\lambda_0, \phi_0)\left(\log\frac{\mathcal{M}^2}{\mu_0^2}\right)^n + \cdots \,, \end{aligned}$$

where we used eq. (99). The ellipses hide terms with positive powers of $\frac{\mathbb{A}}{\mathbb{B}}$, which contain the logarithms of the ratios $\frac{\phi_0}{\mathcal{M}}$. Such terms are subleading for $\mathcal{M}$ given in eq. (111). The first term in the above equation coincides with the leading function (100) of the pivot logarithm. We conclude that eq. (109) necessarily includes a re-summation of a dominant pivot logarithm with

[‡]The choice $\mathcal{M} = \mu_*$ is excluded because, in this case, eq. (106) does not hold. Evidently, eq. (106) is also not valid when $\mathbb{B} = 0$. This implies the above method has to be employed with care in regions where the $\mathbb{B}$ function changes sign.

respect to the mass μ_0. It is not, however, necessary to identify which is this dominant logarithm in a given region of parameter space because of the invariance of eq. (110) under redefinitions of the pivot mass. We have thus overcome the issues outlined in the end of section (3.2.1).

To put it differently, the characteristic displacement t_* given in eq. (110) automatically re-sums the highest powers of dominant logarithms at the mass μ_0 in any region of parameter space where $\mathbb{B} \neq 0$. Therefore, the $\mathcal{O}(\hbar^2)$ terms in eq. (109) are necessarily subleading, i.e., they are not the largest logarithms appearing in the set $\mathbb{S}_2$ of relation (89).

The alert reader will notice a subtlety in the above proof. Upon redefining $\mathcal{M}$ to satisfy the inequality (111), it is possible that $\mathcal{M}$ depends on μ_0. This does not invalidate the above results, for μ_0 is an arbitrary reference mass and, hence, a constant. It was assumed that the pivot mass is not a function of μ, i.e., it cannot change as one travels along the μ-axis in parameter space. However, the pivot mass can be identified with a particular constant, which can be proportional to the boundary value μ_0 without contradiction.

In this way, one can improve the effective potential by re-summing powers of the logarithms that appear in the one-loop correction. This is achieved by evaluating the tree-level potential at the field-dependent scale of eq. (110), which generalises eq. (100), and will be a reliable approximation in perturbation theory as long as the running couplings $\lambda(t_*)$ are small. In appendix B, we will present a more general way of computing the characteristic displacement in perturbation theory and we will give a formula to compute t_* to any order in $\hbar$.

Conclusions

We have presented a method to RG improve the effective potential in the general case in which N_ϕ scalar fields and N_λ couplings are present, without resorting to multi-scale methods. We use the freedom to choose the single subtraction mass μ to evaluate the effective potential of the theory on hypersurface in parameter space in which quantum corrections vanish. While this does not re-sum the leading logarithms as they are defined in the literature, it amounts to a re-summation of all logarithms that appear at one-loop level, with sub-leading logarithmic error. One notes that this is possible by understanding that one may work with different sets of logarithms (cf. eq. (89)) and that the characteristic displacement of eq. (110) automatically re-sums the leading logarithmic contributions to the effective potential.

Moreover, once the one-loop β-functions and anomalous dimensions are known and the boundary values for the running parameters are given, this method can be numerically implemented in a straightforward way, as we will show in Chapters 4, 5 and 6. Indeed, given the definition of t_* in eqs. (108) or (110), it is a simple matter to numerically evaluate $\lambda(t_*)$ at given field values. We therefore conclude that the method presented is a numerically simple alternative to multi-scale techniques.

It is also worth noting that the results of this chapter show that the one-loop RG-improved effective potential will be given by

$$V(\mu; \lambda, \phi) = V^{(0)}(\lambda_*, \phi_*) \, ,$$

also for large field values, as long as $\lambda_* \ll 1$. Indeed, eq. (110) is a reliable approximation in a large region of the scalar-field configuration space if the running couplings are small across a large range of scales. Therefore, to study the stability of the improved effective potential (e.g., boundedness from below), it is sufficient to consider the tree-level form. The RG-improved effective potential will then be bounded from below if (cf. section (2.4))

$$\eta^T \lambda_* \eta \big|_{\text{large fields}} > 0 \, .$$

In this way, to check whether or not the one-loop improved effective potential, which contains contributions from all loop orders, will be bounded, it is sufficient to compute the running couplings at large scales and verify whether or not the running coupling matrix is copositive. Even though expected, this result is not trivial, for quantum corrections could lead to other conditions on stability. In appendix (B), we generalise the results of this chapter to case in which the RG functions are truncated to any loop order. We thus conclude that, precisely because the logarithms can be re-summed into the n-loop running couplings, it is sufficient to analyse the stability constraints on the n-loop running coupling matrix, for any positive integer n.

We are now in a position to analyse several classically conformal models. With the above technique of RG-improvement, we will be able study the effective potential of these models across a large range of scales (field values), which will aid the numerical search for the global electroweak minimum.

Chapter 4

The Conformal Standard Model

In the second part of this thesis, we will be interested in classically conformal extensions of the Standard Model. For this reason, we dedicate this chapter to study the effective potential of the Conformal Standard Model, in which the tree-level Higgs mass parameter vanishes. This implies no symmetry breaking occurs at tree-level and a non-trivial VEV has to be generated by quantum corrections.

4.1 The Tree-Level Mass Spectrum

The scalar-field content of the Conformal Standard Model is comprised of the Higgs $SU(2)$ complex doublet parametrised by

$$H = \frac{1}{\sqrt{2}} \begin{pmatrix} h_1 + ih_2 \\ h_3 + ih_4 \end{pmatrix} ,$$

with the tree-level scalar-sector potential given by

$$V^{(0)} = \lambda (H^\dagger H)^2 = \frac{\lambda}{4} \sum_{a,b=1}^{4} h_a^2 h_b^2 \, . \tag{112}$$

The mass-squared matrix at an arbitrary point of the scalar-field space reads

$$M_{ab}^2 = \frac{\partial^2 V^{(0)}}{\partial h_a \partial h_b} = \lambda \delta_{ab} \sum_{c=1}^{4} h_c^2 + 2\lambda h_a h_b \, . \tag{113}$$

We will be interested in the field-dependent eigenvalues of eq. (113). The action of M^2 on any quadruple $\vec{\psi}$ is

$$\sum_{b=1}^{4} M_{ab}^2 \psi_b = 2\lambda \psi_a (H^\dagger H) + 2\lambda h_a \vec{h} \cdot \vec{\psi} \, , \tag{114}$$

where $\vec{h} = (h_1, h_2, h_3, h_4)$ and $\vec{\psi} = (\psi_1, \psi_2, \psi_3, \psi_4)$. For $\vec{h} \cdot \vec{\psi} = 0$, eq. (114) is an eigenvector equation with eigenvalue $2\lambda H^\dagger H = \lambda \vec{h}^2 \equiv \lambda h^2$. There are three such eigenvectors, which correspond to the Goldstone directions. The remaining eigenvalue can be found by setting $\vec{\psi} = \vec{h}$, which yields the field-dependent mass-squared $6\lambda (H^\dagger H) \equiv 3\lambda h^2$.

Let us now collect the mass eigenvalues for vector bosons and fermions, which are the same as in the non-Conformal Standard Model. These can be straightforwardly computed as the eigenvalues of the vector-boson mass matrix and fermionic mass matrix. Due to the $SU(2)$ symmetry of the model, we find that all mass-squared eigenvalues are proportional to $h^2 = 2H^\dagger H$.

In the vector-boson sector, we find

$$\begin{aligned} m_A^2 &= 0 \,, \\ m_Z^2 &= \frac{g^2 + g'^2}{4} h^2 \,, \\ m_W^2 &= \frac{g^2}{4} h^2 \,, \\ m_{\bar{W}}^2 &= \frac{g^2}{4} h^2 \,. \end{aligned} \tag{115}$$

The zero mass eigenstate is the photon field, which is the gauge boson of the residual $U(1)_{\text{EM}}$ gauge symmetry of the Standard Model. The degenerate states correspond to the charged (complex) vector-boson fields and the remaining state is the neutral (real) vector-boson field. The embedding of the residual gauge group into the full $SU(2) \times U(1)$ group in the Standard Model is characterised by the weak mixing angle, defined by

$$g' = g \tan \theta_W \,.$$

In the fermionic sector, the mass eigenvalues can be computed from the Yukawa interactions of Dirac fermions with the Higgs doublet. We will be interested only in the top quark contribution. The other couplings in the fermionic sector will be set to zero, due to their small values relative to the value of the top Yukawa coupling at the electroweak scale*. We thus find the top quark mass eigenvalue

$$m_t = \frac{Y_t}{\sqrt{2}} h \,. \tag{116}$$

4.2 The One-Loop Effective Potential

The one-loop contributions in the Conformal Standard Model are

$$\begin{aligned} V^{(1)} &= V^{(1)}_{\text{scalar bosons}} + V^{(1)}_{\text{vector bosons}} + V^{(1)}_{\text{Dirac fermions}} \,, \\ V^{(1)}_{\text{scalar bosons}} &= \frac{1}{64\pi^2} \sum_{i=1}^{4} \left[m_i^4 \log\left(\frac{m_i^2}{\mu^2}\right) - \frac{3}{2} m_i^4 \right] \,, \\ V^{(1)}_{\text{vector bosons}} &= \frac{3}{64\pi^2} \left[2m_W^4 \log\left(\frac{m_W^2}{\mu^2}\right) - \frac{5}{3} m_W^4 + m_Z^4 \log\left(\frac{m_Z^2}{\mu^2}\right) - \frac{5}{6} m_Z^4 \right] \,, \\ V^{(1)}_{\text{Dirac fermions}} &= \frac{-4}{64\pi^2} \sum_F \left[m_F^4 \log\left(\frac{m_F^2}{\mu^2}\right) - \frac{3}{2} m_F^4 \right] \approx \frac{-3Y_t^4 h^4}{64\pi^2} \left[\log\left(\frac{Y_t^2}{2} \frac{h^2}{\mu^2}\right) - \frac{3}{2} \right] \,. \end{aligned}$$

*To see that the error in neglecting the contribution from other quarks is negligible, one notes that the top quark mass is considerably larger than all other quark masses. For example, the ratio of the bottom quark mass to the top quark mass is given approximately by 2.41% with the current experimental values.

We will choose the pivot logarithm to be $\frac{1}{2}\log\frac{h^2}{\mu^2}$, such that we can write the one-loop effective potential as (cf.eq. (48))

$$V^{(1)} = h^4\left[\mathbb{A}(\lambda,g,g',Y_t) + \mathbb{B}(\lambda,g,g',Y_t)\log\frac{h^2}{\mu^2}\right] , \tag{117}$$

$$\begin{aligned}\mathbb{A}(\lambda,g,g',Y_t) = \frac{1}{64\pi^2h^4}\Bigg\{&\sum_{i=1}^{4}\left(m_i^4\log\left(\frac{m_i^2}{h^2}\right)-\frac{3}{2}m_i^4\right)+6m_W^4\log\left(\frac{m_W^2}{h^2}\right)-\\ &-5m_W^4+3m_Z^4\log\left(\frac{m_Z^2}{h^2}\right)-\frac{5}{2}m_Z^4-3Y_t^4\left[\log\left(\frac{Y_t^2}{2}\right)-\frac{3}{2}\right]\Bigg\} ,\\ \mathbb{B}(\lambda,g,g',Y_t) = \frac{1}{64\pi^2h^4}&\left[\sum_{i=1}^{4}m_i^4+6m_W^4+3m_Z^4-3Y_t^4h^4\right] .\end{aligned}$$

In particular, we can write the $\mathbb{B}$ function as

$$\mathbb{B}(\lambda,g,g',Y_t) = \frac{1}{64\pi^2}\left\{12\lambda^2+\frac{3}{8}g^4+\frac{3}{16}\left(g^2+g'^2\right)^2-3Y_t^4\right\} . \tag{118}$$

RG Equation and the Scalar-Sector β-function

The RG equation for the effective potential reads

$$\left(\mu\frac{\partial}{\partial\mu}+\beta\frac{\partial}{\partial\lambda}+\beta_g\frac{\partial}{\partial g}+\beta_{g'}\frac{\partial}{\partial g'}+\beta_t\frac{\partial}{\partial Y_t}-\frac{1}{2}\gamma h\frac{\partial}{\partial h}\right)V = 0 , \tag{119}$$

where we used the fact that the effective potential only depends on the radial field h. The running of the gauge and Yukawa couplings and of the Higgs field is determined by well-known Standard Model loop effects. For simplicity, we will only consider the running of the gauge and top Yukawa couplings and the Higgs field. At one-loop level, we find [6, 47, 17]

$$\begin{aligned}\gamma &= \frac{1}{32\pi^2}\left(-9g^2-3g'^2+12Y_t^2\right) ,\\ \beta_g &= -\frac{19g^3}{96\pi^2} ,\\ \beta_{g'} &= \frac{41g'^3}{96\pi^2} ,\\ \beta_t &= \frac{1}{16\pi^2}\left(\frac{9}{2}Y_t^3-8g_s^2Y_t-\frac{9}{4}g^2Y_t-\frac{17}{12}g'^2Y_t\right) ,\\ \beta_{g_s} &= -\frac{7}{16\pi^2}g_s^3 ,\end{aligned} \tag{120}$$

where we included the contribution of the strong coupling g_s to the top Yukawa β-function. Keeping terms up to one-loop order, we can rewrite eq. (119) as [6]

$$\mu\frac{\partial V^{(1)}}{\partial\mu}+\beta\frac{\partial V^{(0)}}{\partial\lambda}-\frac{1}{2}\gamma h\frac{\partial V^{(0)}}{\partial h} = 0 .$$

The terms proportional to $\beta_g, \beta_{g'}$ and β_t vanish because the scalar-sector tree-level potential does not depend on the gauge and Yukawa couplings. Since $\mu\partial_\mu\log\frac{h^2}{\mu^2} = -2$, we obtain

$$\begin{aligned}&\beta\frac{\partial V^{(0)}}{\partial\lambda}-\frac{1}{2}\gamma_h h\frac{\partial V^{(0)}}{\partial h} = 2\mathbb{B}h^4 ,\\ \Rightarrow\ &(\beta-2\lambda\gamma) = 8\mathbb{B} .\end{aligned} \tag{121}$$

Together with eq. (118), this implies

$$\beta(\lambda, g, g', Y_t) = \frac{1}{8\pi^2}\left[12\lambda^2 + \frac{\lambda}{2}\left(-9g^2 - 3g'^2 + 12Y_t^2\right) + \frac{3g^4}{8} + \frac{3(g^2+g'^2)^2}{16} - 3Y_t^4\right] . \quad (122)$$

Running Parameters

The characteristic equations for the gauge and Yukawa couplings read (cf.eq. (120)) [17, 31]

$$\frac{\mathrm{d}g^2}{\mathrm{d}t} = -\frac{19g^4}{48\pi^2} , \quad (123)$$

$$\frac{\mathrm{d}g'^2}{\mathrm{d}t} = \frac{41g'^4}{48\pi^2} , \quad (124)$$

$$\frac{\mathrm{d}g_s^2}{\mathrm{d}t} = -\frac{7}{8\pi^2}g_s^4 , \quad (125)$$

$$\frac{\mathrm{d}Y_t^2}{\mathrm{d}t} = \frac{1}{8\pi^2}\left(\frac{9}{2}Y_t^4 - 8g_s^2Y_t^2 - \frac{9}{4}g^2Y_t^2 - \frac{17}{12}g'^2Y_t^2\right) . \quad (126)$$

The solutions of the gauge couplings are easily found to be

$$\begin{aligned} g^2(t) &= \frac{g^2(0)}{1 + \frac{19}{48\pi^2}g^2(0)t} , \\ g'^2(t) &= \frac{g'^2(0)}{1 - \frac{41}{48\pi^2}g'^2(0)t} , \\ g_s^2(t) &= \frac{g_s^2(0)}{1 + \frac{7}{8\pi^2}g_s^2(0)t} , \end{aligned} \quad (127)$$

where we have set the boundary values at the Z-boson mass $\mu_0 = m_Z \approx 91$ GeV. To solve for the running top Yukawa coupling, we integrate eq. (126) numerically. The experimental values

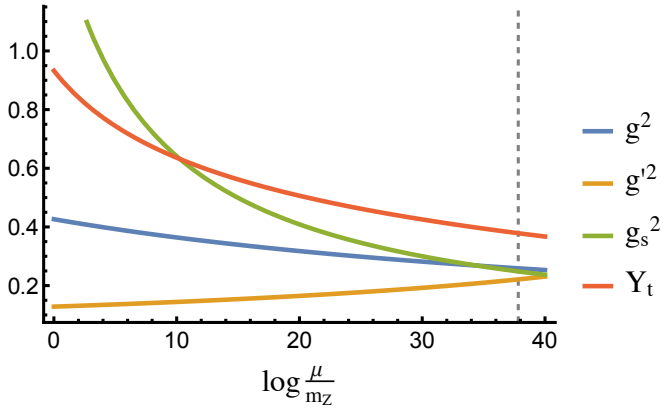

Figure 4.1 – Analytical solution for the squared gauge couplings and numerical solution for the top Yukawa coupling with the boundary values given in eq. (128). The dashed vertical line marks the Planck scale at $t_P \approx 37.8$.

at m_Z are given by

$$\begin{aligned} g(t=0) &\approx 0.652 \,, \\ g'(t=0) &\approx 0.358 \,, \\ g_s(t=0) &\approx 1.22 \,, \\ Y_t(t=0) &\approx 0.933 \,. \end{aligned} \tag{128}$$

The gauge coupling g' exhibits a Landau pole at $t = \frac{48\pi^2}{41 g'^2(0)} \approx 90.07$, in the far ultraviolet. Since this pole is above the Planck scale $t_P = \log \frac{M_P}{m_Z} \approx 37.8$, we expect that a quantum theory of gravitation or a Grand Unified Theory, which we do not contemplate here, will eliminate it. We also note that the gauge and Yukawa couplings vanish in the limit $t \to \infty$, regardless of their initial values. In particular, they have small values around the Planck scale given by

$$\begin{aligned} g(t_P) &\approx 0.509 \,, \\ g'(t_P) &\approx 0.470 \,, \\ g_s(t_P) &\approx 0.498 \,, \\ Y_t(t_P) &\approx 0.379 \,, \\ t_P &\approx 37.8 \,. \end{aligned}$$

The running Higgs field normalisation is a solution to the characteristic equation

$$\frac{\mathrm{d} \log Z}{\mathrm{d}t} = \frac{1}{32\pi^2} \left(-9g^2 - 3g'^2 + 12 Y_t^2 \right) \,, \tag{129}$$

which can be numerically integrated, with boundary value $Z(t=0) = 1$.

Finally, let us set $\lambda(t=0) \approx 0.125$ to match the situation in the Standard Model, i.e., to obtain the correct (experimental) value for the Higgs mass. We can then numerically integrate β in eq. (122). The resulting running Higgs self-coupling is depicted in Figure 4.2.

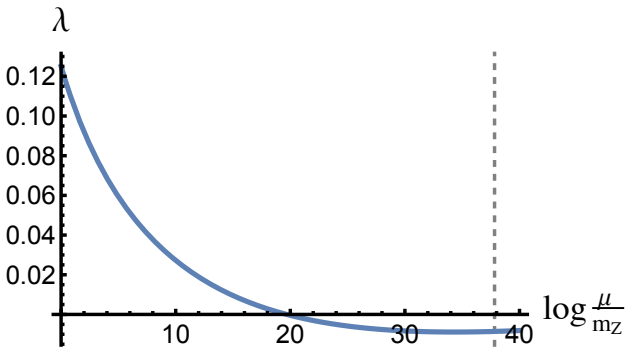

Figure 4.2 – Numerical solution for the Higgs self-coupling in the Conformal Standard Model. The dashed vertical line marks the Planck scale at $t_P \approx 37.8$.

Following the conclusions at the end of section (3.2.2), we see that for this particular boundary value of λ, we obtain a potential which is unbounded from below, due to the negativity of the Higgs self-coupling at large field values, i.e., for $t_* \approx 40$. However, the potential becomes again stable at transplanckian energy scales.

4.2.1 Radiative Extrema

Case I

For the running coupling depicted in Figure 4.2, the Higgs self-coupling vanishes at the masses

$$\begin{aligned} \mu_{\max} &\approx 3.20 \times 10^{10}\ \text{GeV}\ , \\ \mu_{\min} &\approx 4.16 \times 10^{26}\ \text{GeV}\ . \end{aligned} \tag{130}$$

Since the tree level vanishes at these scales, the effective potential is then given by eq. (117) and its second derivative at a stationary point is simply $8\mathbb{B}h^2$. We thus recognise the first (second) mass in eq. (130) as the one at which the one-loop approximation develops a maximum (minimum), since at those scales we have $\mathbb{B} < 0$ ($\mathbb{B} > 0$), as can be verified numerically. We find the corresponding field values at the stationary points

$$\begin{aligned} v_{\max}^2 &= \mu_{\max}^2 \exp\left(-\frac{1}{2} - \left.\frac{\mathbb{A}}{\mathbb{B}}\right|_{\mu_{\max}}\right)\ , \\ v_{\min}^2 &= \mu_{\min}^2 \exp\left(-\frac{1}{2} - \left.\frac{\mathbb{A}}{\mathbb{B}}\right|_{\mu_{\min}}\right)\ , \\ v_{\max} &\approx 1.68 \times 10^{11}\ \text{GeV}\ , \\ v_{\min} &\approx 1.04 \times 10^{27}\ \text{GeV}\ . \end{aligned} \tag{131}$$

For both scales in eq. (130), we find that $\mathbb{A}$ and $\mathbb{B}\log\frac{h^2}{\mu^2}$ are small, which signals that no large logarithms occur. More precisely, it can be numerically checked that all logarithms of the model are not large at the stationary points (131). This implies that the one-loop approximation is reliable at those scales. The running Higgs mass at the scale of the minimum is

$$\frac{m_h^2}{v^2} = 8\mathbb{B}\big|_{\mu_{\min}} \approx 6.88 \times 10^{-4}\ . \tag{132}$$

Case II

Let us now analyse the more general situation in which λ does not vanish. A stationary point of the one-loop effective potential for the Conformal Standard Model is given by the equation

$$\begin{aligned} 0 &= \frac{\mathrm{d}}{\mathrm{d}h}\left\{\left(\frac{\lambda}{4} + \mathbb{A}(\lambda, g, g', Y_t) + \mathbb{B}(\lambda, g, g', Y_t)\log\frac{h^2}{\mu^2}\right)h^4\right\} = \\ &= 4\left(\frac{\lambda}{4} + \mathbb{A}(\lambda, g, g', Y_t) + \frac{1}{2}\mathbb{B}(\lambda, g, g', Y_t) + \mathbb{B}(\lambda, g, g', Y_t)\log\frac{h^2}{\mu^2}\right)h^3\ . \end{aligned}$$

Therefore, non-trivial stationary points are obtained if the couplings at the mass μ obey the constraint

$$\frac{\lambda}{4} + \mathbb{A}(\lambda, g, g', Y_t) + \frac{1}{2}\mathbb{B}(\lambda, g, g', Y_t) + \mathbb{B}(\lambda, g, g', Y_t)\log\frac{v^2}{\mu^2} = 0\ ,$$

where v is the value of the non-trivial VEV. Following [3], we set $\mu = v$ and obtain

$$\lambda + 4\mathbb{A}(\lambda, g, g', Y_t) + 2\mathbb{B}(\lambda, g, g', Y_t) = 0\ . \tag{133}$$

Since $\mathbb{A}(\lambda)$ and $\mathbb{B}(\lambda)$ contain terms of order λ^2 and fourth powers of gauge and Yukawa couplings, we can approximate eq. (133) as

$$\lambda + 4\mathbb{A}(0, g, g', Y_t) + 2\mathbb{B}(0, g, g', Y_t) = 0 \,,$$

as was done in [3] for the massless scalar QED (cf. Chapter 2). This is justified, since from eq. (128) and the running of the parameters (cf. Figures 4.1 and 4.2), we see that λ is much smaller than the gauge and Yukawa couplings for a large range of scales. In this way, a first approximation to $\lambda(\mu = v)$ is entirely determined by the values of gauge and Yukawa couplings at the VEV scale,

$$\lambda(\mu = v) = -4\mathbb{A}(0, g, g', Y_t) - 2\mathbb{B}(0, g, g', Y_t) \,. \tag{134}$$

We can interpret eq. (134) as a definition of v, if the running couplings are known, i.e., the Higgs VEV will be given by the mass scale at which the constraint (134) between the couplings is satisfied. The second derivative reads

$$\begin{aligned} \frac{\mathrm{d}^2}{\mathrm{d}h^2}(V^{(0)} + V^{(1)})\bigg|_{h=\mu=v} &= 12\left(\frac{\lambda}{4} + \mathbb{A}(\lambda, g, g', Y_t) + \frac{7}{6}\mathbb{B}(\lambda, g, g', Y_t)\right)v^2 \approx \\ &\approx 12\left(\frac{\lambda}{4} + \mathbb{A}(0, g, g', Y_t) + \frac{7}{6}\mathbb{B}(0, g, g', Y_t)\right)v^2 = \\ &= 8\mathbb{B}(0, g, g', Y_t)v^2 \,, \end{aligned} \tag{135}$$

where we used eq. (134). To find a minimum, we must solve eq. (134) and select the root for which eq. (135) is positive. For the Higgs self-coupling depicted in Figure 4.2, we find a maximum and a minimum at the scales

$$\begin{aligned} v_{\max} &\approx 1.55 \times 10^{11} \text{ GeV} \,, \\ v_{\min} &\approx 1.08 \times 10^{27} \text{ GeV} \,. \end{aligned} \tag{136}$$

This is in accordance with the results of [12], where the Coleman-Weinberg method was applied to the Standard Model effective potential. The running Higgs mass at the scale of minimum is

$$\frac{m_h^2}{v^2} \approx 8\mathbb{B}(0, g, g', Y_t) \approx 7.21 \times 10^{-4} \,. \tag{137}$$

As before, the extrema in eq. (136) are located at very high energies, which implies the couplings evaluated at these scales are correspondingly very small. This prevents the appearance of large logarithms in $\mathbb{A}$ and $\mathbb{B}$ at the scale of the minimum and guarantees the reliability of the one-loop result. We note that, although the values given in eqs. (132) and (137) differ, one must take into account the fact that the running masses are evaluated at different scales in each case, as a result of different approximations to the one-loop effective potential.

Since the effective potential is obtained from proper vertices evaluated at vanishing external momenta (cf. Chapter 1), the physical (pole) mass of the Higgs boson is obtained by adding the self-energy corrections at non-vanishing external momenta to the Hessian of the effective potential. Moreover, the radiatively generated VEV is not of physical interest, since it will be generally gauge dependent. Thus, the only quantity of physical interest in the above analysis is the mass-to-VEV ratio, given by $8\mathbb{B}$. This quantity is entirely determined by the running of the couplings. We will therefore check the reliability of the one-loop approximation in the following section by RG-improving the potential and verifying that the mass-to-VEV ratio is not considerably altered.

We also note that, once we fix the effective potential at the scale of the minimum $\mu = v$, no non-trivial maximum is present. The converse is also true, i.e., the effective potential at the scale of the maximum exhibits no non-trivial minimum, which can be seen in Figures 4.3 and 4.4 and verified numerically. This can be understood by noting that the one-loop approximation evaluated at $\mu = v$ only holds in the vicinity of the stationary point v, since large logarithms appear for large differences in field values. On the other hand, both extrema will be present in the RG-improved potential, which is valid for a large range of scales.

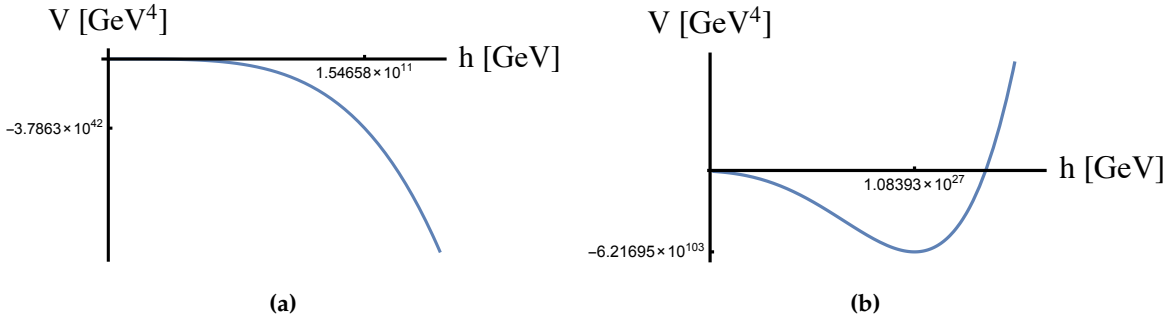

(a) **(b)**

Figure 4.3 – The one-loop effective potential for the Conformal Standard Model, computed at the scale of the minimum.

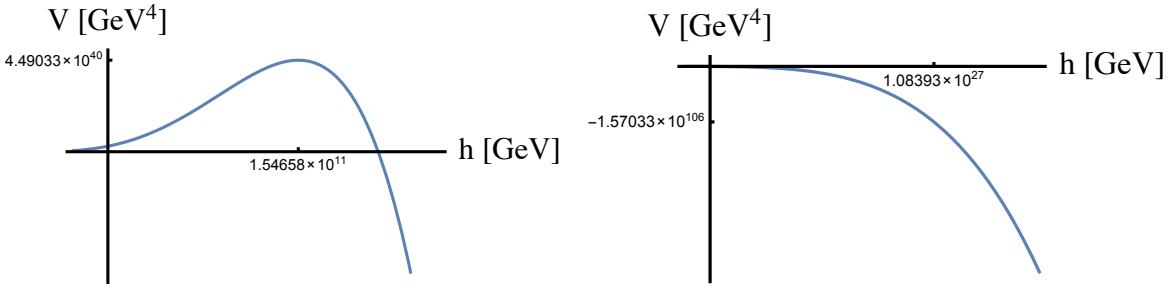

(a) **(b)**

Figure 4.4 – The one-loop effective potential for the Conformal Standard Model, computed at the scale of the maximum.

4.2.2 RG Improvement

We are interested in the large-field behaviour of the effective potential of the Conformal Standard Model and in verifying that the radiative minimum obtained in the previous section continues to hold for the RG improved potential. Following the results of Chapter 3, section (3.2.2), we write the RG-improved effective potential as

$$\begin{aligned} V &= \frac{\lambda(t_*)}{4} Z^{-2}(t_*) h^4 \,, \\ t_*(g, g', Y_t, h) &= \frac{1}{2} \log \frac{h^2}{v^2} + \frac{\mathbb{A}(0, g, g', Y_t)}{2\mathbb{B}(0, g, g', Y_t)} \,. \end{aligned} \tag{138}$$

Let us recall the meaning of eq. (138). We are interested in incorporating higher loop-orders in the effective potential, before we can apply the Coleman-Weinberg method. Given only knowledge of the one-loop RG functions, we start at the mass v , which defines a hyperplane $\mu = v$ in parameter space. As in the previous section, v will be the value of the field at an extremum. We then run the parameters along a characteristic curve to a hypersurface at which loop corrections (approximately) vanish. This characteristic displacement corresponds to a field-dependent rescaling $v \to ve^{t_*}$.

At the hypersurface of vanishing loop corrections, the effective potential has the tree-level form. The higher loop-orders are contained implicitly in the running coupling $\lambda(t_*) \equiv \lambda_*$ and field normalisation $Z(t_*) \equiv Z_*$. Thus, eq. (138) has two interpretations. It can be seen as the tree-level potential evaluated at the scale t_*, or as an improved potential, which formally contains all orders in $\hbar$, evaluated at the mass $\mu = v$. Note that h denotes the value of the Higgs field at $\mu = v$. We have also neglected the λ^2 factors in the $\mathbb{A}$ and $\mathbb{B}$ functions, for consistency with the previous section.

Moreover, since we are dealing with a single scalar field h, the factor $\frac{\mathbb{A}}{2\mathbb{B}}$ only depends on the value of the couplings at $\mu = v$ and is thus an unimportant shift. At large field values, $t_* \approx \log \frac{h}{v}$ and the improved potential (138) coincides with the potential $V(h) = \frac{\lambda(h)}{4} h^4$ frequently used in the literature to study vacuum stability in the Standard Model [9, 11, 10]. Indeed, the Higgs mass term in the effective potential is negligible at large field values, such that the Standard Model is nearly-conformal in the ultraviolet.

Stationary Points

The stationary points of eq. (138) are solutions of the equation

$$0 = \frac{\mathrm{d}V}{\mathrm{d}h} = \lambda(t_*) Z^{-2}(t_*) h^3 + \left[\frac{\beta_*}{4} Z_*^{-2} h^4 - \frac{\lambda_*}{2} \gamma_* Z_*^{-2} h^4 \right] \frac{\mathrm{d}t_*}{\mathrm{d}h} ,$$

which can be written as (compare with eq. (133))

$$\begin{aligned} 0 &= \left\{ \lambda_* + \frac{\beta_*}{4} - \frac{\lambda_*}{2} \gamma_* \right\} Z_*^{-2} h^3 = \\ &= \left\{ \lambda_* + 2\mathbb{B}(\lambda_*, g_*, g'_*, Y_{t*}) \right\} Z_*^{-2} h^3 , \end{aligned} \tag{139}$$

where we used $\frac{\mathrm{d}t_*}{\mathrm{d}h} = \frac{1}{h}$, which follows from eq. (138), and eq. (121). The second derivative of eq. (138) at a stationary point $h = v$ reads

$$m_h^2 \equiv \left. \frac{\mathrm{d}^2 V}{\mathrm{d}h^2} \right|_{h=v} = v^2 Z_*^{-2} \left(\beta_* + \frac{1}{4} \delta\beta_* - \frac{1}{2} \beta_* \gamma_* - \frac{\lambda_*}{2} \delta\gamma_* \right) , \tag{140}$$

where we defined

$$\begin{aligned} \delta\beta_* &:= \left(\beta \frac{\partial \beta}{\partial \lambda} + \beta_g \frac{\partial \beta}{\partial g} + \beta_{g'} \frac{\partial \beta}{\partial g'} + \beta_t \frac{\partial \beta}{\partial Y_t} \right)_{t=t_*} , \\ \delta\gamma_* &:= \left(\beta_g \frac{\partial \gamma}{\partial g} + \beta_{g'} \frac{\partial \gamma}{\partial g'} + \beta_t \frac{\partial \gamma}{\partial Y_t} \right)_{t=t_*} . \end{aligned} \tag{141}$$

Equation (140) defines a running mass parameter for the Higgs field. The scale s at which eq. (139) is satisfied and eq. (140) is positive defines the Higgs VEV through the equation $s = t_*(g, g', Y_t, v)$. Once s is known, one can invert t_* to obtain v. We then find the minimum

$$\begin{aligned} v &\approx 1.04 \times 10^{27} \text{ GeV} , \\ \frac{m_h^2}{v^2} &\approx 7.43 \times 10^{-4} . \end{aligned} \tag{142}$$

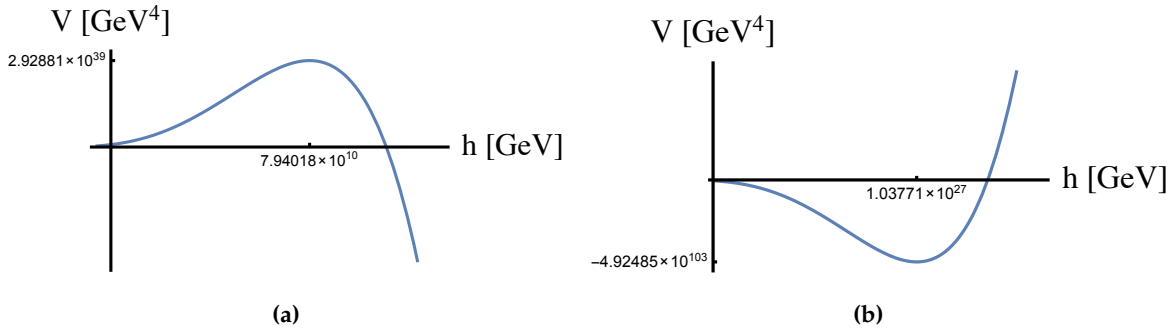

(a) **(b)**

Figure 4.5 – RG-improved potential for the Conformal Standard Model.

By comparing eqs. (136), (137) and (142), we see that the location of the Coleman-Weinberg minimum and the mass-to-VEV ratio do not change considerably by including higher-loop contributions, as expected. The relative differences read

$$\begin{aligned} \delta v &= \frac{1.03771 \times 10^{27} - 1.08393 \times 10^{27}}{1.08393 \times 10^{27}} \approx -4.26\% \,, \\ \delta V_{\text{min}} &= \frac{-4.92485 \times 10^{103} + 6.21695 \times 10^{103}}{6.21695 \times 10^{103}} \approx -20.78\% \,, \\ \delta \left(\frac{m_h^2}{v^2} \right) &= \frac{7.43136 \times 10^{-4} - 7.20594 \times 10^{-4}}{7.20594 \times 10^{-4}} \approx 3.13\% \,. \end{aligned} \tag{143}$$

Moreover, we see that the improved potential exhibits a maximum, which was absent in the one-loop approximation (cf. Figure 4.3). This is not unexpected, since the improved potential is valid for a large range of scales and better approximates the full effective potential. Indeed, eq. (138) remains valid for all scales below the Planck mass, due to the running of λ shown in Figure 4.2. We note that the maximum is at a different location than that in eq. (136), since we are evaluating the improved potential at the scale of the minimum[†].

Indeed, eq. (139) has another root, besides the scale of the minimum. It is straightforward to check that this root corresponds to a maximum located at the field value

$$v_{\text{max}} \approx 1.66 \times 10^{11} \text{ GeV} \,, \tag{144}$$

which differs from that in eq. (136) by

$$\begin{aligned} \delta v_{\text{max}} &= \frac{1.65526 \times 10^{11} - 1.54658 \times 10^{11}}{1.54658 \times 10^{11}} \approx 7.03\% \,, \\ \delta V_{\text{max}} &= \frac{7.36475 \times 10^{40} - 4.49033 \times 10^{40}}{4.49033 \times 10^{40}} \approx 64.01\% \,. \end{aligned} \tag{145}$$

That the relative differences in the $V_{\text{min}}, V_{\text{max}}$ values of the potential at extrema are larger than the corresponding VEV differences is understood from dimensional analysis, since the fields are elevated to the fourth power in the potential. The improved potential computed at v_{max} also

[†]Recall that the improved potential can be seen as the potential evaluated at the scale $\mu = v$, for which terms of all orders in $\hbar$ have been included.

exhibits a minimum, which was not present in the one-loop approximation (cf. Figure 4.4). We refrain from showing the corresponding graphs.

We conclude that the one-loop effective potential determines the extrema reliably, as expected. The higher-loop contributions which are re-summed by the one-loop RG improvement alter the VEVs obtained with the one-loop approximation by less than 8% (cf. eqs. (145)) and, more importantly, the mass-to-VEV ratio changes by less than 4% (cf. eq. (143)).

From the results of both Case I and Case II above, as well as the RG improvement check, we conclude that the running of the Standard Model parameters is not sufficient to dynamically generate the electroweak vacuum, at least up to the one-loop improved potential. One could choose a different boundary condition of the Higgs self-coupling in order to modify the values of the radiatively generated VEV and mass to better approximate the values of the Standard Model. However, one can verify numerically that different values of λ at the scale $\mu_0 = m_Z \approx 91$ GeV do not considerably alter the above conclusions of the one-loop RG improved analysis.

In [47], the authors use the so-called Coleman-Weinberg (CW) renormalisation scheme as opposed to the $\overline{MS}$ scheme to study the effect of higher loop-orders in the analysis of a dynamically generated electroweak vacuum. One of the features of the CW scheme is that the Higgs field normalisation Z is set to be equal to one at $\mu = v$, i.e., at the scale of the Higgs VEV. As studied in [47], the conversion of $\overline{MS}$-scheme functions to CW-scheme functions can be laborious.

However, the above analysis of one-loop RG improvement shows that there is no need to use the CW scheme and one can work with $\overline{MS}$-scheme functions, if one regards the RG improved potential as a potential at the scale $\mu = v$ in which certain contributions to all loop orders have been included. The method of RG improvement presented here is numerically simpler to implement, since one does not have to convert RG functions to the CW-scheme and, once an approximation for t_* is known, the RG improved potential is obtained from the straightforward evaluation of the quantities $\lambda(t_*)$ and $Z(t_*)$.

Moreover, in the terminology of this thesis, we note that the authors of [47] choose the pivot logarithm to be $\log \frac{h^2}{\mu^2}$ in the CW scheme. This choice is justified in the context of a theory with only one scalar field in the CW scheme. In the next chapters, we will examine classically conformal extensions of the Standard Model known as Higgs Portal Models, which are sufficiently robust to generate the electroweak vacuum radiatively.

Chapter 5

Conformal Standard Model with a Real Scalar Singlet

5.1 An Overview of Classically Conformal Extensions of the Standard Model

Since S. Coleman and E. Weinberg published their seminal paper on radiative symmetry breaking [3], a myriad of models have been analysed throughout the literature. A selection of important works has been assembled in the References.

As outlined in section (2.4), there is some freedom in realising the radiative breakdown of conformal symmetry. Models can be collected in two broad classes, which correspond to the Coleman-Weinberg and Gildener-Weinberg cases. We note that both, in principle, can be applied to an arbitrary number of scalar fields, even though it is quite often understood that only the Gildener-Weinberg case is suitable for a multiple-field model.

Simply put, a non-trivial minimum can be generated if the tree-level potential exhibits a flat direction (Case I) or if the couplings satisfy some hierarchy which renders the one-loop correction comparable in magnitude to the classical potential at a given scale (Case II). In each case, pertubativity is guaranteed if no large logarithms are present, which automatically restricts the use of the one-loop effective potential to a small region of parameter space in the neighbourhood of the critical points. To enlarge the region of applicability of the effective potential, one uses the renormalisation group to re-sum certain higher loop-order terms (cf. Chapter 3).

Examples where the Gildener-Weinberg case was adopted can be found in [31, 32, 21, 23, 15, 19, 18], whereas the Coleman-Weinberg method was predominantly used in [22, 24, 29, 30, 33]. Regarding RG-improvement, we note that one does not need to resort to multi-scale techniques in a multiple-field case, contrary to what is proposed in [42, 35, 43, 44]. Indeed, as we analysed in section (3.2.2), with a single subtraction mass one can re-sum higher loop-orders in the effective potential, with an approximation error that can be made of subleading order if the magnitude of the running couplings is sufficiently small. The RG-improvement technique developed in section (3.2.2) was applied in Chapter 4 to study the Conformal Standard Model across all scales below the Planck scale, and will be applied in the next chapter to a classically conformal extension of the Standard Model, providing us with a critical insight of the effect of higher-loop orders in Case I and II of radiative symmetry breaking.

Evidently, increasingly complicated models can be built. Typically, one considers an extended scalar sector, which provides a bridge or portal between the Higgs doublet and a hidden

sector, yet to be discovered. Such models are referred to as Higgs Portal Models. Besides the additional scalars, it is convenient to consider hidden gauge fields and fermions, with a view to phenomena beyond the Standard Model. Let us take the first step.

In this chapter, we will analyse the dynamical breakdown of symmetry for the simplest classically conformal extension of the Standard Model, in which a real scalar singlet field, which does not transform under a transformation of the Standard Model gauge group $SU(2) \times U(1)$, is added to the lagrangian. This additional scalar only couples to the Higgs field. We will study the possibilities of radiative symmetry breaking outlined in section (2.4). The analysis of this model is instructive, as it provides insights into the meaning of the dynamical generation of the electroweak scale and paves the way to more complicated models.

5.2 The One-Loop Effective Potential

The scalar-field content of the model comprises a real scalar singlet φ and the Higgs $SU(2)$ complex doublet with the tree-level scalar-sector potential given by

$$V^{(0)} = \lambda_1 (H^\dagger H)^2 + \frac{\lambda_2}{2}\varphi^2 H^\dagger H + \frac{\lambda_3}{4}\varphi^4 \,. \tag{146}$$

It is straightforward to check that the scalar-sector mass eigenvalues, which diagonalise the Hessian of (146), are given by

$$\begin{aligned}
m_1^2 &= \frac{1}{2}\left(3\lambda_1 + \frac{\lambda_2}{2}\right)h^2 + \frac{1}{2}\left(\frac{\lambda_2}{2} + 3\lambda_3\right)\varphi^2 - \\
&\quad - \frac{1}{2}\sqrt{\left[\left(3\lambda_1 - \frac{\lambda_2}{2}\right)h^2 - \left(3\lambda_3 - \frac{\lambda_2}{2}\right)\varphi^2\right]^2 + 4\lambda_2^2 h^2\varphi^2}\,, \\
m_2^2 &= \lambda_1 h^2 + \frac{\lambda_2}{2}\varphi^2\,, \\
m_3^2 &= \lambda_1 h^2 + \frac{\lambda_2}{2}\varphi^2\,, \\
m_4^2 &= \lambda_1 h^2 + \frac{\lambda_2}{2}\varphi^2\,, \\
m_5^2 &= \frac{1}{2}\left(3\lambda_1 + \frac{\lambda_2}{2}\right)h^2 + \frac{1}{2}\left(\frac{\lambda_2}{2} + 3\lambda_3\right)\varphi^2 + \\
&\quad + \frac{1}{2}\sqrt{\left[\left(3\lambda_1 - \frac{\lambda_2}{2}\right)h^2 - \left(3\lambda_3 - \frac{\lambda_2}{2}\right)\varphi^2\right]^2 + 4\lambda_2^2 h^2\varphi^2}\,,
\end{aligned} \tag{147}$$

where $h^2 \equiv \vec{h}^2$. The vector-boson and fermion masses are the same as in (115) and (116). In the same way we derived (117), we find the one-loop term

$$V^{(1)} = \rho^4\left[\mathbb{A}(\lambda,\theta) + \mathbb{B}(\lambda,\theta)\log\frac{\rho^2}{\mu^2}\right]\,, \tag{148}$$

$$\begin{aligned}
\mathbb{A}(\lambda,\theta) = \frac{1}{64\pi^2\rho^4}\Bigg\{\sum_{i=1}^{5}\left(m_i^4\log\left(\frac{m_i^2}{\rho^2}\right) - \frac{3}{2}m_i^4\right) + 6m_W^4\log\left(\frac{m_W^2}{\rho^2}\right) - \\
-5m_W^4 + 3m_Z^4\log\left(\frac{m_Z^2}{\rho^2}\right) - \frac{5}{2}m_Z^4 - 3Y_t^4\cos^4\theta\left[\log\left(\frac{Y_t^2}{2}\cos^2\theta\right) - \frac{3}{2}\right]\Bigg\}\,,
\end{aligned}$$

$$\mathbb{B}(\lambda,\theta)=\frac{1}{64\pi^2\rho^4}\left[\sum_{i=1}^{5}m_i^4+6m_W^4+3m_Z^4-3Y_t^4h^4\right]\,,$$

where we have chosen the pivot mass to be radius in the scalar-field configuration space and we defined the angle

$$\begin{aligned}\cos^2\theta&:=\frac{h^2}{\rho^2}=\frac{\rho^2-\varphi^2}{\rho^2}=1-\frac{\varphi^2}{\rho^2}=:1-\sin^2\theta\,,\\ h^2&:=h_1^2+h_2^2+h_3^3+h_4^2\,.\end{aligned}$$

In particular, we can write the $\mathbb{B}$ function as (compare with (118))

$$\begin{aligned}64\pi^2\mathbb{B}(\lambda,\theta)=&\left(12\lambda_1^2+\frac{\lambda_2^2}{4}+\frac{3}{8}g^4+\frac{3}{16}(g^2+g'^2)^2-3Y_t^4\right)\cos^4\theta+\\&+\left(6\lambda_1\lambda_2+2\lambda_2^2+3\lambda_2\lambda_3\right)\cos^2\theta\sin^2\theta+\\&+\left(\lambda_2^2+9\lambda_3^2\right)\sin^4\theta\,.\end{aligned}\tag{149}$$

Running Parameters

The RG equation for the effective potential of the Higss portal model reads

$$\left(\mu\frac{\partial}{\partial\mu}+\sum_{j=1}^{3}\beta_j\frac{\partial}{\partial\lambda_j}+\beta_g\frac{\partial}{\partial g}+\beta_{g'}\frac{\partial}{\partial g'}+\beta_t\frac{\partial}{\partial Y_t}-\frac{1}{2}\gamma_h h\frac{\partial}{\partial h}-\frac{1}{2}\gamma_\varphi\varphi\frac{\partial}{\partial\varphi}\right)V=0\,.\tag{150}$$

At one-loop level, the anomalous dimension of the singlet vanishes [6, 17, 47]. Thus, keeping terms up to one-loop order, we can rewrite (150) as

$$\mu\frac{\partial V^{(1)}}{\partial\mu}+\sum_{j=1}^{3}\beta_j\frac{\partial V^{(0)}}{\partial\lambda_j}-\frac{1}{2}\gamma_h h\frac{\partial V^{(0)}}{\partial h}=0\,.$$

Since $\mu\partial_\mu\log\frac{\rho^2}{\mu^2}=-2$, we obtain

$$\begin{aligned}&\sum_{j=1}^{3}\beta_j\frac{\partial V^{(0)}}{\partial\lambda_j}-\frac{1}{2}\gamma_h h\frac{\partial V^{(0)}}{\partial h}=2\mathbb{B}(\lambda,\theta)\rho^4\,,\\ \Rightarrow\;&(\beta_1-2\lambda_1\gamma_h)\cos^4\theta+(\beta_2-\lambda_2\gamma_h)\cos^2\theta\sin^2\theta+\beta_3\sin^4\theta=8\mathbb{B}(\lambda,\theta)\,.\end{aligned}\tag{151}$$

Together with (149), this implies the one-loop scalar-sector β-functions read (compare with (122))

$$\begin{aligned}\beta_1&=\frac{1}{8\pi^2}\left[12\lambda_1^2+\frac{\lambda_2^2}{4}+\frac{\lambda_1}{2}\left(-9g^2-3g'^2+12Y_t^2\right)+\frac{3g^4}{8}+\frac{3(g^2+g'^2)^2}{16}-3Y_t^4\right]\,,\\ \beta_2&=\frac{1}{8\pi^2}\left[6\lambda_1\lambda_2+2\lambda_2^2+3\lambda_2\lambda_3+\frac{\lambda_2}{4}\left(-9g^2-3g'^2+12Y_t^2\right)\right]\,,\\ \beta_3&=\frac{1}{8\pi^2}\left[\lambda_2^2+9\lambda_3^2\right]\,.\end{aligned}\tag{152}$$

5.3 Flat Directions

To probe for non-trivial radiative extrema, we consider the two cases outlined in section (2.4). Let us first consider Case I, in which the tree-level potential exhibits a flat direction when computed at the Gildener-Weinberg mass $\mu_{\rm GW}$.

Intuitively, one expects that the dynamical breakdown of electroweak symmetry will not be realised in this model. Indeed, from eq. (80), we see that a radiative minimum will be present if $\mathbb{B} > 0$. For a fixed angle, we see from eq. (149) that $\mathbb{B}$ will only be positive if the contribution of the top Yukawa coupling is small or the portal coupling λ_2 is sufficiently large so as to counter the Yukawa term.

The top Yukawa coupling will only be small at masses much larger than the Higgs VEV (cf. Figure 4.1). This implies that, if the portal coupling is a small parameter, it will not be possible to set $\mu_{\rm GW} \approx 246$ GeV, i.e., the Gildener-Weinberg mass cannot be close to the Standard Model Higgs VEV, contrary to what one would expect. Nevertheless, it is conceivable that the Higgs VEV at high scales is Standard-Model-like and, more importantly, its running mass is close to the pole mass of 125 GeV. Alternatively, one could set the portal coupling λ_2 to be sufficiently large near $\mu_{\rm GW} \approx 246$ GeV so as to counter the Yukawa contribution.

We note that there are two possibilities for mass generation. One is to consider that the Higgs mass is radiatively generated, such that the physical Higgs field is identified with the field which is parallel to the flat direction of the tree-level potential. In this case, the Higgs mass is (cf. eq. (80))

$$m_h^2 = 8\mathbb{B}v_\rho^2 \,, \tag{153}$$

where v_ρ is the radial VEV. The other possibility is to have the Higgs particle associated with the eigenstate which has non-vanishing tree-level mass, which corresponds to the field orthogonal to the flat direction. We will examine these cases below.

Flat Direction along the Higgs Axis

The tree-level potential (146) exhibits a flat direction along the Higgs axis if

$$\lambda_1(\mu_{\rm GW}) = 0 \,.$$

In this case, the potential will be bounded from below if $\lambda_2(\mu_{\rm GW}), \lambda_3(\mu_{\rm GW}) > 0$. Along the flat direction, the VEV of φ vanishes. To reproduce the Standard Model Higgs mass-to-VEV ratio, we must have

$$8\mathbb{B}|_{\theta=0} \approx \frac{125^2}{246^2} \approx 0.26 \,.$$

From eq. (149), this implies

$$\frac{\lambda_2^2}{4} + \frac{3}{8}g^4 + \frac{3}{16}(g^2 + g'^2)^2 - 3Y_t^4 \approx 2.08\pi^2 \,, \tag{154}$$

i.e., the portal coupling $\lambda_2(\mu_{\rm GW})$ has to be large. By numerically running the gauge and Yukawa couplings (cf. Figure 4.1), we find that, for $\mu_{\rm GW}$ below the Planck mass, the solution of eq. (154) is $\lambda_2(\mu_{\rm GW}) \gtrsim 9$. Although this value is still in the perturbative regime ($\lambda_2 \leq 4\pi$), once it is used as a boundary condition for the numerical integration of eqs. (152), it leads to a Landau pole below the Planck scale, regardless of the (perturbative) initial value of λ_3. Since we are interested in a model which remains perturbative up to the Planck scale, we conclude that there can be no flat direction along the Higgs axis.

General Flat Direction

A general flat direction, obtained from the tree-level stationary point equations, is given by

$$\begin{aligned} \varphi^2 &= -\frac{\lambda_2}{2\lambda_3}h^2 = -\frac{2\lambda_1}{\lambda_2}h^2 \,, \\ 4\lambda_1\lambda_3 &= \lambda_2^2 \,, \end{aligned} \tag{155}$$

where the couplings and fields are evaluated at the Gildener-Weinberg scale. In order for a radiative minimum to be obtained, we must have $\mathbb{B} > 0$ at the point of minimum (cf. section (2.3)). However, as in the case of the flat direction along the Higgs axis, it is not possible to obtain the electroweak vacuum at $\mu_{\text{GW}} \approx 246$ GeV without the presence of Landau pole below the Planck scale. To understand this, we compute the $\mathbb{B}$ function along the flat direction for $\mu \approx 246$ GeV,

$$\mathbb{B} \approx \frac{\lambda_2^2(1.95815 + 16(-1.82546 + (-2\lambda_1 + \lambda_2)^2))}{1024\pi^2(-2\lambda_1 + \lambda_2)^2} \,, \tag{156}$$

where we used eqs. (149) and (155), as well as the values of the gauge and Yukawa couplings at $\mu = 246$ GeV. In Figure 5.1, graphs of $\mathbb{B}$ in eq. (156) are shown for different values of λ_1 and λ_2.

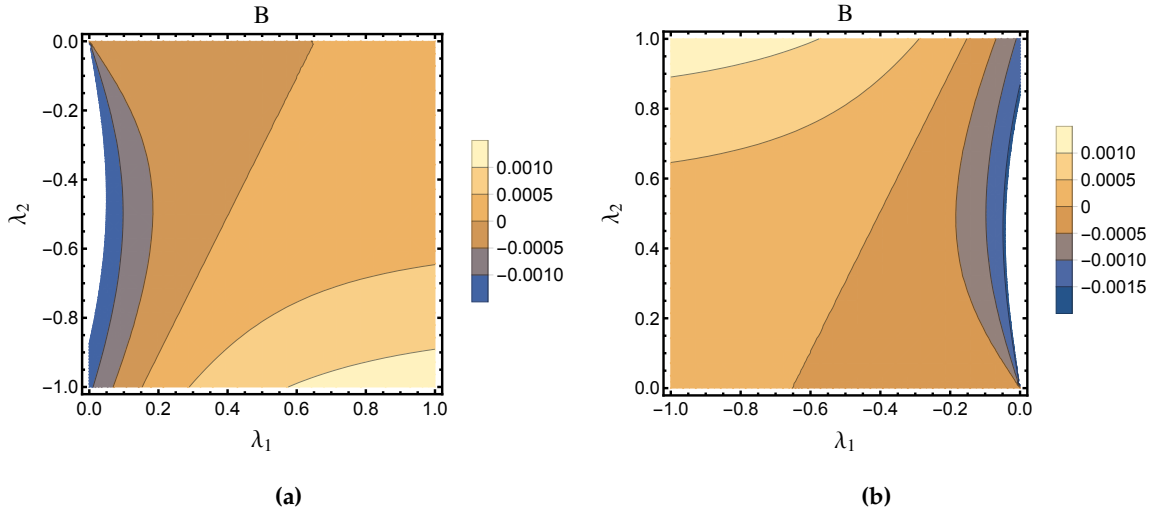

(a) **(b)**

Figure 5.1 – Graphs of $\mathbb{B}$ along the general flat direction for different values of λ_1 and λ_2.

We see that $\mathbb{B}$ is positive along the flat direction for a range of values of λ_1 and λ_2. However, using the values of λ_1 and λ_2 above* for which $\mathbb{B}$ is positive as boundary conditions for the numerical integration of the system of eqs. (152), we find Landau poles below the Planck scale. This signals that, even if the potential is RG-improved, the model does not remain perturbative up to the Planck scale. We, therefore, discard the possibility that the radiative breakdown of symmetry occurs via the Gildener-Weinberg mechanism (Case I).

*We refrain from showing graphs of other regions of parameter space. A numerical integration of the β-functions shows that the values of the couplings in other regions in which $\mathbb{B}$ is positive also lead to instabilities and have the further unpleasant property of allowing for negative values of λ_1.

5.4 Radiative Extrema

Let us now consider Case II, in the regime in which $\mathbf{g} \gtrsim \lambda_1 \gg \lambda_2, \lambda_3$, where $\mathbf{g}$ stands for a typical gauge coupling. To first approximation, we neglect the contributions from the singlet to the effective potential, which then becomes identical to (117). The one-loop effective potential is then approximated by

$$V = \frac{\lambda_1}{4}h^4 + \frac{\lambda_2}{4}h^2\varphi^2 + \frac{\lambda_3}{4}\varphi^4 + \mathbb{A}h^4 + \mathbb{B}h^4 \log\frac{h^2}{\mu^2} \,, \tag{157}$$

where $\mathbb{A}$ and $\mathbb{B}$ are evaluated at $\lambda_2 = \lambda_3 = 0$. This approximation corresponds to keeping only first order in λ_2, λ_3. Moreover, this is equivalent to setting $\varphi = 0$ in the one-loop contribution, which justifies factoring out the pivot mass h instead of the radius ρ. We will denote the field-VEVs as $\langle h \rangle = v$ and $\langle \varphi \rangle = w$ and we will set the subtraction mass to be the VEV of the Higgs field, i.e., $\mu = v$. If we wish to match the situation in the Standard Model, we set $v = 246$ GeV. The stationary point equations read

$$\begin{aligned} 0 &= \lambda_1 v^3 + \frac{\lambda_2}{2}vw^2 + 4\mathbb{A}v^3 + 2\mathbb{B}v^3 \,, \\ 0 &= \frac{\lambda_2}{2}v^2 w + \lambda_3 w^3 \,. \end{aligned} \tag{158}$$

We are not interested in the $w = 0$ solution, since it reproduces the Conformal Standard Model result (133). For $w \neq 0$, we find

$$w^2 = -\frac{\lambda_2}{2\lambda_3}v^2 \,, \tag{159}$$

which implies $\langle \varphi \rangle$ is real if $\lambda_2 < 0$ or $\lambda_3 < 0$. Using eq. (159), we can solve the first of eqs. (158) for λ_3 as a function of λ_1 and λ_2. We find that, if λ_1 is positive (negative), then λ_3 is positive (negative), which implies λ_2 must be negative (positive) in order for the VEV of the singlet to be real. We note that the potential is not bounded from below if $\lambda_1, \lambda_3 < 0$. However, we expect that the one-loop approximation will only be valid in the vicinity of the stationary point and, therefore, the issue of stability of the potential will be left for the RG-improved potential. In this way, we allow negative values of λ_1 and λ_3 in this approximation. At the stationary point, we then find the Hessian matrix

$$\mathrm{M}^2 = v^2 \begin{pmatrix} 2\lambda_1 + 8\mathbb{A} + 4\mathbb{B} & \lambda_2 \frac{w}{v} \\ \lambda_2 \frac{w}{v} & -\lambda_2 \end{pmatrix} \,,$$

with eigenvalues

$$\frac{M_\pm^2}{v^2} = \frac{1}{2}\left(2\lambda_1 + 8\mathbb{A} + 4\mathbb{B} - \lambda_2\right) \pm \frac{1}{2}\sqrt{\left(2\lambda_1 + 8\mathbb{A} + 4\mathbb{B} + \lambda_2\right)^2 + 4\lambda_2^2 \frac{w^2}{v^2}} \,. \tag{160}$$

With the assumed hierarchy of couplings $\mathbf{g} \gtrsim \lambda_1 \gg \lambda_2, \lambda_3$, we expect that the largest eigenvalue in eq. (160) will correspond to the physical Higgs mass and the smallest eigenvalue will yield a light extra scalar. To conform to current experimental bounds, the portal coupling λ_2 must then be very small.

However, a detailed numerical analysis reveals that it is not possible to have both eigenvalues in eq. (160) positive, even for very small values of λ_2. In Figures 5.2 and 5.3, graphs of both eigenvalues in eq. (160) are shown for different values of the parameters λ_1 and λ_2 in the perturbative regime[†]. From Figure 5.2, we see that the stationary point is generally a saddle in the

[†]We discard values for which Landau poles appear before the Planck scale.

regime $\lambda_1 > 0$ and $\lambda_2 < 0$. In particular, in the region in which $\frac{M_+^2}{v^2}$ assumes the Standard Model value for the Higgs mass-to-VEV ratio of approximately 0.26, the eigenvalue $\frac{M_-^2}{v^2}$ is a negative number with small absolute value. On the other hand, in the regime $\lambda_1 < 0$ and $\lambda_2 > 0$, only maxima are found for perturbative values of the couplings, as can be seen in Figure 5.3.

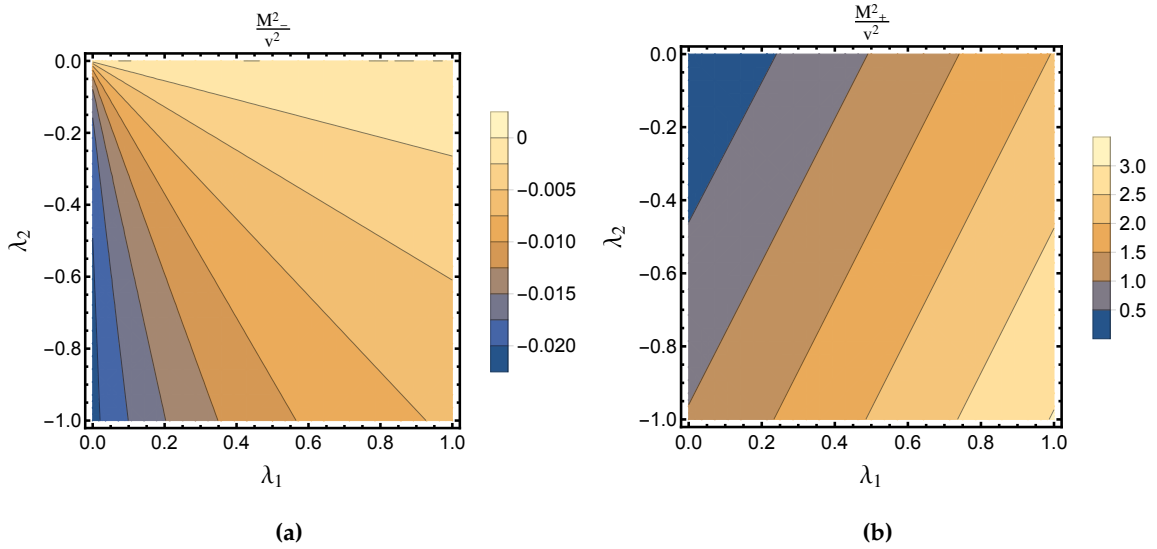

(a) **(b)**

Figure 5.2 – The mass eigenvalues of eq. (160) for positive λ_1 and negative λ_2 in the perturbative regime.

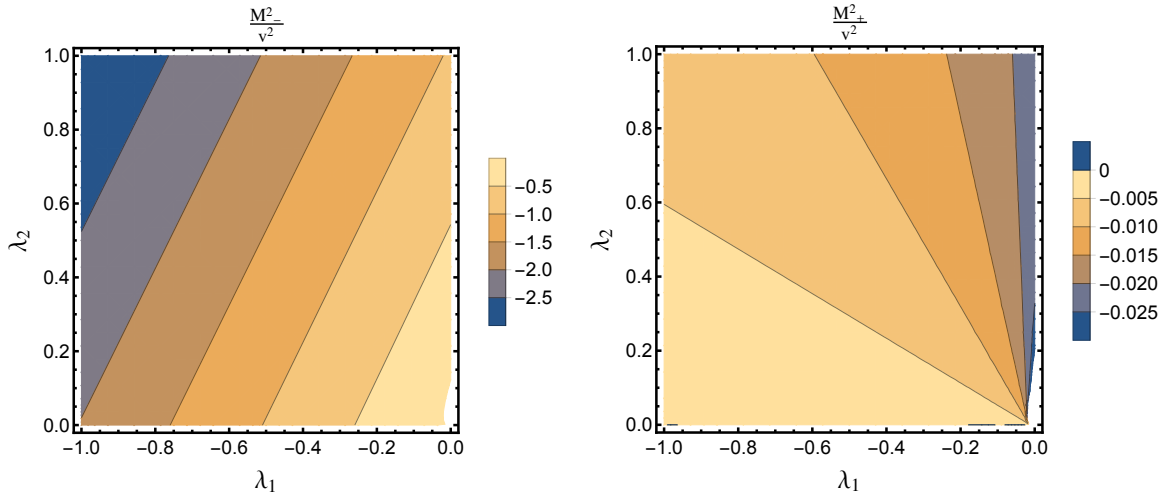

(a) **(b)**

Figure 5.3 – The mass eigenvalues of eq. (160) for negative λ_1 and positive λ_2 in the perturbative regime.

We conclude that imposing a hierarchy of couplings $\mathrm{g} \gtrsim \lambda_1 \gg \lambda_2, \lambda_3$, in the spirit of the orig-

inal paper by S. Coleman and E. Weinberg [3], cannot generate the electroweak vacuum with running couplings that remain perturbative for scales below the Planck scale. Together with the results of the previous section, we thus find that the minimal classically conformal extension of the Standard Model does not accommodate the dynamical generation of the electroweak scale. This is in accord with previous findings in the literature. A recent example is reference [34], in which the authors discuss of this model with a view to early-Universe physics. They conclude that the minimal extension of the Standard Model is excluded by doing a Gildener-Weinberg analysis, although they do not consider the Coleman-Weinberg case. In the next chapter, we will see that adding extra gauge bosons to the hidden sector makes the model sufficiently robust such that dynamical symmetry breaking can occur.

Chapter 6

Conformal Standard Model with a hidden $SU(2)$ Gauge Group

In the previous chapter, we concluded that adding a real scalar singlet to the Conformal Standard Model lagrangian was not sufficient to yield a dynamical generation of the electroweak scale. To increase the sophistication of the model, we could promote the additional field to a complex scalar and make its symmetry group local, i.e., the model could feature a hidden $U(1)$ gauge group. However, from the point of view of an ultraviolet completion of the model, it is more interesting to have a gauge coupling that vanishes in the far ultraviolet. This cannot be achieved with a running $U(1)$ gauge coupling, but rather with an $SU(N)$ coupling parameter.

In this chapter, we will thus consider an extended scalar sector comprised of the Standard Model Higgs doublet and an additional scalar doublet, which transforms under a hidden $SU(2)$ gauge group. This model exhibits all the qualitative features of interest for radiative symmetry breaking and allows for a detailed analysis of the RG-improvement techniques developed in Chapter 3 and appendix B. We will use RG-improvement to analyse the stability and the large field behaviour of the model and we will conclude that perturbation theory remains valid at all scales below the Planck scale for suitable boundary conditions of the running coupling parameters. More complicated models which have been studied in the literature can be analysed and RG-improved in an entirely analogous way.

The tree-level potential for such a classically conformal lagragian is thus of the form

$$V^{(0)} = \lambda_1 (H^\dagger H)^2 + \lambda_2 H^\dagger H \Phi^\dagger \Phi + \lambda_3 (\Phi^\dagger \Phi)^2 \,, \tag{161}$$

where H is the Standard Model Higgs $SU(2)$ complex doublet and Φ is the complex doublet which transforms under the hidden $SU(2)$ gauge group, given by

$$\Phi = \frac{1}{\sqrt{2}} \begin{pmatrix} \varphi_1 + i\varphi_2 \\ \varphi_3 + i\varphi_4 \end{pmatrix} \,.$$

6.1 The One-Loop Effective Potential

The tree-level mass eigenvalues can be straightforwardly computed due to the symmetry of eq. (161). Indeed, if we define $\vec{h} := (h_1, h_2, h_3, h_4)$ and $\vec{\varphi} := (\varphi_1, \varphi_2, \varphi_3, \varphi_4)$, such that $h^2 \equiv \vec{h}^2 =$

$2H^\dagger H$ and $\varphi^2 \equiv \vec{\varphi}^2 = 2\Phi^\dagger\Phi$, we can write the second derivatives of the tree-level potential as

$$\begin{aligned}
\frac{\partial^2 V^{(0)}}{\partial h_a \partial h_b} &= \left(\frac{\delta_{ab}}{h} - \frac{h_a h_b}{h^3}\right)\frac{\partial V^{(0)}}{\partial h} + \frac{h_a h_b}{h^2}\frac{\partial^2 V^{(0)}}{\partial h^2}\,, \\
\frac{\partial^2 V^{(0)}}{\partial h_a \partial \varphi_i} &= \frac{h_a \varphi_i}{h\varphi}\frac{\partial^2 V^{(0)}}{\partial h \partial \varphi}\,, \\
\frac{\partial^2 V^{(0)}}{\partial \varphi_i \partial \varphi_j} &= \left(\frac{\delta_{ij}}{\varphi} - \frac{\varphi_i \varphi_j}{\varphi^3}\right)\frac{\partial V^{(0)}}{\partial \varphi} + \frac{\varphi_i \varphi_j}{\varphi^2}\frac{\partial^2 V^{(0)}}{\partial \varphi^2}\,.
\end{aligned}$$

The action of the Hessian matrix on any multiple $\vec{\psi} = \left(\vec{\xi}, \vec{0}\right)$ is given by

$$\begin{aligned}
\sum_b \frac{\partial^2 V^{(0)}}{\partial h_a \partial h_b}\xi_b &= \left(\frac{\xi_a}{h} - \frac{h_a}{h^3}\vec{h}\cdot\vec{\xi}\right)\frac{\partial V^{(0)}}{\partial h} + \frac{h_a}{h^2}\frac{\partial^2 V^{(0)}}{\partial h^2}\vec{h}\cdot\vec{\xi}\,, \\
\sum_b \frac{\partial^2 V^{(0)}}{\partial \varphi_i \partial h_b}\xi_b &= \frac{\varphi_i}{h\varphi}\frac{\partial^2 V^{(0)}}{\partial h \partial \varphi}\vec{h}\cdot\vec{\xi}\,,
\end{aligned}$$

which becomes an eigenvector equation with eigenvalue $\frac{1}{h}\frac{\partial V^{(0)}}{\partial h}$ if $\vec{h}\cdot\vec{\xi} = 0$. There are three such eigenvectors, which correspond to the Goldstone directions of the Higgs field. Analogously, by analysing the action of the Hessian on a multiple $\vec{\psi} = \left(\vec{0}, \vec{\chi}\right)$, one finds three more eigenvalues, equal to $\frac{1}{\varphi}\frac{\partial V^{(0)}}{\partial \varphi}$, which correspond to the Goldstone masses of the Φ field. Note that the Goldstone masses vanish at stationary points of $V^{(0)}$, as they should. The remaining two eigenvalues can be found by a rotation in the scalar-field configuration space to the basis $\left\{\left(\vec{h}, \vec{0}\right), \left(\vec{0}, \vec{\varphi}\right), \left(\vec{\xi}, \vec{0}\right), \left(\vec{0}, \vec{\chi}\right)\right\}$, in which the Hessian is block diagonal. The unknown eigenvalues are then roots of the secular equation for the non-diagonal block, i.e.,

$$\det\begin{pmatrix} \frac{\partial^2 V^{(0)}}{\partial h^2} - \omega & \frac{\partial^2 V^{(0)}}{\partial h \partial \varphi} \\ \frac{\partial^2 V^{(0)}}{\partial \varphi \partial h} & \frac{\partial^2 V^{(0)}}{\partial \varphi^2} - \omega \end{pmatrix} = 0\,.$$

From eq. (161), we thus obtain the tree-level mass spectrum in the scalar sector (compare with eq. (147))

$$\begin{aligned}
m_1^2 &= \frac{1}{2}\left(3\lambda_1 + \frac{\lambda_2}{2}\right)h^2 + \frac{1}{2}\left(\frac{\lambda_2}{2} + 3\lambda_3\right)\varphi^2 - \\
&\quad - \frac{1}{2}\sqrt{\left[\left(3\lambda_1 - \frac{\lambda_2}{2}\right)h^2 - \left(3\lambda_3 - \frac{\lambda_2}{2}\right)\varphi^2\right]^2 + 4\lambda_2^2 h^2\varphi^2}\,, \\
m_2^2 &= m_3^2 = m_4^2 = \lambda_1 h^2 + \frac{\lambda_2}{2}\varphi^2\,, \\
m_5^2 &= m_6^2 = m_7^2 = \frac{\lambda_2}{2}h^2 + \lambda_3\varphi^2\,, \\
m_8^2 &= \frac{1}{2}\left(3\lambda_1 + \frac{\lambda_2}{2}\right)h^2 + \frac{1}{2}\left(\frac{\lambda_2}{2} + 3\lambda_3\right)\varphi^2 + \\
&\quad + \frac{1}{2}\sqrt{\left[\left(3\lambda_1 - \frac{\lambda_2}{2}\right)h^2 - \left(3\lambda_3 - \frac{\lambda_2}{2}\right)\varphi^2\right]^2 + 4\lambda_2^2 h^2\varphi^2}\,.
\end{aligned} \tag{162}$$

The mass eigenvalues of vector bosons and fermions are the same as in eqs. (115) and (116). We can compute the field-dependent mass of the hidden gauge boson in an entirely analogous way

as the masses in eq. (115). We find the eigenvalue

$$m_d^2 = \frac{g_d^2}{4}\varphi^2 \,, \tag{163}$$

with multiplicity three, where g_d is the gauge coupling of the hidden $SU(2)$ group. The one-loop effective potential is then of the same form as in eq. (148), only now the $\mathbb{A}$ and $\mathbb{B}$ functions read

$$\begin{aligned}
\mathbb{A}(\lambda,\theta) = \frac{1}{64\pi^2\rho^4}\Bigg\{&\sum_{i=1}^{5}\left(m_i^4\log\left(\frac{m_i^2}{\rho^2}\right)-\frac{3}{2}m_i^4\right)+6m_W^4\log\left(\frac{m_W^2}{\rho^2}\right)-\\
&-5m_W^4+3m_Z^4\log\left(\frac{m_Z^2}{\rho^2}\right)-\frac{5}{2}m_Z^4-3Y_t^4\cos^4\theta\left[\log\left(\frac{Y_t^2}{2}\cos^2\theta\right)-\frac{3}{2}\right]+\\
&+9m_d^4\log\left(\frac{m_d^2}{\rho^2}\right)-\frac{15}{2}m_d^4\Bigg\}\,,\\
\mathbb{B}(\lambda,\theta) = \frac{1}{64\pi^2\rho^4}&\left[\sum_{i=1}^{5}m_i^4+6m_W^4+3m_Z^4-3Y_t^4h^4+9m_d^4\right]\,,
\end{aligned}$$

where, as before, the pivot mass is the radius in the scalar-field configuration space and we defined the angle

$$\begin{aligned}
\cos^2\theta &:= \frac{h^2}{\rho^2} = \frac{\rho^2-\varphi^2}{\rho^2} = 1-\frac{\varphi^2}{\rho^2} =: 1-\sin^2\theta\,,\\
h^2 &:= h_1^2+h_2^2+h_3^3+h_4^2\,.
\end{aligned}$$

The $\mathbb{B}$ function now reads (compare with eq. (149))

$$\begin{aligned}
64\pi^2\mathbb{B}(\lambda,\theta) = &\left(12\lambda_1^2+\lambda_2^2+\frac{3}{8}g^4+\frac{3}{16}(g^2+g'^2)^2-3Y_t^4\right)\cos^4\theta+\\
&+\left(6\lambda_1\lambda_2+2\lambda_2^2+6\lambda_2\lambda_3\right)\cos^2\theta\sin^2\theta+\\
&+\left(\lambda_2^2+12\lambda_3^2+\frac{9}{16}g_d^4\right)\sin^4\theta\,.
\end{aligned} \tag{164}$$

Running Parameters

The RG equation for the effective potential of the Higss portal model with a hidden $SU(2)$ gauge field reads

$$\left(\mu\frac{\partial}{\partial\mu}+\sum_{j=1}^{3}\beta_j\frac{\partial}{\partial\lambda_j}+\beta_g\frac{\partial}{\partial g}+\beta_{g'}\frac{\partial}{\partial g'}+\beta_t\frac{\partial}{\partial Y_t}+\beta_d\frac{\partial}{\partial g_d}-\frac{1}{2}\gamma_h h\frac{\partial}{\partial h}-\frac{1}{2}\gamma_\varphi\varphi\frac{\partial}{\partial\varphi}\right)V=0\,.$$

At one-loop level, the anomalous dimension of the extra scalar doublet is

$$\gamma_\varphi = \frac{-9g_d^2}{32\pi^2}\,. \tag{165}$$

By truncating the RG equation to one-loop order, we obtain

$$(\beta_1-2\lambda_1\gamma_h)\cos^4\theta+(\beta_2-\lambda_2\gamma_h-\lambda_2\gamma_\varphi)\cos^2\theta\sin^2\theta+(\beta_3-2\lambda_3\gamma_\varphi)\sin^4\theta = 8\mathbb{B}(\lambda,\theta)\,. \tag{166}$$

Together with (164), this implies the one-loop scalar-sector β-functions read (compare with (152))

$$\begin{aligned}
\beta_1 &= \frac{1}{8\pi^2}\left[12\lambda_1^2 + \lambda_2^2 + \frac{\lambda_1}{2}\left(-9g^2 - 3g'^2 + 12Y_t^2\right) + \frac{3g^4}{8} + \frac{3(g^2+g'^2)^2}{16} - 3Y_t^4\right] , \\
\beta_2 &= \frac{1}{8\pi^2}\left[6\lambda_1\lambda_2 + 2\lambda_2^2 + 6\lambda_2\lambda_3 + \frac{\lambda_2}{4}\left(-9g^2 - 3g'^2 + 12Y_t^2 - 9g_d^2\right)\right] , \\
\beta_3 &= \frac{1}{8\pi^2}\left[\lambda_2^2 + 12\lambda_3^2 - \frac{9}{2}\lambda_3 g_d^2 + \frac{9g_d^4}{16}\right] .
\end{aligned} \tag{167}$$

Moreover, the β-function for the hidden gauge coupling reads [24]

$$\beta_d = \frac{1}{16\pi^2}\left(-\frac{43}{6}g_d^3 - \frac{1}{(4\pi)^2}\frac{259}{6}g_d^5\right) . \tag{168}$$

In Figure 6.1, the running gauge coupling of the hidden $SU(2)$ group is shown. We have chosen the boundary value $g_d(\mu = m_Z) = 1$.

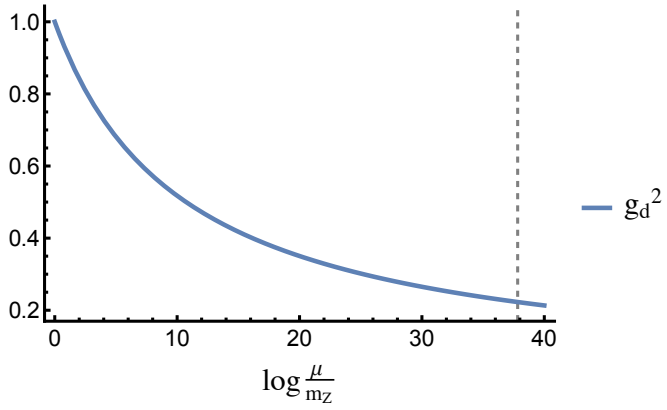

Figure 6.1 – Numerical solution for the gauge coupling of the hidden $SU(2)$ group with the boundary value $g_d(\mu = m_Z) = 1$. The dashed vertical line marks the Planck scale at $t_P \approx 37.8$.

6.2 Hierarchy of Couplings

To search for radiative extrema and avoid large logarithms, we consider Case II outlined in section (2.4), with the hierarchy of couplings $\lambda_1, \lambda_2, \lambda_3 \lesssim \mathcal{O}(\mathbf{g}^4)$, where $\mathbf{g}$ stands for a typical gauge coupling. In this regime, we can neglect the scalar-sector contributions to the one-loop approximation. The effective potential up to one-loop order is then approximated by

$$\begin{aligned}
V = &\frac{\lambda_1}{4}h^4 + \frac{\lambda_2}{4}h^2\varphi^2 + \frac{\lambda_3}{4}\varphi^4 + \\
&+ \mathbb{A}_{\text{SM}}h^4 + \mathbb{B}_{\text{SM}}h^4\log\frac{h^2}{\mu^2} + \frac{9g_d^4}{64\pi^2}\frac{\varphi^4}{16}\left(\log\frac{g_d^2\varphi^2}{4\mu^2} - \frac{5}{6}\right) ,
\end{aligned} \tag{169}$$

where we defined

$$\begin{aligned}\mathbb{A}_{\text{SM}} &:= \frac{1}{64\pi^2 h^4}\left\{6m_W^4\log\left(\frac{m_W^2}{h^2}\right) - 5m_W^4 + 3m_Z^4\log\left(\frac{m_Z^2}{h^2}\right) - \frac{5}{2}m_Z^4 - \right.\\ &\left. -3Y_t^4\left[\log\left(\frac{Y_t^2}{2}\right) - \frac{3}{2}\right]\right\}\,, \\ \mathbb{B}_{\text{SM}} &:= \frac{1}{64\pi^2}\left(\frac{3}{8}g^4 + \frac{3}{16}(g^2+g'^2)^2 - 3Y_t^4\right)\,,\end{aligned} \tag{170}$$

for convenience. As before, we denote the field-VEVs by $\langle h\rangle = v$ and $\langle\varphi\rangle = w$ and we set the subtraction mass to be the VEV of the Higgs field, i.e., $\mu = v = 246$ GeV. The stationary point equations read

$$\begin{aligned}0 &= \lambda_1 v^3 + \frac{\lambda_2}{2}vw^2 + 4\mathbb{A}_{\text{SM}}v^3 + 2\mathbb{B}_{\text{SM}}v^3\,, \\ 0 &= \frac{\lambda_2}{2}v^2 w + \lambda_3 w^3 + \frac{9g_d^4}{64\pi^2}\frac{w^3}{4}\left(\log\frac{g_d^2 w^2}{4v^2} - \frac{1}{3}\right)\,.\end{aligned} \tag{171}$$

The first of eqs. (171) is identical to the corresponding equation obtained in the Standard Model, if we regard the term proportional to w^2 as an effective mass parameter for the Higgs field generated by the VEV of the extra scalar. We will thus regard w as a free parameter, which we will tune to obtain the correct Higgs boson mass below. We note that we can express λ_1 and λ_3 as functions of λ_2 and w by solving eqs. (171). At a stationary point, the Hessian matrix of the potential in eq. (169) reads

$$\mathrm{M}^2 = v^2\begin{pmatrix} 2\lambda_1 + 8\mathbb{A}_{\text{SM}} + 4\mathbb{B}_{\text{SM}} & \lambda_2\frac{w}{v} \\ \lambda_2\frac{w}{v} & 2\lambda_3\frac{w^2}{v^2} + \frac{9g_d^4}{128\pi^2}\frac{w^2}{v^2}\left(\log\frac{g_d^2w^2}{4v^2} + \frac{2}{3}\right)\end{pmatrix}\,. \tag{172}$$

In Figure 6.2, graphs of the eigenvalues of $\frac{\mathrm{M}^2}{v^2}$ in eq. (172) are shown for different values of the free parameters λ_2 and w.
We see that there exists a range of values* of λ_2 and w for which one mass eigenvalue is close to the physical Higgs mass-to-VEV ratio in the Standard Model of approximately 0.26. In this range, the other eigenvalue is positive and larger. We therefore conclude that the Higgs portal model with a hidden $SU(2)$ gauge group is capable of dynamically generating the electroweak vacuum, for a suitable choice of parameters, and we find a heavy extra scalar in addition to the physical Higgs field.

From Figure 6.2, we choose the boundary value

$$\lambda_2(\mu = v) = -0.001\,, \tag{173}$$

for which the smallest mass eigenvalue equals 0.26 if the extra scalar has a VEV equal to

$$w = 4129.61\text{ GeV}\,. \tag{174}$$

With these values, we can solve eqs. (171) for λ_1 and λ_3 to obtain

$$\begin{aligned}\lambda_1(\mu = v) &\approx 0.12\,, \\ \lambda_3(\mu = v) &\approx -0.011\,.\end{aligned} \tag{175}$$

Note that the tree-level potential is unbounded from below for negative λ_3. This is, however, not an issue, since the one-loop approximation (169) will only be valid when the logarithmic terms

*One may verify that positive values of λ_2 lead to a saddle point, which is not of interest.

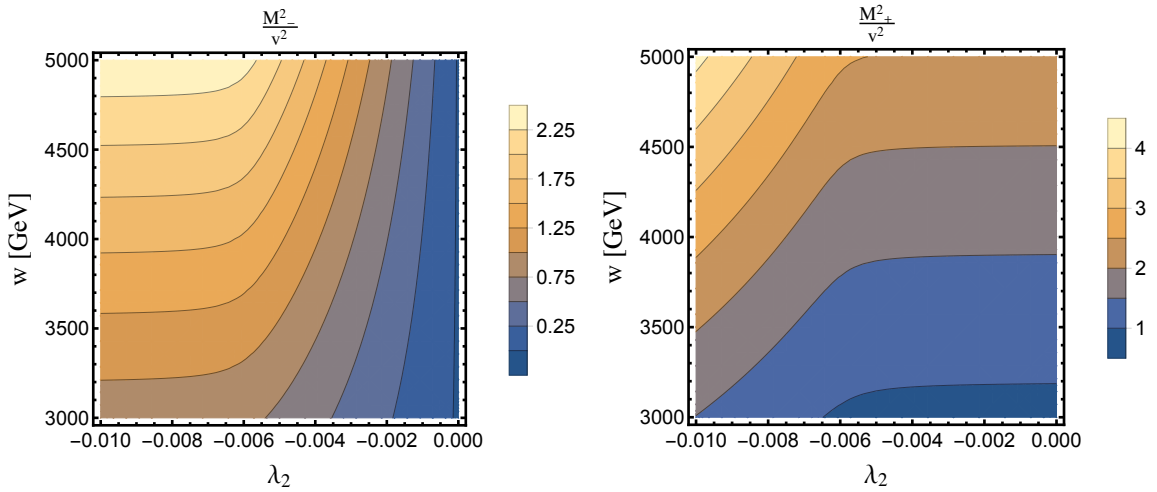

(a) **(b)**

Figure 6.2 – Mass eigenvalues of the Hessian in eq. (172) for different values of the free parameters λ_2 and w.

are negligible. For large field values, such logarithms grow large and eq. (169) is no longer a reliable approximation of the effective potential. We must, therefore, RG-improve the effective potential to study stability. We will do so in the next section.

With the boundary values in eqs. (173) and (175), one may explicitly verify that no large logarithmic contributions are featured in eq. (169). The products of logarithms with couplings are all less than $3.5 < 4\pi$ at the radiative minimum. Analogously, one may compute the scalar-sector contributions to the one-loop term and verify that they are indeed negligible around the stationary point. Thus, the one-loop approximation (169) is reliable and we may trust the electroweak vacuum found above. At the minimum, the mass eigenvalues of eq. (172) are

$$\begin{aligned} m_h &\equiv M_- \approx 125.44 \text{ GeV} , \\ m_\varphi &\equiv M_+ \approx 318.91 \text{ GeV} . \end{aligned} \tag{176}$$

The extra scalar particle is therefore heavier than the physical Higgs. In Figures 6.3 and 6.4, the graphs of the one-loop approximation (169) are shown.
In particular, from Figure 6.4, we see that the potential along the Higgs direction is almost constant, which can be understood from the high value of the hidden $SU(2)$ gauge coupling at the scale of the minimum,

$$g_d^2(\mu = v) \approx 0.91 .$$

A numerical search confirms that there is indeed a global minimum at $(h = v, \varphi = w)$.

Finally, by implementing the boundary conditions of eqs. (173) and (175) and integrating the β-functions in eq. (167), we find the running scalar-sector couplings depicted in Figure 6.5. For the tree-level potential given in eq. (161), the copositivity of the coupling matrix translates into the conditions

$$\lambda_1 > 0 , \ \lambda_3 > 0 , \ 4\lambda_1\lambda_3 - \lambda_2^2 > 0 .$$

From Figure 6.5, we see that the determinant of the coupling matrix, $4\lambda_1\lambda_3 - \lambda_2^2$, and both self-couplings λ_1 and λ_3 are positive at high energies. We thus conclude that the RG-improved

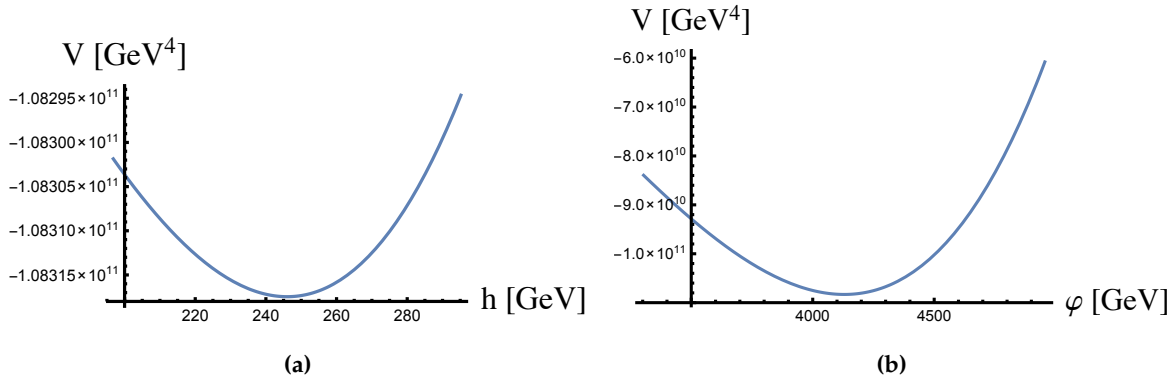

(a) **(b)**

Figure 6.3 – (a) Graph of the potential in eq. (169) for different values of the Higgs field h, with the value of extra scalar fixed to $\varphi = w$. A minimum is present at $h = 246$ GeV. (b) Graph of the potential in eq. (169) for different values of the extra doublet field φ, with the value of Higgs field fixed to $h = v$. A minimum is present at $\varphi = 4129.61$ GeV.

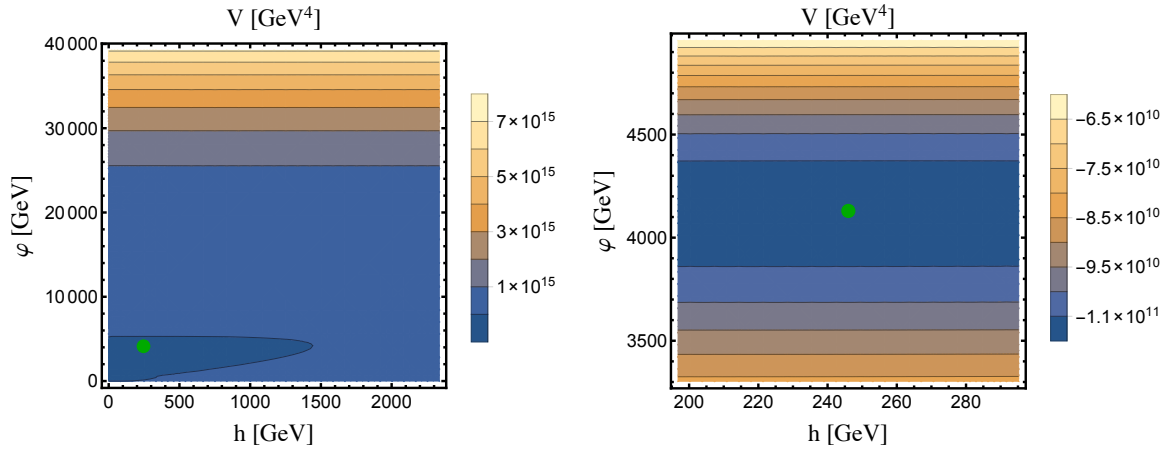

(a) **(b)**

Figure 6.4 – Contour plots of the potential in eq. (169) for different values of the scalar fields. The electroweak vacuum is denoted by the green dot.

potential and, therefore, the full effective potential (cf. Chapter 3) will be bounded from below for this model. Moreover, all couplings remain perturbative up to the Planck scale and we conclude that the Higgs portal model with a hidden $SU(2)$ gauge group is capable of accommodating the dynamical generation of the electroweak scale and remains valid for all scales below the Planck scale.

This model was studied in a slightly different fashion in [24]. In that reference, the authors choose to reproduce the Coleman-Weinberg reasoning for scalar QED in the Higgs portal model. They first work in the decoupling limit $\lambda_2 \to 0$ to impose that radiative symmetry breaking occurs in the hidden sector at the scale of the VEV for the extra doublet, which then is tuned such that the mass parameter for the Higgs field in Standard Model is reproduced. This method can correctly reproduce the observed Higgs mass, as was shown in [24]. However, we see from the

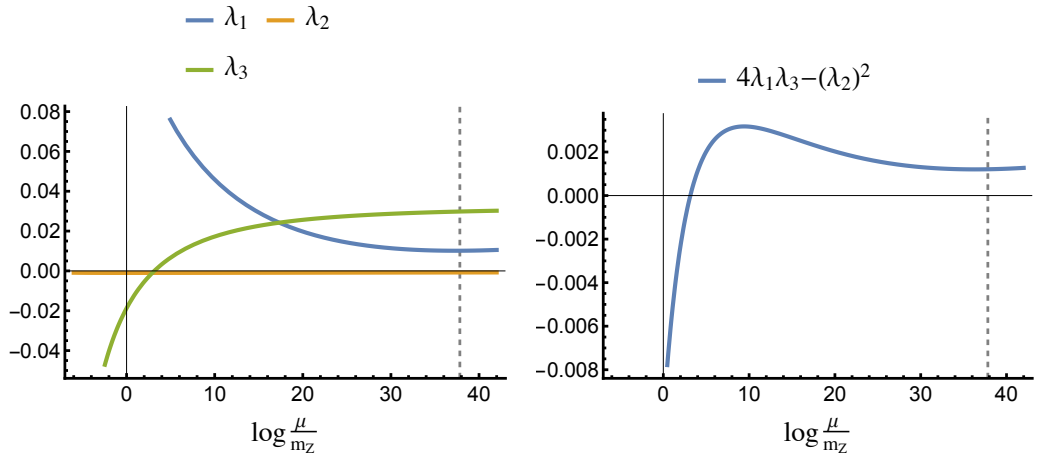

Figure 6.5 – (a) Running coupling parameters in the scalar sector with boundary values given in eqs. (173) and (175). (b) Running determinant of the coupling matrix for the scalar-sector. The dashed vertical line marks the Planck scale at $t_P \approx 37.8$.

above analysis that such a sequential approach to the problem, in which one first considers the Coleman-Weinberg case in the hidden sector and then tunes the scale $\mu = \langle\varphi\rangle$, is not necessary.

Indeed, if we follow the insight of S. Coleman and E. Weinberg and consider an adequate hierarchy of couplings (as was outlined in section 2.4), we see that there is no need to consider the decoupling limit, since both stationary point eqs. (171) can be solved simultaneously in the one-loop approximation, as we showed. Moreover, instead of fixing $\mu = \langle\varphi\rangle$, we can choose $\mu = \langle h\rangle = 246$ GeV directly, which clarifies the meaning of the radiative generation of the electroweak scale.

To see this, we note that, even though the pole mass is obtained by taking into account the self-energy corrections at non-zero external momenta, which are not captured by Hessian in eq. (172), the running Higgs mass at the electroweak scale should be an adequate approximation of the pole mass, if the one-loop approximation is reliable. Therefore, we understand that the electroweak vacuum is dynamically generated if, at the scale of the radiative VEV of the Higgs field, the running masses of the particles approximate their Standard Model values. This is achieved in the above model.

Although the model correctly reproduces the electroweak vacuum, it can lead to different measurable cross sections in comparison to the Standard Model. For example, we may study the effective self-couplings of the physical Higgs particle, which is the mass-eigenstate with eigenvalue close to 125 GeV in eq. (176). To do this, we must first change basis in the scalar-field configuration space to the basis of mass-eigenstates,

$$\begin{aligned}\tilde{h} &= h\cos\theta + \varphi\sin\theta\,,\\ \tilde{\varphi} &= -h\sin\theta + \varphi\cos\theta\,,\end{aligned}$$

where θ is the mixing angle of the two scalar fields, such that $\tilde{h}$ and $\tilde{\varphi}$ satisfy (cf. eq. 176)

$$M\begin{pmatrix}\tilde{h}\\0\end{pmatrix} \approx 125.44\begin{pmatrix}\tilde{h}\\0\end{pmatrix}\,,\; M\begin{pmatrix}0\\\tilde{\varphi}\end{pmatrix} \approx 318.91\begin{pmatrix}0\\\tilde{\varphi}\end{pmatrix}\,.$$

We can then define the effective trilinear and quartic Higgs self-couplings as

$$\begin{aligned}\lambda_{\text{eff}}^{(3)} &:= \frac{1}{6}\frac{\partial^3 V}{\partial \tilde{h}^3}\,, \\ \lambda_{\text{eff}}^{(4)} &:= \frac{1}{6}\frac{\partial^4 V}{\partial \tilde{h}^4}\,.\end{aligned} \tag{177}$$

In Table 6.1, we collect the predicted values of the effective Higgs self-couplings and the mass of the extra scalar for different values of the portal coupling λ_2. In each case, one must set the VEV of the extra scalar such that the smallest mass eigenvalue reproduces the Higgs mass. We also include the relative differences of the predicted effective self-couplings to their corresponding values in the Standard Model,

$$\delta_{\text{SM}}\lambda^{(i)} := \frac{\lambda_{\text{eff}}^{(i)} - \lambda_{\text{SM}}^{(i)}}{\lambda_{\text{SM}}^{(i)}}\,,\ (i = 3, 4)\,.$$

We refrain from computing values of the portal coupling which are larger than 0.011 in magnitude because a numerical integration of the β-functions then leads to a Landau pole below the Planck scale.

λ_2	$\lambda_{\text{eff}}^{(3)}$	$\delta_{\text{SM}}\lambda^{(3)}$	$\lambda_{\text{eff}}^{(4)}$	$\delta_{\text{SM}}\lambda^{(4)}$	m_φ
-10^{-7}	30.21 GeV	-5.54%	0.10	-22.16%	31868.20 GeV
-10^{-6}	30.21 GeV	-5.54%	0.10	-22.16%	10077.60 GeV
-10^{-5}	30.21 GeV	-5.54%	0.10	-22.16%	3186.82 GeV
-0.0001	30.21 GeV	-5.54%	0.10	-22.16%	1007.77 GeV
-0.001	30.20 GeV	-5.56%	0.10	-22.11%	318.91 GeV
-0.004	28.61 GeV	-10.55%	0.097	-25.53%	163.20 GeV
-0.006	17.21 GeV	-46.19%	0.048	-62.88%	145.64 GeV
-0.01	7.90 GeV	-75.30%	0.010	-92.06%	168.00 GeV
-0.011	7.81 GeV	-75.57%	0.010	-92.24%	175.45 GeV

Table 6.1 – The predicted values for the effective Higgs self-couplings and mass of the extra-scalar in the Conformal Standard Model with a hidden $SU(2)$ gauge group for different values of the portal coupling λ_2. All values are approximated to two decimal places.

We note that smaller portal couplings yield a heavier extra scalar and better agreement with the Higgs self-couplings of the Standard Model.

6.3 RG Improvement

To analyse the large-field behaviour of the effective potential of the Higgs portal model with a hidden $SU(2)$ gauge group, we need to RG-improve the potential. Improvement will also allows to verify the reliability of the one-loop approximation. The RG-improved effective potential reads (cf. section (3.2.2))

$$\begin{aligned}V &= \frac{\lambda_1(t_*)}{4}Z_h^{-2}(t_*)h^4 + \frac{\lambda_2(t_*)}{4}Z_h^{-1}(t_*)Z_\varphi^{-1}(t_*)h^2\varphi^2 + \frac{\lambda_3(t_*)}{4}Z_\varphi^{-2}(t_*)\varphi^4\,, \\ t_* &= \frac{\mathbb{A}_{\text{SM}}h^4 + \mathbb{B}_{\text{SM}}h^4\log\frac{h^2}{v^2} + \frac{9g_d^4}{64\pi^2}\frac{\varphi^4}{16}\left(\log\frac{g_d^2\varphi^2}{4v^2} - \frac{5}{6}\right)}{\frac{1}{32\pi^2}\left(3m_Z^4 + 6m_W^4 - 3Y_t^4h^4 + 9m_d^4\right)}\,,\end{aligned} \tag{178}$$

where Z_h and Z_φ are the normalisations of the Higgs and extra doublet fields, respectively.

Let us recall that the meaning of eq. (178). We start at mass $v = 246$ GeV and run the parameters along a characteristic curve to a hypersurface at which loop corrections vanish. The characteristic displacement is, to lowest order, t_*. If we regard the potential (178) as evaluated at the mass $\mu = v = 246$ GeV, then all orders in $\hbar$ are re-summed in the running couplings $\lambda(t_*) \equiv \lambda_*$ and field normalisations $Z(t_*) \equiv Z_*$. We note that h and φ denote the values of the Higgs and extra doublet fields, respectively, at $\mu = v = 246$ GeV. Moreover, for consistency with the previous section and due to the assumed hierarchy of couplings at this scale, we neglect the scalar-sector contributions in the numerator and denominator of t_*.

In Figures 6.6 and 6.7, graphs of the RG-improved potential are shown. By comparing Figures 6.3, 6.4, 6.6 and 6.7, we see that the improved potential does not change considerably around the minimum, which confirms the reliability of the above one-loop approximation.

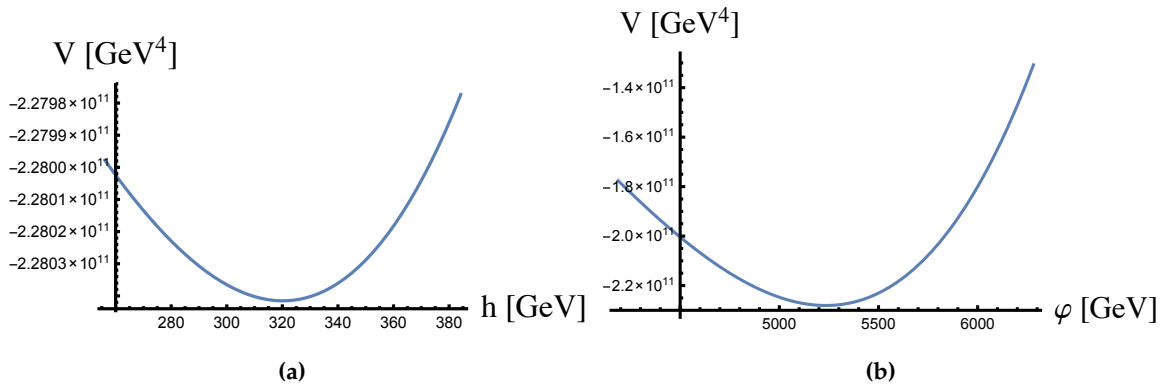

Figure 6.6 – (a) Graph of the RG-improved potential in eq. (178) for different values of the Higgs field h, with the value of extra scalar fixed to its value at the stationary point. A minimum is present at $h \approx 320.16$ GeV. (b) Graph of the RG-improved potential in eq. (178) for different values of the extra doublet field φ, with the value of Higgs field fixed to its value at the stationary point. A minimum is present at $\varphi \approx 5234.32$ GeV.

After a numerical search, one finds that the improved potential has a global minimum at the field values

$$\begin{aligned} h &\approx 320.16 \text{ GeV} , \\ \varphi &\approx 5234.32 \text{ GeV} , \end{aligned} \tag{179}$$

which differ from the values of the previous section by

$$\begin{aligned} \delta v &= \frac{320.16 - 246}{246} \approx 30.15\% , \\ \delta w &= \frac{5234.32 - 4129.61}{4129.61} \approx 26.75\% . \end{aligned}$$

These differences are understood from the fact that higher loop-orders can affect the one-loop results. Numerical precision also has to be taken into account and the use of values for the couplings and masses that are more precise than those employed here can lead to more accurate results.

We conclude that the Higgs portal model with a hidden $SU(2)$ gauge group can generate the electroweak vacuum for the choice of running couplings depicted in Figure 6.5. The model is perturbative at all scales below the Planck scale. Moreover, from the running of the couplings

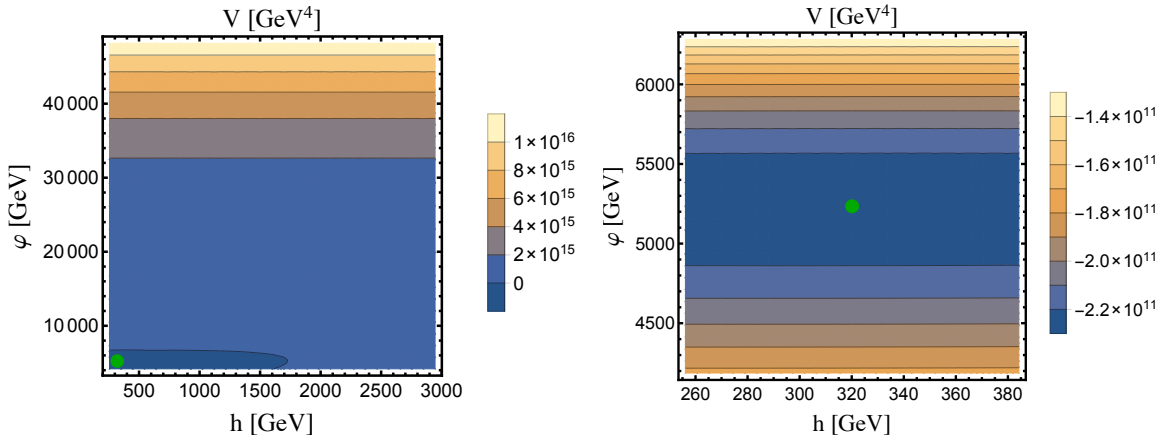

(a) **(b)**

Figure 6.7 – Contour plots of the RG-improved potential in eq. (178) for different values of the scalar fields. The global minimum in eq. (179), found numerically, is denoted by a green dot.

and the evaluation of the RG-improved potential for field values up to the Planck mass, we may infer that the one-loop improved effective potential is bounded from below (cf. section (3.2.2)).

The above results were achieved via the Coleman-Weinberg approach (Case II). Instead of attempting to repeat the above results in the Gildener Weinberg approach, we will slightly change the parameters of the model and study a Case I example which fails to identify the global minimum of the effective potential. This will illustrate the importance of correctly identifying in which case the model belongs and the utility of RG-improvement.

6.4 A Gildener-Weinberg Example

To illustrate the importance of distinguishing between Case I and Case II outlined in section (2.4), we will consider an interesting example where the Gildener-Weinberg approach, presented in section (2.3), fails to capture the global minimum, which is found with the improved version of the potential. This example also makes clear the importance of RG-improving. Indeed, the improved potential is valid in a much larger region of parameter space than the one-loop approximation and is thus able to correctly identify the global minimum.

Let us then consider the classically conformal model of Chapter 6 with a different choice of boundary values for running couplings. We choose the boundary conditions

$$\begin{aligned} g_{CW}(\mu = m_Z) &= 0.840125\,, \\ \lambda_1(\mu = m_Z) &= 0.140938\,, \\ \lambda_2(\mu = m_Z) &= -0.017367\,, \\ \lambda_3(\mu = m_Z) &= -0.00122639\,, \end{aligned} \tag{180}$$

for which the running of the scalar-sector couplings are depicted in Figure 6.8.

We see that the model is bounded from below, since the coupling matrix is copositive at high energies (cf. Chapter 3). This is not surprising since this model is very similar to the one analysed in Chapter 6, in which we used the hierarchy of couplings $\lambda_1, \lambda_2, \lambda_3 \lesssim \mathcal{O}(\mathbf{g}^4)$ to compute the one-loop approximation and found that it correctly determined the global minimum.

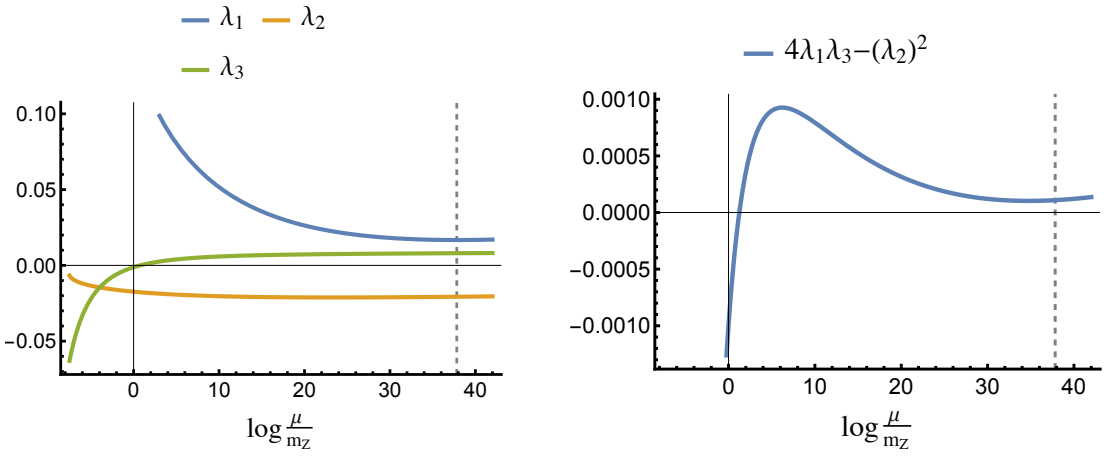

Figure 6.8 – (a) Running coupling parameters in the scalar sector with boundary values given in eq. (180). (b) Running determinant of the coupling matrix for the scalar-sector. The dashed vertical line marks the Planck scale at $t_P \approx 37.8$.

In the current example, we will ignore the fact that the model is Case II, and we will apply the Gildener-Weinberg approach (Case I). We will find that this approach does not identify the correct global minimum. This implies that a correct application of Case I or Case II is paramount to a reliable use of the one-loop approximation.

The potential acquires a flat direction when the determinant of the coupling matrix, given by $4\lambda_1\lambda_3 - \lambda_2^2$, vanishes. For the model at hand, this happens at the mass (cf. Figure 6.8)

$$\mu_{\rm GW} \approx 318.28 \text{ GeV} . \tag{181}$$

Along the flat direction, the square of the ratio of the Higgs field to the extra doublet field is

$$\frac{\varphi^2}{h^2} = -\frac{\lambda_2(\mu_{\rm GW})}{2\lambda_3(\mu_{\rm GW})} \approx 13.41 .$$

At this scale, the $\mathbb{B}$ function in eq. (164) reads $\mathbb{B} \approx 3.16 \times 10^{-4} > 0$. This signals that there will be a radiative minimum at the Gildener-Weinberg mass. We can compute the Higgs VEV from eq. (79). The result is

$$\langle h \rangle = v \approx 243.31 \text{ GeV} .$$

Furthermore, the only non-vanishing tree-level mass eigenvalue, which corresponds to the state orthogonal to the flat direction, is

$$m_h \approx 123.81 \text{ GeV} ,$$

i.e., the Higgs has a vacuum expectation value which is Standard-Model-like at the Gildener-Weinberg scale and the physical Higgs field can be identified with the state orthogonal to the flat direction. The state along the flat direction acquires a radiatively generated mass equal to

$$m_\varphi = v \sqrt{8\mathbb{B}\left(1 - \frac{\lambda_2}{2\lambda_3}\right)^2}\Bigg|_{\mu=\mu_{\rm GW}} \approx 46.47 \text{ GeV} .$$

We thus see that the extra scalar field is lighter than the physical Higgs particle, in contrast to what was found in the model of section (6.2) (cf. eq. (176)). The criterion used in the previous section, which established that the electroweak minimum should be generated at the scale of the Higgs VEV is also not realised, since the Gildener-Weinberg mass in eq. (181) is larger than the Higgs VEV. Nevertheless, the current model exhibits the electroweak minimum, in the sense that the Higgs mass and vacuum expectation value are approximately reproduced at the Gildener-Weinberg scale.

Let us now consider the RG-improved potential, given by eq. (178). Recall that, due to the hierarchy $\lambda_1, \lambda_2, \lambda_3 \lesssim \mathcal{O}(\mathbf{g}^4)$, we ignore the scalar-sector contributions to the one-loop term. A numerical search shows that the global minimum of the improved potential is located far away from the Gildener-Weinberg minimum, approximately at the field values

$$\langle h \rangle = v \approx 2489.21 \text{ GeV} \, , \langle \varphi \rangle = w \approx 6896.44 \text{ GeV} \, .$$

Furthermore, a numerical computation of the Hessian shows that the Gildener-Weinberg minimum ceases to be a stationary point after improvement. In Figure 6.9, the minimum of the one-loop approximation and the global minimum of the one-loop improved potential are shown.

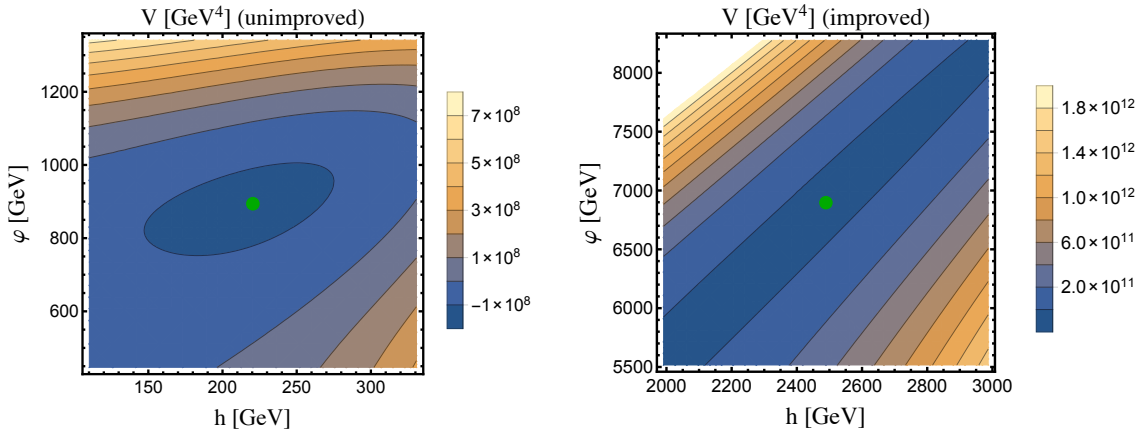

(a) **(b)**

Figure 6.9 – (a) The electroweak minimum (green dot) of the one-loop effective potential computed at the Gildener-Weinberg mass given in eq. (181). (b) The global minimum (green dot) of the one-loop improved effective potential.

From Figure 6.9(b), it seems that the global minimum of the one-loop improved potential is located at an almost flat direction. This is an effect of resolution of the contour plot, since a numerical computation of derivatives shows that the point labelled by the green dot is indeed a global minimum.

We thus conclude that the Gildener-Weinberg approach (Case I) fails to capture the radiative global minimum in this case. The reason for this is that the hierarchy of couplings was disregarded, in contrast to Chapter 6, where we correctly considered that the above example should be analysed as Case II, not Case I. We regard this as an important observation that could lead to incorrect conclusions about radiatively generated extrema if overlooked. Moreover, this example illustrates the importance of RG-improvement, which is what we advocate here.

Conclusions

Classically conformal extensions of the Standard Model are simple, yet predictive, models that can accommodate a rich phenomenology. There is a pressing need to extend the current theory to incorporate gravity, dark energy, dark matter, massive neutrinos, baryogenesis and other phenomena which lie beyond the scope of the Standard Model. As the LHC has yet to detect signs of superpartners, alternatives to supersymmetry become increasingly favourable. Moreover, the near vanishing of the Higgs mass parameter in the ultraviolet indicates that the current theory is nearly-conformal around the Planck scale.

Therefore, given the current data, a minimalistic approach would reject supersymmetry or even Grand Unified Theories. In this way, the possibility of a new physical scale between the electroweak and Planck scales is discarded. If we follow the hint of the ultraviolet behaviour of the Standard Model, we see that we should consider a theory which has conformal symmetry at tree level. Moreover, conformal symmetry should be realised in the full quantum theory at an (unkown) UV fixed point. Soft breaking of this symmetry occurs via quantum and thermal corrections, which generate all mass scales, including the mass of the physical Higgs boson. Such a scenario is certainly appealing, for, if it is realised in Nature, mass is then simply a consequence of the quantum theory. Furthermore, this framework also paves the way to a simple resolution of the Hierachy problem because the Higgs mass can be protected from radiative corrections by the custodial conformal symmetry present at tree level.

If quantum (loop) corrections are to be responsible for mass generation, one needs to understand under what conditions this is possible. We placed particular emphasis on the importance of correctly identifying the mechanisms through which radiative symmetry breaking occurs. In Chapter 2, we outlined the two general cases that are possible. Either the tree-level contribution is larger than the loop corrections or otherwise. This simple statement has important consequences. If the tree-level term dominates over loop corrections, a non-trivial minimum can only be generated at points in which the tree-level contribution vanishes. This typically leads to the requirement that the classical potential exhibits a flat direction. Conversely, loop corrections might be the dominant contributions at a given point in parameter space. Both cases are related to a hierarchy of the coupling parameters of the theory, as was outlined in section (2.4). Disregarding such hierarchy can lead to incorrect conclusions, as we pointed out in section (6.4). There we showed that, even though the classical potential might exhibit a flat direction on which a radiative minimum occurs, if it does not dominate over loop corrections, a global minimum can be located elsewhere. This simple fact is frequently overlooked in the literature.

Besides determining whether or not quantum corrections generate a global minimum, we must also determine stability properties of the potential, e.g., boundedness and verify the validity of a given loop-order approximation. Since the effective potential exhibits large logarithmic contributions away for field values which are much different from those at the minimum, a perturbative expansion of the potential is valid only in a limited region of parameter space. Nevertheless, one may develop a technique to restore or enhance the validity of perturbation theory. This is usually done with the aid of the renormalisation group (RG). In Chapter 3, we developed a novel technique of RG-improving the potential, motivated by stability considerations and by a search for a simple alternative to multi-scale methods, which have been used previously in the literature. The implementation of such methods is rather involved. Multi-scale techniques can also be related to the decoupling theorem [45].

With the method developed in Chapter 3 and further developed in appendix B, we are able to RG-improve a potential with an arbitrary number of scalar fields using only the conventional RG equation. We showed that this method automatically re-sums the leading contributions

from higher loop-orders when it is applicable and justifies a frequently used criterion of stability, namely that the stability of the tree-level form in the large-field limit is a sufficient indicator of stability of the (improved) effective potential. With this new tools at hand, we proceeded to examine the dynamical generation of the electroweak scale.

We adopted the following criteria to search for models in which the electroweak scale is dynamically generated. The effective potential of a given quantum field theory must exhibit a global minimum which reproduces the Standard Model Higgs vacuum expectation value and running mass. The correct Higgs vacuum expectation value is needed to ignite the usual Brout-Englert-Higgs mechanism through which vector bosons and fermions acquire mass. The Higgs running mass does not need to coincide with its pole mass. However, the running mass is a good approximation to the pole mass of a particle if the effective potential is evaluated at scales which are near the vacuum expectation value of the particle.

Therefore, we searched for classically conformal models in which the effective potential, when evaluated at the scale of the Higgs vacuum expectation value, exhibited a non-trivial global minimum. Moreover, at this minimum there should be a mass-eigenstate with the measured value of the Higgs boson mass, around 125 GeV. Regarding the validity of perturbation theory, we took as our guiding principle the fact that there should be no new physical scales below the Planck scale. This implies that the running couplings of the theory cannot exhibit a Landau pole between the electroweak and Planck scales. Our analysis was limited to one-loop renormalisation group functions, but since all couplings should remain small parameters across a large range of scales, we expect that higher loop-orders will bring only small corrections. We adopted the Landau gauge throughout the text for convenience, since in this gauge the Faddeev-Popov-ghost contributions to the effective potential can be disregarded.

As we saw in Chapter 4, current data rule out a dynamical generation of the electroweak scale in the Conformal Standard Model, since the running of the Standard Model parameters can only generate a non-trivial minimum at large energies. Therefore, if the Higgs mass is to be a radiative effect, we need to consider non-minimal extensions. We have focused on Higgs portal models, which were studied in Chapters 5 and 6. The key idea is simple. One extends the scalar sector, adding additional scalar fields which are singlets under the Standard Model gauge group. The interaction of such scalars to the Standard Model occurs only via the Higgs field. In this way, the coupling of the additional fields with beyond-the-Standard-Model particles is hidden, i.e., it can only be detected through the Higgs portal. It is advantageous to consider these hidden sectors to model a diverse range of phenomena beyond the Standard Model.

In Chapter 5, we thoroughly analysed the simplest classically conformal extension, which features an additional real scalar singlet[†]. We saw that, although it is possible to reproduce the electroweak vacuum in this model, this comes at the expense of Landau poles below the Planck mass. The reason for this is that, in order to generate real and positive masses, the portal coupling generally needs to be large to balance the negative contribution of the top quark Yukawa coupling. Our perturbativity criterion then lead us to discard this model. Clearly, one could then study arbitrarily complicated models, with hidden sectors tailored to admit complex phenomenology.

Fortunately, we concluded in Chapter 6 that a very simple extension can correctly generate the electroweak scale. This model features an additional scalar field which transforms under a hidden $SU(2)$ gauge group, and has been also considered in [24]. The role of the gauge coupling is counteract the dominant influence of the top quark Yukawa coupling in the running of the parameters. Indeed, since the $SU(2)$ gauge coupling decreases as energies increase, this does not lead to Landau poles below the Planck scale, contrary to the case of the singlet model. Evidently, one can also consider hidden $SU(N)$, $(N > 2)$, gauge groups, which will have

[†]The $O(N)$-symmetric model is analysed in appendix C.

an effective low energy physics which differs from the $SU(2)$ case. Nevertheless, all the key properties of the dynamical breakdown of symmetry are encapsulated by the simple $SU(2)$ model and complications should only come at the interest of phenomenology.

To sum up, in this thesis we have thoroughly examined the possibilities for a dynamical generation of the electroweak scale. With the aid of a new method of RG-improvement, we concluded that one-loop approximations to certain Higgs portal models are reliable and correctly identify a global electroweak vacuum. This implies that it is possible that the Higgs mass and subsequently all mass scales originate from a dynamical breakdown of symmetry, in which case the electroweak vacuum is stable and the metastability of the Standard Model is lifted. It also explains the origin of the mass of the physical Higgs boson. In the specific model analysed in chapter 6, we found an extra heavy scalar in addition to the Higgs particle and computed the effective trilinear and quartic Higgs self-couplings, which can differ considerably from those in the Standard Model.

The future prospects of this area of research are encouraging. We conclude that there are sufficiently simple models with classical conformal symmetry that are predictive model and can be tested in particle accelerators. Moreover, the coupling parameters can be chosen so as to remain perturbative up to the Planck scale. Thus, there is no need to consider supersymmetric extensions, Grand Unified Theories, or large numbers of spectator states (as in [25]). Quantum-gravitational effects will most likely become relevant around the Planck scale, but no new physical scale arises below it. In this way, corroboration of such models in future experiments would provide insight into physics across a large range of scales, all the way up to quantum gravity. It remains to be seen.

Appendix A

The Method of Characteristics

In solving the renormalisation group (RG) equation, it is useful to use the *method of characteristics* for partial differential equations (PDEs). We will review the method, providing basic examples of solutions of PDEs.

Fixing the Notation

We will use a slightly modified version of the notation used in [49]. A point in $\mathbb{R}^n$ or a n-component vector will be denoted by $x = (x_1, ..., x_n)$. The canonical basis in $\mathbb{R}^n$ is given by unit vectors e_i such that $\sum_k (e_i)_k (e_j)_k = \delta_{ij}$. The gradient of a scalar function is defined as $\nabla = \sum_i e_i \partial_i$. A point in $\mathbb{Z}^n$ with non-negative components is called a multi-index and will be denoted by greek letters, for example $\alpha = (\alpha_1, ..., \alpha_n)$. For convenience, we define

$$\begin{aligned} |\alpha| &:= \sum_{i=1}^{n} \alpha_i = \alpha_1 + \cdots + \alpha_n \ , \ \alpha \in \mathbb{Z}^n \ , \\ x^\alpha &:= \prod_{i=1}^{n} x_i^{\alpha_i} = x_1^{\alpha_1} \cdots x_n^{\alpha_n} \ , \ x \in \mathbb{R}^n \ , \\ A_\alpha &:= A_{\alpha_1 \ldots \alpha_n} \ , \end{aligned} \tag{182}$$

where A is a tensor field. The most general $|\alpha|$-th order derivative of a function $u : \mathbb{R}^n \to \mathbb{R}$ will be denoted by

$$\nabla^\alpha u := \frac{\partial^{|\alpha|} u}{\partial x_1^{\alpha_1} \cdots \partial x_n^{\alpha_n}} = \partial_1^{\alpha_1} \cdots \partial_n^{\alpha_n} u \ . \tag{183}$$

A.1 The Cauchy Boundary Value Problem

We will be mostly interested in linear differential equations and we will not discuss the non-linear case or systems of differential equations. For a more complete treatment of the subject, we refer the reader to [49], upon which we based this section.

A.1.1 The Characteristic Form

A general m-th order linear differential equation for a function $u : \mathbb{R}^n \to \mathbb{R}$ can be written as

$$\mathcal{L}u(x) = \sum_{|\alpha| \leq m} A_\alpha(x) \nabla^\alpha u(x) = B(x) \,, \tag{184}$$

where A_α and B are functions from $\mathbb{R}^n$ to $\mathbb{R}$ and $\mathcal{L}$ is the differential operator

$$\begin{aligned} \mathcal{L} &:= \sum_{|\alpha| \leq m} A_\alpha \nabla^\alpha = \sum_{|\alpha| < m} A_\alpha \nabla^\alpha + L \\ L &:= \sum_{|\alpha| = m} A_\alpha \nabla^\alpha \,. \end{aligned} \tag{185}$$

L is called the principal part of $\mathcal{L}$. We can define the *characteristic form* of L as the contraction

$$\Xi(v) = \sum_{|\alpha| = m} A_\alpha v^\alpha \;\;, \forall v \in \mathbb{R}^n \,, \tag{186}$$

such that, formally, $\Xi(\nabla) = L$.

Under a change of variables $y = y(x)$, by the chain rule,

$$\begin{aligned} \frac{\partial}{\partial x_i} &= \sum_j \frac{\partial y_j}{\partial x_i} \frac{\partial}{\partial y_j} \equiv \sum_j C_{ij} \frac{\partial}{\partial y_j} \,, \\ \nabla \equiv \nabla_x &= C \nabla_y \,. \end{aligned}$$

We find that a k-th order derivative with respect to the variable x_i can be written as a linear combination of derivatives with respect to the y variables of order less than or equal to k.

$$\partial_i^k = \frac{\partial^k}{\partial x_i^k} = \sum_j C_{ij_1} \cdots C_{ij_k} \frac{\partial}{\partial y_{j_1}} \cdots \frac{\partial}{\partial y_{j_k}} + \cdots \,,$$

where we have hidden derivatives of order less than k in the ellipses. Therefore,

$$\nabla^\alpha \equiv \nabla_x^\alpha = (C \nabla_y)^\alpha + \cdots \,,$$

where derivatives of order less than $|\alpha|$ are omitted. The principal part of $\mathcal{L}$ can then be written as

$$L = \sum_{|\alpha| = m} A_\alpha \nabla^\alpha = \sum_{|\alpha| = m} A_\alpha (C \nabla_y)^\alpha \,, \tag{187}$$

and the characteristic form in the y variables reads

$$\Xi_y(v) = \sum_{|\alpha| = m} A_\alpha (Cv)^\alpha \;\;, \forall v \in \mathbb{R}^n \,,$$

such that, formally, $\Xi_y(\nabla_y) = L$.

A.1.2 (Non)Characteristic Hypersurfaces

Given a hypersurface $S \subset \mathbb{R}^n$ defined by the equation

$$\Sigma(x) = 0 \,, \tag{188}$$

where Σ is a C^m function, we say that S is *regular* if $\nabla\Sigma \neq 0$. The *Cauchy boundary value problem* consists of the differential equation (184) and boundary data, i.e., the values of u and its normal derivatives of order less than m on S. A solution of the problem then satisfies (184) and its values on S are determined by the boundary data.

Consider the example $\Sigma(x) = x_n$. Then S is defined by $x_n = 0$ with normal vector e_n and normal derivative given by $\sum_i (e_n)_i \partial_i = \sum_i \delta_{in}\partial_i = \partial_n$. The boundary data can be written as

$$\partial_n^k u(x) = \phi_k(x_1, ..., x_{n-1}) \quad , \quad k = 0, ..., m-1 \,. \tag{189}$$

In particular, this implies that

$$\nabla^\alpha u = \partial_1^{\alpha_1} \cdots \partial_{n-1}^{\alpha_{n-1}} \phi_{\alpha_n} \,,$$

for $\alpha_1 + \cdots + \alpha_n < m$. Therefore, on S, eq. (184) reduces to

$$A_{0\ldots0,m}(x)\partial_n^m u(x) = B(x) - \sum_{|\alpha|<m} A_\alpha(x)\partial_1^{\alpha_1}\cdots\partial_{n-1}^{\alpha_{n-1}}\phi_{\alpha_n}(x) \,,$$

which has a unique solution for $\partial_n^m u(x)$ if $A_{0\ldots0,m}(x) \neq 0$ for $x \in S$.

With further generalisations in mind, note that $A_{0\ldots0,m} = \Xi(e_n) = \Xi(\nabla\Sigma)$. Therefore, we can determine $\partial_n^m u(x)$ and, in fact, all derivatives $\nabla^\alpha u(x)$ with $|\alpha| = m$ on S from eq. (184) and the boundary data if $\Xi(\nabla\Sigma) \neq 0$. In this case, we say that S is *noncharacteristic*. Otherwise, S is a *characteristic* hypersurface and we cannot determine all of the $\nabla^\alpha u(x)$ derivatives with $|\alpha| = m$ on S, and therefore we cannot solve the Cauchy boundary value problem.

Suppose now that Σ is an arbitrary C^m function. Since S is regular, for any $x \in S$, $\partial_n\Sigma \neq 0$ in a neighbourhood of x. This allows us to define the (invertible) change of variables

$$y_i = \begin{cases} x_i & i = 1, ..., n-1 \\ \Sigma(x) & i = n \end{cases} \,, \tag{190}$$

such that S is defined by the equation $y_n = 0$. With respect to the y variables, S is noncharacteristic if $\Xi_y(\nabla_y\Sigma) \neq 0$, where, in terms of the y variables, $\Sigma(y) = y_n$. Note, however, that $\Xi_y(\nabla_y\Sigma) = \Xi(\nabla\Sigma)$. Therefore, without loss of generality, we conclude that a regular hypersurface S is noncharacteristic if $\Xi(\nabla\Sigma) \neq 0$ and characteristic otherwise.

The condition $\Xi(\nabla\Sigma) = 0$ is a first-order PDE for Σ. We can find a family of characteristic hypersurfaces by solving this PDE. In the non-linear case, Ξ not only depends on the independent variables x but also on the boundary data. The solutions to the characteristic condition $\Xi(\nabla\Sigma) = 0$ form a family of characteristic manifolds.

Note that (real) characteristic manifolds need not exist. Consider the example of the Laplace operator $\Delta = \sum_i \partial_i^2$. The characteristic form is

$$\Xi(v) = \sum_i v_i^2 \,,$$

which is positive-definite and thus can never vanish for regular hypersurfaces.

A.1.3 First-Order PDEs

If (184) is a first-order PDE, then $m = 1$ and, upon a suitable change of notation, we can rewrite it as

$$\mathcal{L}u(x) = A(x)u(x) + \sum_{i=1}^{n} B_i(x)\partial_i u(x) = C(x) \,, \tag{191}$$

where A, B_i and C are functions from $\mathbb{R}^n$ to $\mathbb{R}$ and the differential operator $\mathcal{L}$ has principal part L given by

$$\begin{aligned} L &= \sum_{i=1}^{n} B_i \partial_i = \Xi(\nabla) \\ \Xi(v) &= \sum_{i=1}^{n} B_i v_i \ , \ \forall v \in \mathbb{R}^n \ . \end{aligned}$$

To solve a Cauchy problem for the PDE (191), we collect the boundary data for u on some noncharacteristic hypersurface M defined by the equation $G(x) = 0$, where G is a C^m function with $\Xi(\nabla G) \neq 0$. Given a chart (U, f) for M, the boundary data is given by

$$u(x) = \phi(f(\hat{x})) \ , \ x \in U \subset M \ , \tag{192}$$

where $\hat{x}$ is a set of $n-1$ independent variables, obtained from x by eliminating one variable via the equation $G(x) = 0$. Let us denote the local coordinates by $f(\hat{x}) = \xi$. Since f must be a homeomorphism, it can be inverted to yield $\hat{x} = f^{-1}(\xi)$, i.e., $n-1$ independent variables as a function of the local coordinates on M. Thus, we can denote a point $x \in M$ by $x(\hat{x}) = x(f^{-1}(\xi))$ to make explicit that only $n-1$ variables are independent.

We can find characteristic hypersurfaces by solving the first-order equation

$$\Xi(\nabla\Sigma) = \sum_{i=1}^{n} B_i \partial_i \Sigma = 0 \,,$$

which gives an orthogonality condition between the vector $B(x)$ and $\nabla\Sigma(x)$ for any point x in the hypersurface S given by $\Sigma(x) = 0$. This implies that $B(x)$ is an element of the tangent space of the hypersurface S at x, i.e., $B(x) \in T_x S$. We can associate B with a parametrised curve in S,

$$\begin{aligned} \gamma : \mathbb{R} &\to \mathbb{R}^n \\ t &\mapsto \gamma(t) \ , \\ \frac{\mathrm{d}\gamma}{\mathrm{d}t} &\equiv B(\gamma(t)) \ . \end{aligned}$$

Note that if S intersects M, we can solve the Cauchy problem with boundary data on M by running along such a parametrised curve. Concretely, given local coordinates ξ on M, we associate B with a family of curves with boundary conditions

$$\begin{aligned} \gamma : \mathbb{R}^n &\to \mathbb{R}^n \\ (t, \xi) &\mapsto \gamma(t, \xi) \ , \\ \gamma(0, \xi) &= x(f^{-1}(\xi)) \in M \ , \\ \frac{\partial\gamma}{\partial t} &= B(\gamma(t, \xi)) \ . \end{aligned} \tag{193}$$

These curves are called *characteristic curves*[*] for (191). Thus, for all points in S, eq. (191) can be rewritten as

$$\sum_{i=1}^{n} \frac{\partial \gamma_i}{\partial t} \partial_i u = F(\gamma(t,\xi), u) \; ,$$

with $F(\gamma(t,\xi), u) = C(\gamma(t,\xi)) - A(\gamma(t,\xi))u$. Therefore, by the chain rule, we obtain

$$\frac{\partial u}{\partial t} = F(\gamma(t,\xi), u) \; .$$

In this way, the Cauchy problem for the linear first-order PDE (191) can be recast as system of differential equations along a characteristic curve γ with boundary conditions.

$$\begin{aligned} &\frac{\partial \gamma}{\partial t} = B(\gamma(t,\xi)) \; , \\ &\frac{\partial u}{\partial t} = F(\gamma(t,\xi), u) \; , \\ &\gamma(0,\xi) = x(f^{-1}(\xi)) \in M \; , \\ &u(\gamma(0,\xi)) = \phi(\xi) \; . \end{aligned} \tag{194}$$

These equations are called *characteristic equations*. For a fixed ξ, the solution along the characteristic curve will be $u(\gamma(t,\xi))$. By varying (t,ξ), we obtain the solution $u(\gamma(t,\xi))$ for the whole domain $\mathbb{R}^n$. To express it in terms of the original independent variables $x = \gamma(t,\xi)$, we invert the function γ to obtain $(t,\xi) = \gamma^{-1}(x)$ such that $u(\gamma(t,\xi)) = u(x)$.

To see that it is possible to invert γ, consider first the case in which $G(x) = x_n$ and $B_n \neq 0$. Then $\Xi(\nabla G) = B_n \neq 0$ and the hypersurface M described by $x_n = 0$ is a noncharacteristic hyperplane. In this setting, we can choose f to be the identity, such that we obtain

$$\begin{aligned} &x = (x_1, ..., x_n) \; , \\ &\hat{x} = (x_1, ..., x_{n-1}) \; , \\ &\xi = (\xi_1, ..., \xi_{n-1}) = f(\hat{x}) = \hat{x} \; , \\ &x(f^{-1}(\xi)) \equiv (x_1, ..., x_{n-1}, 0) \; . \end{aligned}$$

Then the jacobian matrix of γ for any point $(\xi, t=0)$ in M is given by

$$\mathrm{jac}(\gamma)|_{t=0} = \begin{pmatrix} \frac{\partial \gamma_1}{\partial t} & \frac{\partial \gamma_1}{\partial \xi_1} & \cdots & \frac{\partial \gamma_1}{\partial \xi_{n-1}} \\ \vdots & \vdots & \ddots & \vdots \\ \frac{\partial \gamma_n}{\partial t} & \frac{\partial \gamma_n}{\partial \xi_1} & \cdots & \frac{\partial \gamma_n}{\partial \xi_{n-1}} \end{pmatrix} = \begin{pmatrix} B_1 & 1 & \cdots & 0 \\ \vdots & \vdots & \ddots & \vdots \\ B_{n-1} & 0 & \cdots & 1 \\ B_n & 0 & \cdots & 0 \end{pmatrix} \; ,$$

the determinant of which is $\det \mathrm{jac}(\gamma) \,|_{t=0} = (-1)^{n-1} B_n \neq 0$. By the *Inverse Function Theorem*, this implies that there is a local inverse of γ in the vicinity of $(\xi, t=0)$.

Now consider a general C^m function $G(x)$, such that $\Xi(\nabla G) \neq 0$ and $G(x) = 0$ gives the noncharacteristic hypersurface M. Since M must be regular, $\nabla G \neq 0$ in the vicinity of any point in M. Let us perform the (invertible) change of variables,

$$y_i = \begin{cases} x_i & i = 1, ..., n-1 \\ G(x) & i = n \end{cases} \; .$$

[*]Sometimes (193) is called a *projected* characteristic curve to distinguish it from a similar curve in $\mathbb{R}^{n+1}$ in which one also includes the dependent coordinate u as component.

We already know that $0 \neq \Xi(\nabla G) = \Xi_y(\nabla_y G)$, where $G(y) = y_n$. In terms of the y variables, the first-order PDE (191) reads

$$\sum_{i=1}^{n} \tilde{B}_i(y) \frac{\partial u}{\partial y_i} = \tilde{F}(y, u) \ ,$$

where $\tilde{F}(y, u) = C(x(y)) - A(x(y))u$ and

$$\tilde{B}_i = \sum_{j=1}^{n} B_j \frac{\partial y_i}{\partial x_j} = \begin{cases} B_i & (i = 1, ..., n-1) \\ \Xi(\nabla G) & (i = n) \ . \end{cases}$$

In particular, $\tilde{B}_n \neq 0$. Therefore, we see that we can take $G(x) = x_n$ and $B_n \neq 0$ without loss of generality. This guarantees that γ has a local inverse and we can solve the system (194). We provide simple examples of this powerful method below.

An Example: The Transport Equation

To illustrate the method of characteristics, an archetypical example is the solution to the transport equation. A possible Cauchy problem is

$$\begin{aligned} &\partial_x u + c \, \partial_y u = 0 \ , \\ &u(0, y) = \sin(y) \ , \end{aligned}$$

where c is a fixed constant. The characteristic form is $\Xi(v_x, v_y) = v_x + c \ v_y$ and the line parametrised by $(0, \xi)$ is therefore noncharacteristic (it is also clearly regular). This means the problem can be solved with the given boundary data. The corresponding characteristic equations and boundary conditions are

$$\begin{aligned} &\frac{\partial \gamma_1}{\partial t} = 1 \ , \\ &\frac{\partial \gamma_2}{\partial t} = c \ , \\ &\frac{\partial u}{\partial t} = 0 \ , \\ &\gamma_1(0, \xi) = 0 \ , \\ &\gamma_2(0, \xi) = \xi \ , \\ &u(0, \xi) = \sin(\xi) \ . \end{aligned}$$

The solution to the system is straightforward to find and reads

$$\begin{aligned} &\gamma_1(t, \xi) = t + a_1(\xi) \ , \\ &\gamma_2(t, \xi) = ct + a_2(\xi) \ , \\ &u(\gamma_1(t, \xi), \gamma_2(t, \xi)) = a_3(\xi) \ , \end{aligned}$$

where a_1, a_2 and a_3 are *a priori* arbitrary functions of ξ. In particular, we see that u must be constant along a particular characteristic curve. The boundary conditions impose $a_1(\xi) = 0$, $a_2(\xi) = \xi$ and $a_3(\xi) = \sin(\xi)$. We can invert γ to express the solution in terms of $x = \gamma_1(t, \xi)$ and $y = \gamma_2(t, \xi)$. Indeed,

$$\begin{aligned} &x = \gamma_1(t, \xi) = t \ , y = \gamma_2(t, \xi) = ct + \xi \\ &\xi = y - cx \ . \end{aligned}$$

Therefore, the solution is $u(x, y) = \sin(y - cx)$.

Appendix B

The Hypersurface of Vanishing Loop Corrections: A General Approach

In this appendix, we will generalise the results of Chapter 3, in which we proved that the effective potential can be evaluated at a hypersurface where the one-loop corrections vanish and that knowledge of the one-loop RG functions is sufficient to re-sum the largest logarithmic contributions to the effective potential. We will prove that, in fact, there exists a hypersurface on which all loop corrections vanish. The corresponding field-dependent scale can be computed as a power series in $\hbar$. To lowest order, the results of this appendix will agree with those of Chapter 3. We will show that higher orders contribute with subleading terms that were not contemplated in that chapter. We will conclude that this general method, which can be easily implemented numerically, is a viable alternative to multi-scale techniques.

Fixing the Notation

As before, we will consider a theory with N_ϕ scalar fields, N_λ couplings, vector and fermionic fields and N_m mass eigenvalues. The couplings (possibly including mass terms) are denoted by $\lambda = (\lambda_1, ..., \lambda_{N_\lambda})$, the classical scalar fields by $\phi = (\phi_1, ..., \phi_{N_\phi})$ and the mass eigenvalues by $m = (m_1, ..., m_{N_m})$. The mass logarithms will be defined as

$$L_a = \log \frac{m_a^2(\lambda, \phi)}{\mu^2} \ , \ a = 1, ..., N_m \ , \tag{195}$$

where we make explicit the dependence of the mass eigenvalues on the couplings as well as on the fields. We will also denote the effective potential by $V(\mu; \lambda, \phi)$, which is a function defined on a domain of the parameter space spanned by $(\mu; \lambda, \phi)$. We will use the modified multi-index notation adopted in appendix A. Given a multi-index $\alpha = (\alpha_1, ..., \alpha_N)$, we will denote

$$\begin{aligned} |\alpha| &:= \sum_{i=1}^{N} \alpha_i \ , \\ x^{\boldsymbol{\alpha}} &:= \prod_{i=1}^{n} x_i^{\alpha_i} = x_1^{\alpha_1} \cdots x_n^{\alpha_n} \ , \\ A_{\boldsymbol{\alpha}} &:= A_{\alpha_1 ... \alpha_N} \ , \end{aligned}$$

where x is a vector field and A is a tensor field. We will denote a reduced multi-index as

$$\{\alpha\} := (\alpha_1, ..., \alpha_{N-1}) \,,$$

which is simply a multi-index with the last component removed. Given some function $f(\alpha) = f(\alpha_1, ..., \alpha_N)$, we will also make use of the change of variables

$$\begin{aligned}
&\sum_{\alpha_1=0}^{\infty} \cdots \sum_{\alpha_N=0}^{\infty} f(\alpha) = \\
&= \sum_{\alpha=0}^{\infty} \sum_{\alpha_1=0}^{\alpha} \sum_{\alpha_2=0}^{\alpha-\alpha_1} \cdots \sum_{\alpha_{N-1}=0}^{\alpha-\alpha_1-...-\alpha_{N-2}} f(\alpha_1, \alpha_2, ..., \alpha_{N-1}, \alpha - \alpha_1 - ... - \alpha_{N-1}) \equiv \\
&\equiv \sum_{\alpha=0}^{\infty} \sum_{\{a\}=0}^{\alpha} f(\alpha) \,,
\end{aligned}$$

where in the last line we defined a convenient short-hand notation. For example, we may write

$$\sum_{\{n\}=0}^{n} \phi^{\mathbf{n}} = \sum_{n_1=0}^{n} \sum_{n_2=0}^{n-n_1} \cdots \sum_{n_{N_\phi-1}=0}^{n-n_1-...-n_{N_\phi-2}} \phi_1^{n_1} \cdots \phi_{N_\phi}^{n_{N_\phi}} \,.$$

B.1 The Perturbative Structure of the Effective Potential

In perturbation theory, the effective potential is written as the loop expansion in eq. (82). The general structure of the renormalised l-th loop order term in the $\overline{MS}$ scheme is [37, 41, 42]

$$V^{(l)}(\mu; \lambda, \phi) = \sum_{n=0}^{l} \sum_{\{n\}=0}^{n} v_{\mathbf{n}}^{(l)} \prod_{a=1}^{N_m} L_a^{n_a} \equiv \sum_{n=0}^{l} \sum_{\{n\}=0}^{n} v_{\mathbf{n}}^{(l)} L^{\mathbf{n}} \,, \tag{196}$$

where the coefficients $v_{\mathbf{n}}^{(l)} = v_{n_1...n_{N_\phi}}^{(l)}$ are functions of the couplings and the fields. The potential depends logarithmically on the subtraction mass μ through the powers of the mass logarithms, which originate from the regularisation of momentum integrals.

In certain regions of parameter space, in particular for large field values, it is necessary to reorganise the perturbative expansion in eq. (82) in order to re-sum the large logarithms that appear in eq. (196). To achieve this, we make use of the renormalisation group (RG), which we studied in Chapter 3. A typical reorganisation or improvement of the effective potential can be written as

$$V(\mu; \lambda, \phi) = \sum_{l=0}^{\infty} \hbar^l V^{(l)}(\mu, \lambda, \phi) = \sum_{l=0}^{\infty} \hbar^l f_l(\hbar; \mu, \lambda, \phi) \,, \tag{197}$$

where the functions f_l may contain all powers of $\hbar$. We will call f_l the l-th-to-leading functions [37, 41]. If such functions can be found in closed form and satisfy

$$\left| \frac{f_{l+1}}{f_l} \right| < 1 \,,$$

than one can truncate the right hand side of eq. (197) to a given order in $\hbar$. For suitable choices of f_l, the region of parameter space for which the right hand side of eq. (197) is perturbative can thus be larger than the corresponding region for which the left hand side is perturbative [42].

A trivial choice of f_l is

$$f_l(\hbar;\mu,\lambda,\phi) = V^{(l)}(\mu,\lambda,\phi)\ ,$$

which will only guarantee perturbativity if no mass logarithms are large. In the case of large logarithms, we could define the l-th-to-leading logarithms in analogy to the one field case studied in the previous chapter (cf. eq. (58)). This can be done by changing the summation variables in eqs. (82) and (196) to obtain

$$\begin{aligned} V(\mu;\lambda,\phi) &= \sum_{l=0}^{\infty}\hbar^l\sum_{n=0}^{l}\sum_{\{n\}=0}^{n} v_{\mathbf{n}}^{l}L^{\mathbf{n}} = \\ &= \sum_{l=0}^{\infty}\sum_{n=0}^{\infty}\hbar^{l+n}\sum_{\{n\}=0}^{n} v_{\mathbf{n}}^{l+n}L^{\mathbf{n}} = \\ &= \sum_{l=0}^{\infty}\hbar^l f_l(\hbar;\mu,\lambda,\phi)\ , \end{aligned} \tag{198}$$

where

$$f_l(\hbar;\mu,\lambda,\phi) = \sum_{n=0}^{\infty}\hbar^n\sum_{\{n\}=0}^{n} v_{\mathbf{n}}^{l+n}L^{\mathbf{n}}\ , \tag{199}$$

provided the sums converge. We will refer to eq. (199) as the l-th-to-leading logarithms, since this is how they are usually defined in the literature [42]. If $N_m = 1$, we recover the one-field case,

$$\begin{aligned} V(\mu;\lambda,\phi) &= \sum_{l=0}^{\infty}\sum_{n=0}^{\infty}\hbar^{l+n}\sum_{\{n\}=0}^{n} v_{\mathbf{n}}^{l+n}L^{\mathbf{n}} \overset{N_m=1}{=} \\ &\overset{N_m=1}{=} \sum_{l=0}^{\infty}\sum_{n=0}^{\infty}\hbar^{l+n}v_n^{l+n}\left[\log\frac{m^2}{\mu^2}\right]^n\ , \end{aligned}$$

which agrees with eq. (58). Re-summing these logarithms, i.e., finding closed-form expressions to each f_l, is not a practical task, unless all logarithms are equal ($N_m = 1$), as we saw in section (2.1.1). In the case in which very different logarithms are present, one needs to employ multi-scale techniques in order to to find closed expressions for eq. (199).

In Chapter 3, we presented an alternative method to re-sum logarithms. It relied on changing the focus from the leading logarithms, as they are usually defined, and instead considering the pivot logarithm and logarithms of the ratios $\frac{\phi}{\mathcal{M}}$, as was discussed in section (3.1). We analysed this method with one-loop RG functions and showed that it automatically re-summed the leading functions of the pivot logarithm (cf. eq. (101)).

In this appendix, we will extend this method to RG functions truncated to any loop order, which will allow us to re-sum all the l-th-to-leading functions, when they are suitably defined. First, in section (B.2), we will derive equations for all the l-th-to-leading functions in the pivot logarithm expansion. Then, in section (B.3), we will prove that it is possible to write the full effective potential as the tree-level form, i.e., there exists a scale at which all quantum corrections vanish. We will show that evaluating the effective potential at this scale automatically re-sums (sub)leading terms in the pivot logarithm expansion and that this scale can be determined in perturbation theory, without resorting to multi-scale techniques. Finally, we will discuss the reliability of the approximations obtained by truncating this scale at a given order.

B.2 (Sub)Leading Contributions in the Pivot Logarithm Expansion

In section (3.2.1), we showed that knowledge of the one-loop β-functions and anomalous dimensions was sufficient to re-sum the leading function of the pivot logarithm expansion (cf. eq. (101)). We will now follow the work of B. Kastening in [37], in which the pivot logarithm method was applied to $O(N)$-symmetric ϕ^4-theory, and establish a general way of computing the k-th-to-leading functions in the pivot logarithm expansion.

Instead of using eqs. (97) and (98) to re-sum (sub)leading functions, it is more convenient to follow [36, 37] and use recursive relations for the f_k functions. In order to obtain these relations, we define

$$L_{\mathcal{M}} = \frac{\hbar}{2} \log \frac{\mathcal{M}^2}{\mu^2} \tag{200}$$

and write f_k as function of the pivot logarithm,

$$f_k(\hbar; \mu, \lambda, \phi) \equiv f_k(L_{\mathcal{M}}, \lambda, \phi) = \sum_{n=0}^{\infty} 2^n \tilde{w}_n^{(n+k)} (\lambda, \phi) L_{\mathcal{M}}^n ,$$

such that the insertion of eq. (95) into eq. (93) now yields

$$\begin{aligned}
0 &= \sum_{k=0}^{\infty} \hbar^k \mu \frac{\mathrm{d} f_k}{\mathrm{d}\mu} = \\
&= \sum_{k=0}^{\infty} \hbar^k \left(-\hbar \frac{\partial f_k}{\partial L_{\mathcal{M}}} + \sum_{i=1}^{N_\lambda} \beta_i \frac{\partial f_k}{\partial \lambda_i} - \frac{1}{2} \sum_{a=1}^{N_\phi} \gamma_a \phi_a \frac{\partial f_k}{\partial \phi_a} \right) = \\
&= \sum_{k=0}^{\infty} \hbar^{k+1} \left(-\frac{\partial f_k}{\partial L_{\mathcal{M}}} + \sum_{l=1}^{k+1} \sum_{i=1}^{N_\lambda} \beta_i^{(l)} \frac{\partial f_{k-l+1}}{\partial \lambda_i} - \frac{1}{2} \sum_{l=1}^{k+1} \sum_{a=1}^{N_\phi} \gamma_a^{(l)} \phi_a \frac{\partial f_{k-l+1}}{\partial \phi_a} \right) .
\end{aligned}$$

We thus obtain the recursive equations

$$\frac{\partial f_k}{\partial L_{\mathcal{M}}} - \sum_{l=1}^{k+1} \sum_{i=1}^{N_\lambda} \beta_i^{(l)} \frac{\partial f_{k-l+1}}{\partial \lambda_i} + \frac{1}{2} \sum_{l=1}^{k+1} \sum_{a=1}^{N_\phi} \gamma_a^{(l)} \phi_a \frac{\partial f_{k-l+1}}{\partial \phi_a} = 0 , \tag{201}$$

supplemented by the boundary conditions

$$f_k(0, \lambda, \phi) = \tilde{w}_0^{(k)} . \tag{202}$$

Let us solve eq. (201) for the first leading function. The Cauchy problem for f_0 is

$$\begin{aligned}
&\frac{\partial f_0}{\partial L_{\mathcal{M}}} - \sum_{i=1}^{N_\lambda} \beta_i^{(1)} \frac{\partial f_0}{\partial \lambda_i} + \frac{1}{2} \sum_{a=1}^{N_\phi} \gamma_a^{(1)} \phi_a \frac{\partial f_0}{\partial \phi_a} = 0 , \\
&f_0(0, \lambda, \phi) = \tilde{w}_0^{(0)} \equiv \tilde{V}^{(0)} ,
\end{aligned}$$

which can be solved with the method of characteristics (cf. Appendix A). The boundary hyperplane is chosen to be $L_{\mathcal{M}} = 0$, which is a regular and noncharacteristic hypersurface. We can

parametrise the boundary by $\xi = (\lambda_0, \phi_0)$. The characteristic equations and boundary conditions are

$$\begin{aligned}
\frac{\partial \bar{L}_{\mathcal{M}}}{\partial t}(t,\xi) &= 1 \,, \\
\frac{\partial \bar{\lambda}_i}{\partial t}(t,\xi) &= -\beta_i^{(1)}(\bar{\lambda}) \,, \\
\frac{\partial \bar{\phi}_a}{\partial t}(t,\xi) &= \frac{1}{2}\gamma_a^{(1)}(\bar{\lambda})\bar{\phi}_a \,, \\
\frac{\partial f_0}{\partial t}(t,\xi) &= 0 \,, \\
\bar{L}_{\mathcal{M}}(0,\xi) &= 0 \,, \\
\bar{\lambda}_i(0,\xi) &= \lambda_{i,0} \,, \\
\bar{\phi}_a(0,\xi) &= \phi_{a,0} \,, \\
f_0(0,\xi) &= \tilde{V}^{(0)}(\xi) \,.
\end{aligned}$$

The solution then reads

$$\begin{aligned}
L_{\mathcal{M}} = \bar{L}_{\mathcal{M}}(t,\lambda_0,\phi_0) &= t \,, \\
\lambda_i = \bar{\lambda}_i(t,\lambda_0,\phi_0) &\,, \\
\phi_a = \bar{\phi}_a(t,\lambda_0,\phi_0) &\,, \\
f_0(t,\lambda_0,\phi_0) = \tilde{V}^{(0)}(\lambda_0,\phi_0) &\,.
\end{aligned}$$

Upon inverting the characteristic curve family, we find

$$\begin{aligned}
t(L_{\mathcal{M}},\lambda,\phi) &= L_{\mathcal{M}} \,, \\
\lambda_{i,0}(L_{\mathcal{M}},\lambda,\phi) &= \bar{\lambda}_i(-t,\lambda,\phi) \,, \\
\phi_{a,0}(L_{\mathcal{M}},\lambda,\phi) &= \bar{\phi}_a(-t,\lambda,\phi) \,, \\
f_0(L_{\mathcal{M}},\lambda,\mathcal{M}) &= \tilde{V}^{(0)}(\lambda_0,\phi_0) \,,
\end{aligned}$$

which agrees with eq. (101). In general, we can use the method of characteristics to solve eq. (201) for f_k with f_s $(0 \leq s < k)$ as sources. Due to the boundary conditions (202), knowledge of the RG functions up to $(k+1)$-th loop order is necessary to compute the k-th-to-leading function. In particular, one needs only the one-loop order RG functions to compute the leading function f_0, as we saw in Chapter 3.

Evidently, the difficulty in determining the (dominant) pivot logarithm for each region in parameter space remains. We will now generalise the method of Chapter 3 and verify that it indeed solves the issue.

B.3 Vanishing Loop Corrections: General Formulas

As was studied in section (3.2.2), the effective potential remains constant along characteristic curves, via the solution to the Cauchy problem given in eq. (105). Indeed, we saw that it is not possible to choose a scale t such that the full effective potential vanishes, for the Cauchy problem was ill-posed. Nevertheless, we found a hypersurface at which the one-loop corrections disappear.

Let us now search for a field-dependent scale at which all loop-corrections vanish, as opposed to just the one-loop term. For this, we write the effective potential of the theory as

$$\tilde{V}(\mu;\lambda,\phi) = \tilde{V}^{(0)}(\lambda,\phi) + q(\mu,\lambda,\phi) \,, \tag{203}$$

where we defined the variable

$$q \equiv q(\mu,\lambda,\phi) = \sum_{l=1}^{\infty} \hbar^l \tilde{V}^{(l)}(\mu,\lambda,\phi) \,, \tag{204}$$

which encodes the quantum corrections. We note that the solution to the equation

$$q(\mu(t),\lambda(t),\phi(t)) = 0 \,, \tag{205}$$

which we will denote by

$$t_* \equiv t_*(\mu_0,\lambda_0,\phi_0) \,, \tag{206}$$

defines a displacement along the characteristic curve to a point of vanishing quantum corrections. For brevity, let us denote

$$\begin{aligned} \mu_* &\equiv \mu(t_*) = \mu_0 e^{t_*} \,, \\ \lambda_{i*} &\equiv \lambda_i(t_*) \,, \\ \phi_{a*} &\equiv \phi_a(t_*) \,. \end{aligned} \tag{207}$$

Due to solution (105), we obtain

$$\tilde{V}^{(0)}(\lambda_*,\phi_*) = \tilde{V}^{(0)}(\lambda(t_*),\phi(t_*)) + q(\mu(t_*),\lambda(t_*),\phi(t_*)) = \tilde{V}(\mu_0;\lambda_0,\phi_0) \,. \tag{208}$$

Moreover, the quantum corrections will satisfy

$$\begin{aligned} 0 = q(\mu(t_*),\lambda(t_*),\phi(t_*)) &= q(\mu_0,\lambda_0,\phi_0) + \sum_{n=1}^{\infty} \frac{1}{n!} \left.\frac{\mathrm{d}^n q}{\mathrm{d}t^n}\right|_{t=0} t_*^n = \\ &= q(\mu_0,\lambda_0,\phi_0) - \sum_{n=1}^{\infty} \frac{1}{n!} \left.\frac{\mathrm{d}^n \tilde{V}^{(0)}}{\mathrm{d}t^n}\right|_{t=0} t_*^n \,, \end{aligned} \tag{209}$$

where we used the fact that eq. (104) implies $\frac{\mathrm{d}^n \tilde{V}}{\mathrm{d}t^n} \equiv 0$ and, therefore,

$$\frac{\mathrm{d}^n \tilde{V}^{(0)}}{\mathrm{d}t^n} = -\frac{\mathrm{d}^n q}{\mathrm{d}t^n} \,,\ n > 0 \,. \tag{210}$$

Using eq. (209), we find

$$\begin{aligned} \tilde{V}^{(0)}(\lambda_*,\phi_*) &= \tilde{V}^{(0)}(\lambda_0,\phi_0) + \sum_{n=1}^{\infty} \frac{1}{n!} \left.\frac{\mathrm{d}^n \tilde{V}^{(0)}}{\mathrm{d}t^n}\right|_{t=0} t_*^n = \\ &= \tilde{V}^{(0)}(\lambda_0,\phi_0) + q(\mu_0,\lambda_0,\phi_0) \,, \end{aligned} \tag{211}$$

which is merely a rewriting of eq. (208).

On the hypersurface $q = 0$, the potential can be written as the tree-level form $\tilde{V}^{(0)}(\lambda_*,\phi_*)$ and only the running couplings $\lambda_* \equiv \lambda(t_*)$ and fields $\phi_* \equiv \phi(t_*)$ appear. In this way, any logarithmic dependence is implicit. This amounts to a re-summation of all logarithms. A perturbative treatment will be valid if the running couplings are small and, therefore, running towards

this tree-level hypersurface will minimise the effect of radiative corrections in truncations of the effective potential at a given loop order.

We can solve for t_* in perturbation theory using eq. (209). We refer the reader back to the multi-index notation presented at the beginning of this appendix, which we will employ here. We write

$$t_* = \sum_{l=0}^{\infty} \hbar^l t_*^{(l)} \,, \tag{212}$$

which we insert in

$$q(\mu_0, \lambda_0, \phi_0) = \sum_{n=1}^{\infty} \frac{1}{n!} \left. \frac{\mathrm{d}^n \tilde{V}^{(0)}}{\mathrm{d}t^n} \right|_{t=0} t_*^n \,,$$

to obtain

$$\begin{aligned}
\sum_{s=1}^{\infty} \hbar^s \tilde{V}^{(s)}(\mu_0, \lambda_0, \phi_0) &= \sum_{n=1}^{\infty} \frac{1}{n!} \sum_{l_1,\ldots,l_n=1}^{\infty} \hbar^{l_1+\cdots+l_n} \prod_{a=1}^{n} \left[\mathrm{d}^{(l_a)}\right]_{t=0} \tilde{V}^{(0)} \times \\
&\times \sum_{k_1,\ldots,k_n=0}^{\infty} \hbar^{k_1+\cdots+k_n} \prod_{b=1}^{n} t_*^{(k_b)} = \\
&= \sum_{n=1}^{\infty} \sum_{l=0}^{\infty} \sum_{k=0}^{\infty} \frac{\hbar^{l+n+k}}{n!} \left[\sum_{\{l\}=1}^{l+n} \prod_{a=1}^{n} \mathrm{d}^{(l_a)} \tilde{V}^{(0)} \right]_{t=0} \sum_{\{k\}=0}^{k} \prod_{b=1}^{n} t_*^{(k_b)} = \\
&= \sum_{s=1}^{\infty} \hbar^s \sum_{n=1}^{s} \sum_{l=0}^{s-n} \frac{1}{n!} \left[\sum_{\{l\}=1}^{l+n} \prod_{a=1}^{n} \mathrm{d}^{(l_a)} \tilde{V}^{(0)} \right]_{t=0} \sum_{\{k\}=0}^{s-n-l} \prod_{b=1}^{n} t_*^{(k_b)} \,.
\end{aligned}$$

Note that we have employed changes of summation variables to write the right-hand side of the above equation in a similar form to the left-hand side. Indeed, assuming all sums converge, we are lead to the formula

$$\sum_{n=1}^{s} \sum_{l=0}^{s-n} \frac{1}{n!} \left[\sum_{\{l\}=1}^{l+n} \prod_{a=1}^{n} \mathrm{d}^{(l_a)} \tilde{V}^{(0)} \right]_{t=0} \sum_{\{k\}=0}^{s-n-l} \prod_{b=1}^{n} t_*^{(k_b)} = \tilde{V}^{(s)}(\mu_0, \lambda_0, \phi_0) \,, \ (s \geq 1) \,. \tag{213}$$

To lowest order ($s = 1$), formula (213) gives

$$\begin{aligned}
\left[\left(\mathrm{d}^{(1)}\right) \tilde{V}^{(0)} \right]_{t=0} t_*^{(0)} &= \tilde{V}^{(1)}(\mu_0, \lambda_0, \phi_0) \,, \\
t_*^{(0)} &= \frac{\tilde{V}^{(1)}(\mu_0, \lambda_0, \phi_0)}{\left[\left(\mathrm{d}^{(1)}\right) \tilde{V}^{(0)} \right]_{t=0}} \,,
\end{aligned} \tag{214}$$

which agrees with eq. (110), once one notes that we have $\left[\left(\mathrm{d}^{(1)}\right) \tilde{V}^{(0)} \right]_{t=0} = 2\mathbb{B}\mathcal{M}^4$ from eq. (99). The next order ($s = 2$) is obtained with the equation

$$\begin{aligned}
&\sum_{n=1}^{2} \sum_{l=0}^{2-n} \frac{1}{n!} \left[\sum_{\{l\}=1}^{l+n} \prod_{a=1}^{n} \mathrm{d}^{(l_a)} \tilde{V}^{(0)} \right]_{t=0} \sum_{\{k\}=0}^{2-n-l} \prod_{b=1}^{n} t_*^{(k_b)} = \tilde{V}^{(2)}(\mu_0, \lambda_0, \phi_0) \,, \\
&\left[\mathrm{d}^{(1)} \tilde{V}^{(0)} \right]_{t=0} t_*^{(1)} + \left[\mathrm{d}^{(2)} \tilde{V}^{(0)} \right]_{t=0} t_*^{(0)} + \frac{1}{2} \left[\left(\mathrm{d}^{(1)}\right)^2 \tilde{V}^{(0)} \right]_{t=0} \left(t_*^{(0)}\right)^2 = \tilde{V}^{(2)}(\mu_0, \lambda_0, \phi_0) \,,
\end{aligned}$$

which yields

$$t_*^{(1)} = \frac{\tilde{V}^{(2)}(\mu_0,\lambda_0,\phi_0) - \left[\mathrm{d}^{(2)}\tilde{V}^{(0)}\right]_{t=0} t_*^{(0)} - \frac{1}{2}\left[\left(\mathrm{d}^{(1)}\right)^2\tilde{V}^{(0)}\right]_{t=0}\left(t_*^{(0)}\right)^2}{\left[\mathrm{d}^{(1)}\tilde{V}^{(0)}\right]_{t=0}} \,. \tag{215}$$

One can continue in this way to determine $t_* \equiv t_*(\mu_0,\lambda_0,\phi_0)$ to an arbitrary loop order using formula (213). In particular, we note that t_* inherits from the effective potential the invariance under redefinitions of the pivot mass at each order in perturbation theory. This can be explicitly verified in eqs. (214) and (215).

Let us now define the s-th-to-leading functions. In the same way we derived eq. (213), we can write

$$\begin{aligned}
\tilde{V}(\mu_0;\lambda_0,\phi_0) = \tilde{V}^{(0)}(\lambda_*,\phi_*) &= \tilde{V}^{(0)}(\lambda_0,\phi_0) + \sum_{n=1}^{\infty}\frac{1}{n!}\left.\frac{\mathrm{d}^n\tilde{V}^{(0)}}{\mathrm{d}t^n}\right|_{t=0} t_*^n = \\
&= \tilde{V}^{(0)}(\lambda_0,\phi_0) + \sum_{n=1}^{\infty}\sum_{l=0}^{\infty}\sum_{k=0}^{\infty}\frac{\hbar^{l+k+n}}{n!}\sum_{\{l\}=1}^{l+n}\sum_{\{k\}=0}^{k}\prod_{a=1}^{n}\left[\mathrm{d}^{(l_a)}\right]_{t=0}\tilde{V}^{(0)}\prod_{b=1}^{n}t_*^{(k_b)} = \\
&= \tilde{V}^{(0)}(\lambda_0,\phi_0) + \sum_{s=0}^{\infty}\hbar^s\sum_{n=1}^{\infty}\frac{\hbar^n}{n!}\sum_{l=0}^{s}\sum_{\{l\}=1}^{l+n}\sum_{\{k\}=0}^{s-l}\prod_{a=1}^{n}\left[\mathrm{d}^{(l_a)}\right]_{t=0}\tilde{V}^{(0)}\prod_{b=1}^{n}t_*^{(k_b)} \,.
\end{aligned}$$

Let us now define

$$T_n^{(s+n)} := \frac{1}{n!}\sum_{l=0}^{s}\sum_{\{l\}=1}^{l+n}\sum_{\{k\}=0}^{s-l}\prod_{a=1}^{n}\left[\mathrm{d}^{(l_a)}\right]_{t=0}\tilde{V}^{(0)}\prod_{b=1}^{n}t_*^{(k_b)} \,, \tag{216}$$

such that we obtain

$$\tilde{V}(\mu_0;\lambda_0,\phi_0) = \tilde{V}^{(0)}(\lambda_0,\phi_0) + \sum_{s=0}^{\infty}\hbar^s\sum_{n=1}^{\infty}\hbar^n T_n^{(s+n)} = \sum_{s=0}^{\infty}\hbar^s f_s(\hbar;\mu_0,\lambda_0,\phi_0) \,,$$

where the s-th-to-leading function is defined as

$$f_s(\hbar;\mu_0,\lambda_0,\phi_0) = \delta_{s,0}\tilde{V}^{(0)}(\lambda_0,\phi_0) + \sum_{n=1}^{\infty}\hbar^n T_n^{(s+n)} \,. \tag{217}$$

In particular, the leading function reads

$$\begin{aligned}
f_0(\hbar;\mu_0,\lambda_0,\phi_0) &= \tilde{V}^{(0)}(\lambda_0,\phi_0) + \sum_{n=1}^{\infty}\hbar^n T_n^{(n)} = \\
&= \tilde{V}^{(0)}(\lambda_0,\phi_0) + \sum_{n=1}^{\infty}\frac{1}{n!}\left[\left(\hbar\mathrm{d}^{(1)}\right)^n\tilde{V}^{(0)}\right]_{t=0}\left(t_*^{(0)}\right)^n = \\
&= \tilde{V}^{(0)}\left(\bar{\lambda}\left(t_*^{(0)}\right),\bar{\phi}\left(t_*^{(0)}\right)\right) \,,
\end{aligned} \tag{218}$$

where we defined the one-loop running parameters

$$\begin{aligned}
&\bar{\lambda}(t) : \frac{\mathrm{d}\bar{\lambda}}{\mathrm{d}t} = \hbar\beta^{(1)}(\bar{\lambda}) \,,\ \bar{\lambda}(0) = \lambda_0 \,, \\
&\bar{\phi}(t) : \frac{\mathrm{d}\bar{\phi}}{\mathrm{d}t} = -\frac{\hbar}{2}\gamma^{(1)}(\bar{\lambda})\bar{\phi} \,,\ \bar{\phi}(0) = \phi_0 \,.
\end{aligned} \tag{219}$$

Note that to compute the leading function, one needs only knowledge of the one-loop RG functions. The objects $T_n^{(s+n)}$ were defined such that they are formally of order $\hbar^{s+n}$, in analogy to the usual definition of the s-th-to-leading logarithms.

From eq. (214), we see that the leading function in eq. (218) automatically includes the leading function in eq. (100) and, therefore, the expansion in powers of $t_*^{(0)}$ re-sums the leading powers of a pivot logarithm and also includes terms that are subleading, which are precisely the logarithms of the ratios $\frac{\phi_0}{\mathcal{M}_0}$. As we showed in Chapter 3, the invariance under redefinitions of $\mathcal{M}_0$ guarantees that the dominant logarithms are captured in this re-summation. The subleading terms, which are proportional to logarithms of the ratios $\frac{\phi_0}{\mathcal{M}_0}$ will be re-summed with higher orders in t_* (cf. eq. 213) which yield the subleading functions as defined in eq. (217).

Conclusions

We have generalised the method presented in Chapter 3 to all loop orders. This method can be used to RG-improve the effective potential in a general theory with N_ϕ scalar fields and N_λ couplings, without resorting to multi-scale methods. The key step is to evaluate the effective potential on a hypersurface in parameter space in which all quantum corrections vanish. This amounts to a re-summation of all logarithms of the theory. Naturally, to fully determine the field-dependent value of the subtraction mass on this surface, knowledge of all loop-orders is necessary.

However, this method can be made practical by noting that truncations of the RG functions at any given loop order can produce reliable approximations of the full effective potential if the running couplings are sufficiently small. In particular, truncation of the β-functions and anomaous dimensions to one-loop order yields the results of Chapter 3. The error made by truncating the RG functions is of subleading-logarithmic order, in the sense of the set $\mathbb{S}_2$ of relation (89), due to the invariance of t_* under redefinitions of the pivot mass, at each order in perturbation theory. We note that the method here developed ceases to be valid if the hypersurface on which quantum corrections vanish is characteristic, for the Cauchy problem is ill-posed in this case.

Furthermore, the results of this chapter show that the full effective potential is given by the tree-level form

$$V(\mu;\lambda,\phi) = V^{(0)}(\lambda_*,\phi_*)\ ,$$

as long as $\lambda_* \ll 1$, which generalises the conclusions on stability made at the end of Chapter 3. Thus, to study the stability of the n-loop RG-improved effective potential, it is sufficient to consider the tree-level form with n-loop running couplings, evaluated at the n-th loop-order truncation of t_*.

In the next appendix, we will study applications of the above method and its utility in identifying global minima of the effective potential and verifying the reliability of the one-loop approximation. We will also verify its limitations when Landau poles are present.

Appendix C

An Application of RG-Improvement

To illustrate our method of RG-improvement, we will apply the techniques developed in Chapter 3 and appendix B to massless $O(N)$-symmetric ϕ^4-theory.

C.1 Massless $O(N)$-symmetric ϕ^4-theory

Massless ϕ^4-theory is an example of a classically conformal theory. This implies there is no vacuum energy and no mass parameters at tree-level. We will consider $N_\phi = N$ scalar fields and $N_\lambda = 1$ coupling, such that the theory has $O(N)$ symmetry. For convenience, we set $\hbar = 1$. In the $\overline{MS}$ scheme, the renormalised effective potential up to two-loop order is [36, 38]

$$
\begin{aligned}
V(\mu,\lambda,\phi) &= V^{(0)}(\lambda,\phi) + V^{(1)}(\mu,\lambda,\phi) + V^{(2)}(\mu,\lambda,\phi)\,, \\
V^{(0)}(\lambda,\phi) &= \frac{\lambda}{4!}\rho^4\,, \\
V^{(1)}(\mu,\lambda,\phi) &= \frac{1}{64\pi^2}\left[m_H^4\left(\log\frac{m_H^2}{\mu^2}-\frac{3}{2}\right)+(N-1)m_G^4\left(\log\frac{m_G^2}{\mu^2}-\frac{3}{2}\right)\right]\,, \\
V^{(2)}(\mu,\lambda,\phi) &= \frac{1}{8(4\pi)^4}\lambda^2\rho^2 m_H^2\left(\log^2\frac{m_H^2}{\mu^2}-4\log\frac{m_H^2}{\mu^2}+8\Omega(1)+5\right)+ \\
&\quad+\frac{1}{8(4\pi)^4}\lambda m_H^4\left(\log\frac{m_H^2}{\mu^2}-1\right)^2+\frac{N-1}{(4\pi)^4}\left\{\frac{1}{72}\lambda^2\rho^2\left[(m_H^2+2m_G^2)\left(\log^2\frac{m_G^2}{\mu^2}-\right.\right.\right. \\
&\quad-\left.\left.\left.4\log\frac{m_G^2}{\mu^2}+8\Omega\left(\frac{m_H^2}{m_G^2}\right)+5\right)+2m_H^2\log\frac{m_H^2}{m_G^2}\left(\log\frac{m_G^2}{\mu^2}-4\right)\right]+ \right. \\
&\quad+\left.\frac{1}{12}\lambda m_H^2 m_G^2\left[\log\frac{m_H^2}{\mu^2}\log\frac{m_G^2}{\mu^2}-\log\frac{m_H}{\mu^2}-\log\frac{m_G^2}{\mu^2}+1\right]\right\}+ \\
&\quad+\frac{N^2-1}{(4\pi)^4}\frac{\lambda}{24}m_G^4\left(\log\frac{m_G^2}{\mu^2}-1\right)^2\,,
\end{aligned}
\tag{220}
$$

where we defined

$$\begin{aligned}
\rho^2 &= \sum_{a=1}^{N} \phi_a^2 \,, \\
m_H^2 &= \frac{\lambda}{2}\rho^2 \,,\; m_G^2 = \frac{\lambda}{6}\rho^2 \,, \\
\Omega(x) &= \begin{cases} \frac{\sqrt{x(4-x)}}{x+2} \int_0^{\arcsin\left(\frac{\sqrt{x}}{2}\right)} \log(2\sin t)\mathrm{d}t & \text{for } x \le 4 \\ \frac{\sqrt{x(x-4)}}{x+2} \int_0^{\operatorname{arccosh}\left(\frac{\sqrt{x}}{2}\right)} \log(2\cosh t)\mathrm{d}t & \text{for } x > 4 \end{cases} .
\end{aligned} \tag{221}$$

In terms of the pivot mass $\mathcal{M} = \rho$, we can rewrite (220) as follows.

$$\begin{aligned}
V(\mu,\lambda,\phi) &= w_0(\lambda) + w_1(\lambda)\log\frac{\rho^2}{\mu^2} + w_2(\lambda)\log^2\frac{\rho^2}{\mu^2} \,, \\
w_0(\lambda) &= w_0^{(0)}(\lambda) + w_0^{(1)}(\lambda) + w_0^{(2)}(\lambda) \,, \\
w_1(\lambda) &= w_1^{(1)}(\lambda) + w_1^{(2)}(\lambda) \,, \\
w_2(\lambda) &= w_2^{(2)}(\lambda) \,, \\
w_0^{(0)}(\lambda) &= \frac{\lambda}{4!}\rho^4 \,, \\
w_0^{(1)}(\lambda) &= \frac{1}{64\pi^2}\left[m_H^4\left(\log\frac{m_H^2}{\rho^2} - \frac{3}{2}\right) + (N-1)m_G^4\left(\log\frac{m_G^2}{\rho^2} - \frac{3}{2}\right)\right] \,, \\
w_0^{(2)}(\lambda) &= \frac{1}{8(4\pi)^4}\lambda^2\rho^2 m_H^2\left(\log^2\frac{m_H^2}{\rho^2} - 4\log\frac{m_H^2}{\rho^2} + 8\Omega(1) + 5\right) + \\
&\quad + \frac{1}{8(4\pi)^4}\lambda m_H^4\left(\log\frac{m_H^2}{\rho^2} - 1\right)^2 + \frac{N-1}{(4\pi)^4}\left\{\frac{1}{72}\lambda^2\rho^2\left[(m_H^2 + 2m_G^2)\left(\log^2\frac{m_G^2}{\rho^2} - \right.\right.\right. \\
&\quad - \left.\left.\left. 4\log\frac{m_G^2}{\rho^2} + 8\Omega\left(\frac{m_H^2}{m_G^2}\right) + 5\right) + 2m_H^2\log\frac{m_H^2}{m_G^2}\left(\log\frac{m_G^2}{\rho^2} - 4\right)\right] + \right. \\
&\quad + \left.\frac{1}{12}\lambda m_H^2 m_G^2\left[\log\frac{m_H^2}{\rho^2}\log\frac{m_G^2}{\rho^2} - \log\frac{m_H}{\rho^2} - \log\frac{m_G^2}{\rho^2} + 1\right]\right\} + \\
&\quad + \frac{N^2-1}{(4\pi)^4}\frac{\lambda}{24}m_G^4\left(\log\frac{m_G^2}{\rho^2} - 1\right)^2 \,, \\
w_1^{(1)}(\lambda) &= \frac{1}{64\pi^2}\left[m_H^4 + (N-1)m_G^4\right] \,, \\
w_1^{(2)}(\lambda) &= \frac{1}{8(4\pi)^4}\lambda^2\rho^2 m_H^2\left(2\log\frac{m_H^2}{\rho^2} - 4\right) + \frac{1}{4(4\pi)^4}\lambda m_H^4\left(\log\frac{m_H^2}{\rho^2} - 1\right) + \\
&\quad + \frac{N-1}{(4\pi)^4}\left\{\frac{1}{72}\lambda^2\rho^2\left[(m_H^2 + 2m_G^2)\left(2\log\frac{m_G^2}{\rho^2} - 4\right) + 2m_H^2\log\frac{m_H^2}{m_G^2}\right] + \right. \\
&\quad + \left.\frac{1}{12}\lambda m_H^2 m_G^2\left[\log\frac{m_H^2}{\rho^2} + \log\frac{m_G^2}{\rho^2} - 2\right]\right\} + \frac{N^2-1}{(4\pi)^4}\frac{\lambda}{12}m_G^4\left(\log\frac{m_G^2}{\rho^2} - 1\right) \,, \\
w_2^{(2)}(\lambda) &= \frac{1}{8(4\pi)^4}\lambda^2\rho^2 m_H^2 + \frac{1}{8(4\pi)^4}\lambda m_H^4 + \frac{N-1}{(4\pi)^4}\left\{\frac{1}{72}\lambda^2\rho^2\left[m_H^2 + 2m_G^2\right] + \frac{1}{12}\lambda m_H^2 m_G^2\right\} + \\
&\quad + \frac{N^2-1}{(4\pi)^4}\frac{\lambda}{24}m_G^4 \,.
\end{aligned}$$

The β-function and anomalous dimension can be computed with standard techniques and, up to two-loop order, read [6, 42, 38]

$$\begin{aligned}
\beta^{(1)} &= \frac{N+8}{3(4\pi)^2}\lambda^2 \,, \\
\beta^{(2)} &= -\frac{3N+14}{3(4\pi)^4}\lambda^3 \,, \\
\gamma^{(1)} &= 0 \,, \\
\gamma^{(2)} &= \frac{N+2}{18(4\pi)^4}\lambda^2 \,.
\end{aligned} \tag{222}$$

Let us now verify the solutions of eq. (99). Taking a first derivative, we obtain

$$\mathrm{d}^{(1)} w_0^{(0)} = \beta^{(1)} \frac{\partial w_0^{(0)}}{\partial \lambda} = \frac{N+8}{3(4\pi)^2}\lambda^2 \frac{\rho^4}{4!} \,.$$

With the definitions of m_H and m_G given in eq. (221) and the formulas given on the previous page, one may easily verify that the right hand side of the above equation is indeed equal to $2w_1^{(1)}$. Then, taking a second derivative, we find

$$\left[\mathrm{d}^{(1)}\right]^2 w_0^{(0)} = 2\beta^{(1)} \frac{\partial w_1^{(1)}}{\partial \lambda} = \frac{\lambda^3}{36} \frac{(N+8)^2}{3(4\pi)^4} \rho^4 \,.$$

Again, it is straightforward to verify that the right hand side of the above equation is equal to $8w_2^{(2)}$, with the formulas previously given.

We can now compute $t_*^{(0)}$ and $t_*^{(1)}$ using eqs. (214), (215) and (222). From the results of Chapter 3 and appendix B, we expect that $t_*^{(1)}$ will be a small correction to $t_*^{(0)}$ and that the relative differences in the values of the running couplings $\lambda(t_*^{(0)})$ and $\lambda(t_*^{(0)} + t_*^{(1)})$ will also be small, as long as the running coupling $\lambda(t)$ remains a small parameter across a large range of scales and no Landau poles occur. In Figure C.1, the graphs of the ratio $\frac{t_*^{(1)}}{t_*^{(0)}}$ are shown for different values of the number N of scalar fields, the coupling λ and the ratio $\frac{\rho}{\mu}$.
We note that, as expected, the ratio $t_*^{(1)}/t_*^{(0)}$ remains small across a large region of parameter space. This can be understood by using the above values of λ as boundary conditions for the running, in each case, and noting that the running coupling remains a small parameter and no Landau poles are present. For example, for $N = 10$ scalar fields and* $\lambda = 0.1$, we obtain a running coupling free of poles. If we understand $\lambda(t_*^{(0)})$ to be the one-loop running coupling evaluated at the field-dependent scale $t_*^{(0)}$ and, analogously, the quantity $\lambda(t_*^{(0)} + t_*^{(1)})$ to be the two-loop running coupling evaluated at the field-dependent scale $t_*^{(0)} + t_*^{(1)}$, we can define the relative difference

$$\delta\lambda := \frac{\lambda(t_*^{(0)} + t_*^{(1)}) - \lambda(t_*^{(0)})}{\lambda(t_*^{(0)})} \,. \tag{223}$$

In the same way, we define the one-loop and two-loop improved potentials and their relative difference as

$$V_{\text{one-loop improved}} \equiv V_1 := \frac{\lambda(t_*^{(0)})}{4!}\rho^4 \,,$$

*Values of λ close to 1 generally lead to Landau poles at large scales. However, even in those cases, a perturbative treatment is warranted for scales sufficiently short of the Landau pole.

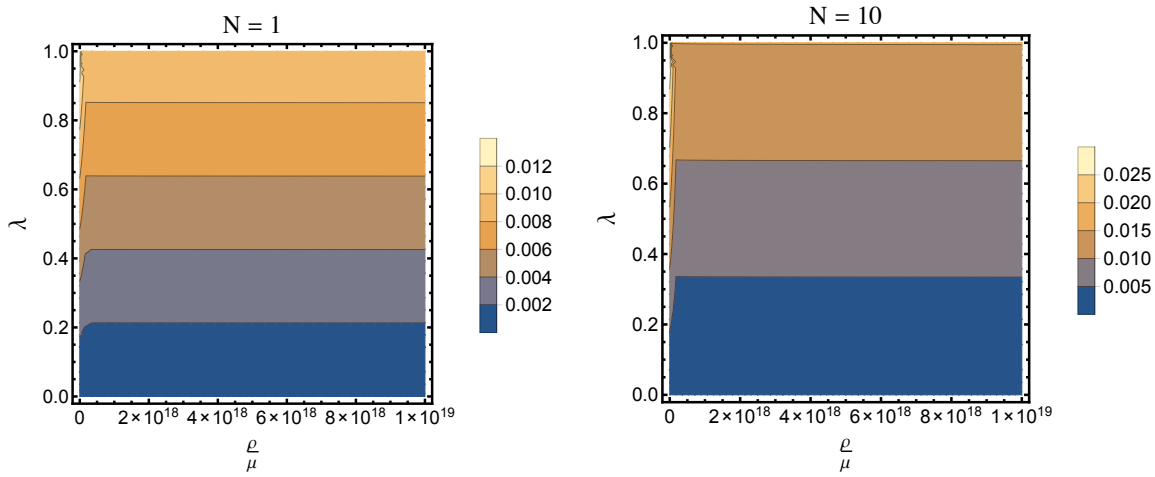

(a) **(b)**

Figure C.1 – (a) The ratio $t_*^{(1)}/t_*^{(0)}$ for $N = 1$ scalar field for different values of the coupling λ and the ratio $\frac{\varrho}{\mu}$. (b) The ratio $t_*^{(1)}/t_*^{(0)}$ for $N = 10$ scalar fields for different values of the coupling λ and the ratio $\frac{\varrho}{\mu}$.

$$V_{\text{two-loop improved}} \equiv V_2 := \frac{\lambda(t_*^{(0)}) + \lambda(t_*^{(1)})}{4!}\rho^4(t_*^{(0)} + t_*^{(1)}) \,,$$
$$\delta V := \frac{V_2 - V_1}{V_1} \,. \tag{224}$$

In Figure C.2, we show the relative differences of eqs. (223) and (224) across a large range of field values. As expected, the differences are small. This implies that truncating the RG functions to one-loop order provides a reliable approximation of the full effective potential.

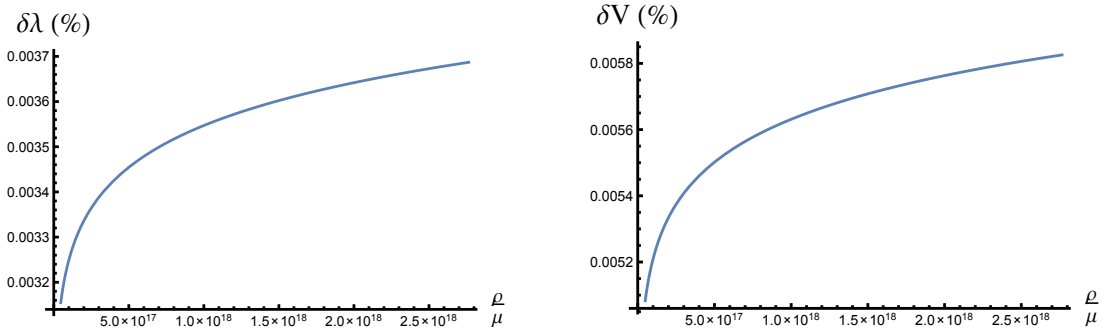

(a) **(b)**

Figure C.2 – The relative differences between the one-loop and two-loop running coupling and improved potentials for $N = 10$ scalar fields. Due to the absence of Landau poles, the differences remain small.

Let us now analyse a case in which Landau-pole divergences occur near the boundary scale

μ. In Figure C.3(a), the graph of the ratio $\frac{t_*^{(1)}}{t_*^{(0)}}$ is shown for different values of the coupling λ and the ratio $\frac{\rho}{\mu}$, when $N = 1000$ scalar fields are present, while we show the graph of the one-loop running coupling with boundary value $\lambda = 1$ in Figure C.3(b).

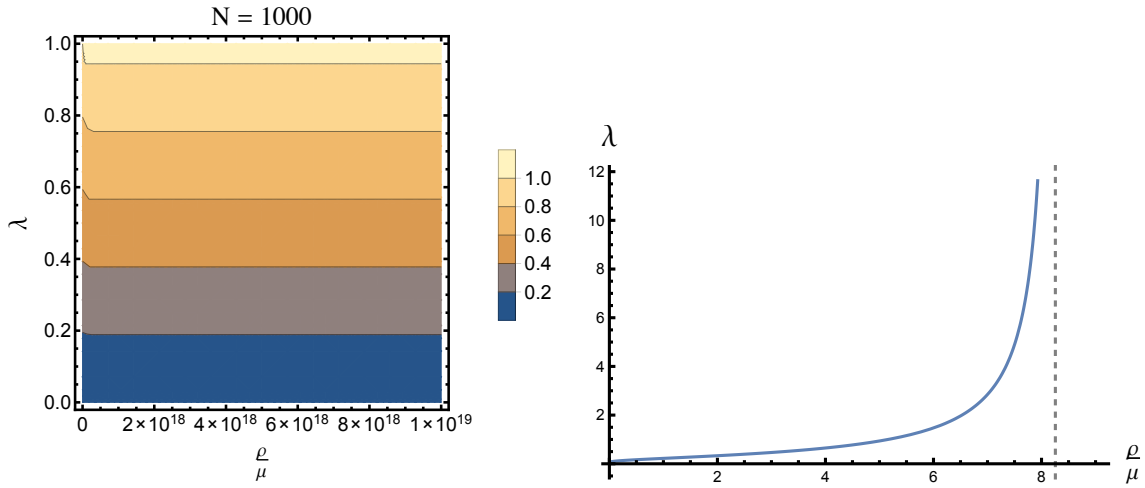

(a) **(b)**

Figure C.3 – (a) The ratio $t_*^{(1)}/t_*^{(0)}$ for $N = 1000$ scalar fields for different values of the coupling λ and the ratio $\frac{\rho}{\mu}$. (b) The one-loop running coupling for $N = 1000$ scalar fields and with a boundary value $\lambda = 1$. The dashed vertical line marks the location of a Landau pole.

We see from Figure (C.3)(a) that, for $N = 1000$ scalar fields and large boundary values of λ, the ratio $t_*^{(1)}/t_*^{(0)}$ also grows large. In this case, we expect that the one-loop improved potential will not be a reliable truncation of the full effective potential. This is confirmed by Figure (C.3)(b), in which we see that a Landau pole is present for field values close to the boundary μ. We thus conclude that, as expected from the results of Chapter 3 and appendix B, this method of RG-improving the potential is indeed reliable as long as the coupling parameter remains small. In the presence of a Landau pole, it is not enough to truncate the RG functions to one-loop order and higher-loop corrections are needed.

References

Effective Actions, Vacuum Stability and Radiative Symmetry Breaking

[1] J. Goldstone, A. Salam and S. Weinberg, *Broken Symmetries*, Phys. Rev. 127, 965, DOI: 10.1103/PhysRev.127.965 (1962).

[2] G. Jona-Lasinio, *Relativistic Field Theories with Symmetry-Breaking Solutions*, Nuovo Cimento 34 (1964) 1790, DOI: 10.1007/BF02750573.

[3] S. Coleman and E. Weinberg, *Radiative Corrections as the Origin of Spontaneous Symmetry Breaking*, Phys. Rev. D 7, 1888, DOI: 10.1103/PhysRevD.7.1888 (1973).

[4] R. Jackiw, *Functional Evaluation of the Effective Potential*, Phys. Rev. D 9, 1686, DOI: 10.1103/PhysRevD.9.1686 (1974).

[5] E. Gildener and S. Weinberg, *Symmetry Breaking and Scalar Bosons*, Phys. Rev. D 13, 3333, DOI: 10.1103/PhysRevD.13.3333 (1976).

[6] M. Sher, *Electroweak Higgs Potentials and Vacuum Stability*, Phys.Rept. 179 (1989) 273-418, DOI: 10.1016/0370-1573(89)90061-6.

[7] V.A. Miransky, *Dynamical Symmetry Breaking in Quantum Field Theories*, World Scientific Publishing Co. (1993).

[8] M. Quirós, *Finite Temperature Field Theory and Phase Transitions*, IEM-FT-187/99, hep-ph/9901312v1, (1999).

[9] Degrassi et al., *Higgs Mass and Vacuum Stability in the Standard Model at NNLO*, JHEP 1208 (2012) 098, DOI: 10.1007/JHEP08(2012)098.

[10] J. Elias-Miró, J.R. Espinosa, G.F. Giudice, H.M. Lee and A. Strumia, *Stabilization of the Electroweak Vacuum by a Scalar Threshold Effect*, J. High Energ. Phys. (2012) 2012: 31, DOI: 10.1007/JHEP06(2012)031.

[11] J.R. Espinosa, *Vacuum Stability and the Higgs Boson*, LATTICE 2013 hep-lat/1311.1970v1.

[12] A. Andreassen, W. Frost and M.D. Schwartz, *Consistent Use of the Standard Model Effective Potential*, Phys. Rev. Lett. 113, 241801 (2014), DOI: 10.1103/PhysRevLett.113.241801.

[13] B.N. Swiezewska, *Higgs Boson and Vacuum Stability in Models with Extendend Scalar Sector*, PhD Thesis, University of Warsaw (2016).

[14] W.A. Bardeen, *On Naturalness in the Standard Model*, FERMILAB-CONF-95-391-T, C95-08-27.3 (1995).

[15] R. Hempfling, *The Next-to-Minimal Coleman-Weinberg Model*, Phys. Lett. B 379 (1996) 153-158, DOI: 10.1016/0370-2693(96)00446-7.

[16] M. Shaposhnikov, *Is There a New Physics Between Electroweak and Planck scales?* (Talk), C07-06-21 hep-th/0708.3550v1 (2007).

[17] K. A. Meissner and H. Nicolai, *Conformal Symmetry and the Standard Model*, Phys.Lett. B648 (2007) 312-317, DOI: 10.1016/j.physletb.2007.03.023, hep-th/0612165.

[18] W.F. Chang, J.N. Ng and J.M.S. Wu, *Shadow Higgs from a Scale-Invariant Hidden $U(1)_s$ Model*, Phys. Rev. D 75, 115016, DOI: 10.1103/PhysRevD.75.115016 (2007).

[19] R. Foot, A. Kobakhidze and R.R. Volkas, *Electroweak Higgs as a pseudo-Goldstone Boson of Broken Scale Invariance*, Phys. Lett. B 655: 156-161, 2007, DOI: 10.1016/j.physletb.2007.06.084.

[20] R. Foot, A. Kobakhidze, K.L. McDonald and R.R. Volkas, *A Solution to the Hierarchy Problem from an Almost Decoupled Hidden Sector Within a Classically Scale Invariant Theory*, Phys. Rev. D 77, 035006, DOI: 10.1103/PhysRevD.77.035006 (2008).

[21] A. Farzinnia, H.J. He and J. Ren, *Natural Electroweak Symmetry Breaking from Scale Invariant Higgs Mechanism*, Phys. Lett. B 727 (2013) 141-150, DOI:10.1016/j.physletb.2013.09.060.

[22] C. Englert, J. Jaeckel, V.V. Khoze and M. Spannowsky, *Emergence of the Electroweak Scale through the Higgs Portal*, DCPT/13/04, IPPP/13/02, DOI: 10.1007/JHEP04(2013)060.

[23] A. Farzinnia and J. Ren, *Higgs Partner Searches and Dark Matter Phenomenology in a Classically Scale Invariant Higgs Boson Sector*, Phys. Rev. D 90, 015019, DOI:10.1103/PhysRevD.90.015019 (2014).

[24] V.V. Khoze and C. McCabe and G. Ro, *Higgs Vacuum Stability from the Dark Matter Portal*, JHEP 1408 (2014) 026, DOI: 10.1007/JHEP08(2014)026.

[25] D. Chway, R. Dermisek, T. H. Jung and H. Do Kim, *Radiative Electroweak Symmetry Breaking Model Perturbative All the Way to the Planck Scale*, Phys. Rev. Lett. 113, 051801 (2014), DOI: 10.1103/PhysRevLett.113.051801.

[26] C.T. Hill, *Is the Higgs boson associated with Coleman-Weinberg dynamical symmetry breaking?*, Phys. Rev. D 89, 073003 (2014), DOI: 10.1103/PhysRevD.89.073003.

[27] A. Gorsky, A. Mironov, A. Morozov and T.N. Tomaras, *Is the Standard Model saved asymptotically by conformal symmetry?*, J. Exp. Theor. Phys. (2015) 120: 344, DOI: 10.1134/S1063776115030218

[28] A. Karam and K. Tamvakis, *Dark Matter and Neutrino Masses from a Scale-Invariant Multi-Higgs Portal*, Phys. Rev. D 92, 075010 (2015), DOI: 10.1103/PhysRevD.92.075010.

[29] N. Haba, H. Ishida, N. Okada and Y. Yamaguchi, *Electroweak Symmetry Breaking Through Bosonic Seesaw Mechanism in a Classically Conformal Extension of the Standard Model*, SU-HET-11-2015, hep-ph/1509.01923v1.

[30] Altmannshofer et al., *Light Dark Matter, Naturalness, and the Radiative Origin of the Electroweak Scale*, J. High Energ. Phys. (2015) 2015: 32, DOI: 10.1007/JHEP01(2015)032.

[31] ZW. Wang, T.G. Steele, T. Hanif and R.B. Mann, *Conformal Complex Singlet Extension of the Standard Model: Scenario for Dark Matter and a Second Higgs Boson*, JHEP 1608 (2016) 065, DOI: 10.1007/JHEP08(2016)065.

[32] A. Karam and K. Tamvakis, *Dark Matter from a Classically Scale-Invariant $SU(3)_X$*, Phys. Rev. D94 (2016) 055004 DOI: 10.1103/PhysRevD.94.055004 (2016).

[33] A. Das, N. Okada and N. Papapietro, *Electroweak Vacuum Stability in Classically Conformal $B-L$ Extension of the Standard Model*, hep-ph/1509.01466 (2017).

[34] L. Marzola, A. Racioppi and V. Vaskonen, *Phase transition and gravitational wave phenomenology of scalar conformal extensions of the Standard Model*, hep-ph/1704.01034 (2017).

Renormalisation Group Improvement of Effective Potentials

[35] M.B. Einhorn and D.R.T. Jones, *A New Renormalization Group Approach to Multiscale Problems*, Nucl. Phys. B 230 (1984) 261-272, DOI: 10.1016/0550-3213(84)90127-5.

[36] B. Kastening, *Renormalization Group Improvement of the Effective Potential in Massive ϕ^4-theory*, Phys. Lett. B 283 (1992) 287-292, DOI: 10.1016/0370-2693(92)90021-U.

[37] B. Kastening, *Renormalization Group Improvement of the Effective Potential in Massive $O(N)$ Symmetric ϕ^4 Theory*, UCLA Report No. UCLA/92/TEP/26, hep-ph/9207252 (1992) (unpublished).

[38] C. Ford, D.R.T. Jones, *The effective potential and the differential equations method for Feynman integrals*, Phys. Lett. B 274 (1992) 409-414, DOI: 10.1016/0370-2693(92)92007-4,
Erratum B285 (1992) 399, DOI: 10.1016/0370-2693(92)91523-C.

[39] C. Ford, D.R.T. Jones, P.W. Stephenson and M.B. Einhorn, *The Effective Potential and the Renormalisation Group*, Nucl. Phys. B 395 (1993) 17-34, DOI: 10.1016/0550-3213(93)90206-5.

[40] M. Bando, T. Kugo, N. Maekawa and H. Nakano, *Improving the Effective Potential*, Phys. Lett. B 301 (1993) 83-89, DOI:10.1016/0370-2693(93)90725-W.

[41] M. Bando, T. Kugo, N. Maekawa and H. Nakano, *Improving the Effective Potential: Multi-Mass-Scale Case*, Prog Theor Phys (1993) 90 (2): 405-417, DOI: 10.1143/ptp/90.2.405.

[42] C. Ford, *Multi-scale Renormalisation Group Improvement of the Effective Potential*, Phys. Rev. D 50 (1994) 7531-7537, DOI: 10.1103/PhysRevD.50.7531.

[43] C. Ford and C. Wiesendanger, *Multi-scale Renormalization*, Phys. Lett. B 398 (1997) 342-346, DOI: 10.1016/S0370-2693(97)00237-2.

[44] C. Ford and C. Wiesendanger, *A Multi-scale Subtraction Scheme and Partial Renormalization Group Equations in the $O(N)$-symmetric ϕ^4-theory*, Phys. Rev. D 55 (1997) 2202-2217, DOI: 10.1103/PhysRevD.55.2202.

[45] J.A. Casas, V. Di Clemente, M. Quirós, *The Effective Potential in the Presence of Several Mass Scales*, Nucl.Phys. B553 (1999) 511-530, DOI: 10.1016/S0550-3213(99)00262-X.

[46] K. A. Meissner and H. Nicolai, *Renormalization Group and Effective Potential in Classically Conformal Theories*, Acta Phys. Polon. B40 (2009) 2737-2752, hep-th/0809.1338v3 (2009).

[47] F.A. Chishtie, T. Hanif, J. Jia, R.B. Mann, D.G.C. McKeon, T.N. Sherry and T.G. Steele, *Can the Renormalization Group Improved Effective Potential be used to estimate the Higgs Mass in the Conformal Limit of the Standard Model?*, Phys. Rev. D 83, 105009 (2011), DOI:10.1103/PhysRevD.83.105009.

[48] T.G. Steele, ZW. Wang and D.G.C. McKeon, *Multi-scale Renormalization Group Methods for Effective Potentials with Multiple Scalar Fields*, Phys. Rev. D 90, 105012 (2014), DOI: 10.1103/PhysRevD.90.105012.

Quantum Field Theory and Mathematical Methods

[49] F. John, *Partial Differential Equations*, Applied Mathematical Sciences Volume 1, Fourth Edition, Springer (1982).

[50] K.P. Hadeler, *On Copositive Matrices*, Linear Algebra and its Applications Volume 49 (1983) 79-89, DOI: 10.1016/0024-3795(83)90095-2.

[51] T.P. Cheng and L.F. Li, *Gauge Theory of Elementary Particle Physics*, Oxford Science Publications, Oxford University Press, First Edition (1984, 2000 reprint).

[52] S. Weinberg, *The Quantum Theory of Fields*, Vols. I and II, Cambridge University Press; First edition (2005 reprint).

[53] L.C. Evans, *Partial Differential Equations*, Graduate Studies in Mathematics Volume 19, Second Edition, American Mathematical Society (2010).

[54] B. de Wit, E. Laenen and J. Smith *Field Theory in Particle Physics*, lecture notes (2016).